# Third Annual Report for NSF EAR-0724958 entitled "Transformative Behavior of Water, Energy and Carbon in the Critical Zone: An Observatory to Quantify Linkages among Ecohydrology, Biogeochemistry, and Landscape Evolution" (Jemez-Santa Catalina CZO). August 31, 2012.

## JRB-SCM CZO Team:

**Principal investigators:** Jon Chorover, Peter Troch, Paul Brooks, Jon Pelletier, Craig Rasmussen, Greg Barron-Gafford, David Breshears, Travis Huxman, Jennifer McIntosh, Thomas Meixner, Shirley Papuga, Marcel Schaap (University of Arizona). **Collaborators:** Enrique Vivoni (ASU), Marcy Litvak (UNM), Robert Parmenter (Valles Caldera National Preserve), Kathleen Lohse (ISU).

**Postdoctoral scientists:** Ciaran Harman, Adrian Harpold, Bhaskar Mitra, and Julia Perdrial.

**Graduate Students (supported at least in part in third year of CZO):** Angelica Vazquez-Ortega, Ingo Heidbuechel, Jessica Driscoll Angie Jardine, Krystine Nelson, Xavier Zapata-Rios, Courtney Porter, Clare Stielstra, Rebecca Lybrand, Caitlin Orem, Emily Charaska, Chris Jones, Molly Holleran, Michael Pohlmann, David Huckle, Rachel Maxwell, Emily Charaska, Tyson Swetnam.

**Data and Field Management Scientists:** Matej Durcik, Nathan Abramson, Mark Losleben, Scott Compton.

Information included in the first and second annual reports are either not repeated or only briefly summarized here. The purpose of the current report is to provide an update on the more recent activities and findings during Year 3 of the Jemez-Santa Catalina CZO project.

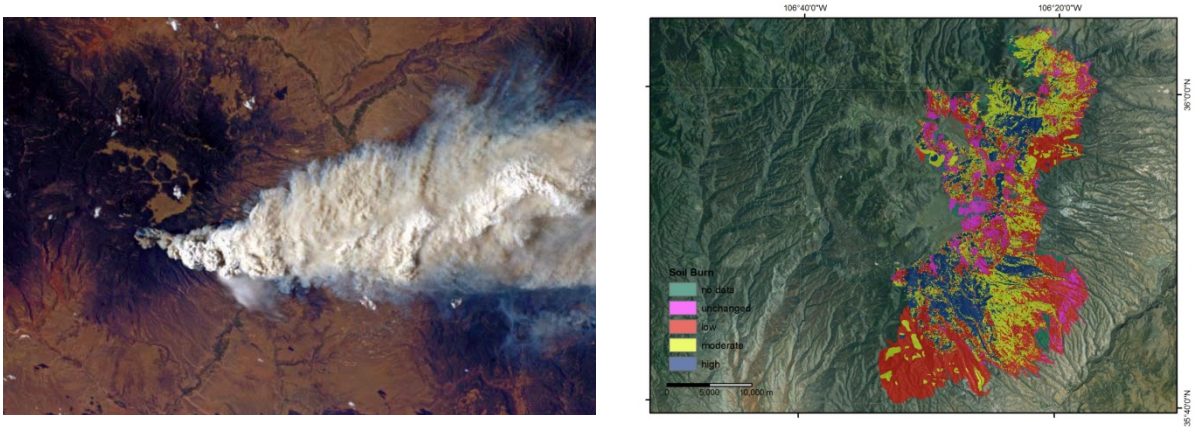


**Figure 1.** Ignition of the Las Conchas Fire in June, 2011 (left side) burned a large portion of Jemez River Basin under varying levels of severity (right side). The newly instrumented "Burned ZOB" on Rabbit Mountain (see also Fig. 2-3) is located east of the unburned Valle Grande, approximately half way up the north-south direction of extent of the fire.

**1. Major Research and Education Activities.** Project funding was initiated in September 2009. The UA portion of the CZO team, comprising 12 faculty, 4 postdoctoral scientists, 17 affiliated graduate students, two field technical staff, and a data management specialist, derive from five departments at the University of Arizona. This group meets weekly to discuss research and education progress toward building a CZO that has two observatory locations: The Jemez River Basin NM (JRB) and the Santa Catalina Mountains AZ (SCM).

We hypothesize that *effective energy and mass transfer* (EEMT, MJ $m^{-2}$ $y^{-1}$) quantifies climatic forcings that shape the co-evolution of vegetation, soils and landscapes in the critical zone (Rasmussen et al., 2010; Pelletier et al., *in review*). Testing of this hypothesis occurs across EEMT gradients in the JRB-SCM CZO that also span granite, rhyolite and schist rock types. We expect that gradients in EEMT and lithology will predict key aspects of CZ structure formation from molecular to grain to pedon to watershed scales.

Rock types include granite and schist in SCM, and rhyolite in JRB). In the SCM, instrumented ZOBs have been installed at low (ca. 1100 m) intermediate (ca. 2100 m) and high (ca. 2400 m) elevations. In the JRB, a high elevation ZOB (ca. 3000 m) was instrumented in spring, summer and fall of 2010. Following the Las Conchas wildfire of June-July 2011 (for details see second year annual report), a fire-disturbed ZOB was installed in a similar (but burned) mixed conifer vegetation type. Instrumentation across sites includes selected sites for Eddy flux towers, meteorological stations, precipitation collectors, soil moisture, potential and temperature probes, soil solution samplers, piezometers, flumes, pressure transducers and ISCO samplers.

***New CZO Infrastructure Installations***

Following the Las Conchas wildfire of 2011 (**Fig. 1**), our CZO team discussed the new opportunity that was presented by instrumenting a mixed-conifer catchment that had been severely burned by the fire. We recognized that by instrumenting such a site, because of resource limitations, we would be unable, in the current grant cycle, to instrument lower elevation sites in the JRB as originally planned. However, we also recognized that this fire represented a unique opportunity to explore the impacts on CZ function of the most important type of disturbance to impact forested mountain landscapes in the semi-arid Southwest. It is also noteworthy that this modification to our initial build-out plan is responsive to the CZO steering committee report of June, 2011, which states " …*many (CZO) study sites are in pristine areas with little current or expected land disturbance activities…less attention (is being paid) to human impacts like fire, atmospheric deposition, proximity to roads and power plants, soil cultivation, etc… that overprint all the processes the CZOs are studying*…". The JRB-SCM CZO team mobilized quickly to re-prioritize instrumenting a burned mixed-conifer catchment in order to enable the observation of CZ post-disturbance response.

Therefore, installations that have been completed since the submission of our Second Annual Report (September 2011), include the JRB burned ZOB on Rabbit Mountain (**Figs. 2-3**), which was equipped to provide a direct a means of direct comparison of the disturbed site with the unburned mixed conifer ZOB on Redondo Mountain (see First and Second Annual reports). Installations were scheduled and completed as soon as feasible once CZO personnel were permitted to re-enter the site (October, 2011, **Fig. 2**), and included two meterological stations, three piezometers, three snow depth sensors, and six soil pedon excavations that permitted installation of soil moisture, temperature and potential probes, plus wick and Prenart type lysimeters, as a function of soil depth (**Fig. 3**). Data acquisition began immediately following installations.

**Figure 2.** Installation of equipment in the "Burned ZOB" on Rabbit Mountain, JRB-CZO (October 2011). The catchment was subjected to high intensity burn, particularly in higher elevation locations. Installation of equipment involved a cross-section of CZO students, postdocs and staff.

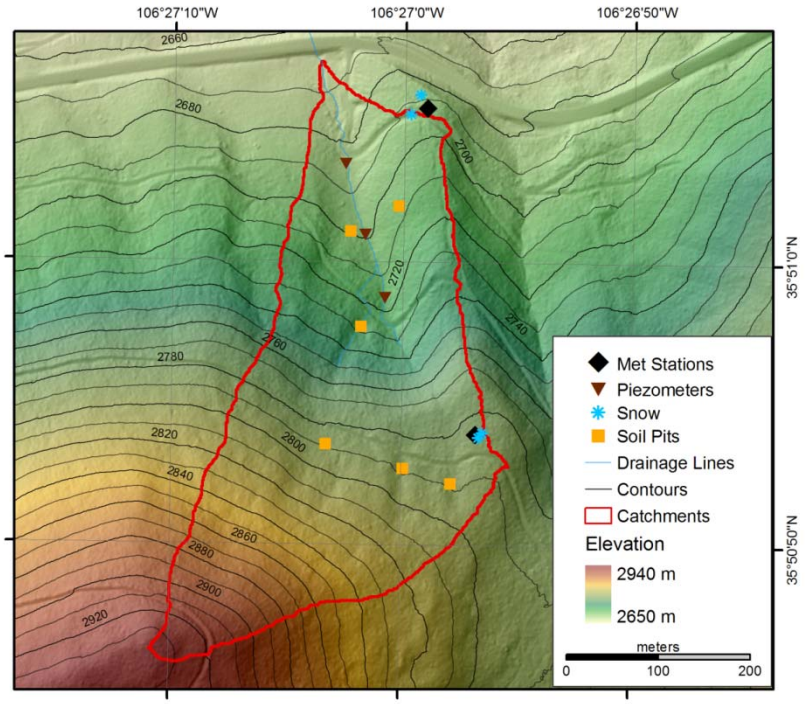


**Figure 3.** Shaded relief map overlain on JRB-CZO LiDAR data showing the precise locations of equipment installations in the Burned ZOB on Rabbit Mountain (JRB-CZO). Layout provides direct comparability to the Mixed Conifer ZOB on Redondo Mountain, and includes two meteorological stations, three piezometers, three snow ldepth sensors, and six soil pits each instrumented with sensors and samplers for depth resolved continuous measurement of soil moisture, water potential and temperature (Decagon probes), and both wick and Prenart type soil solution samplers.

## ***2. Activities in each of the JRB-SCM Science Themes.***

The JRB-SCM CZO is designed to quantify contemporary fluxes of energy, water, carbon and other solutes in the CZ in order to better predict long term CZ evolution and structure in semi-arid southwestern environments. Research is conducted in conjunction with the four, cross-cutting scientific "themes" of EHP, SSB, SWD and LSE.

1. ***Ecohydrology and Hydrologic Partitioning*** (EHP)
2. ***Subsurface Biogeochemistry*** (SSB)
3. ***Surface Water Dynamics*** (SWD)
4. ***Landscape Evolution*** (LSE)

Work in each of these themes proceeds through development of complementary research lines that probe common ground with a variety of disciplines and techniques. For example, while our LSE theme investigates how long term EEMT forcing of rock weathering and ecosystem change drives soil production and erosion over millennia, EHP, SSB and SWD also have the goal of quantifying contemporary rates of water-, carbon- and weathering-driven processes. Contemporary rates of carbon, water and weathering flux will constrain an evolving LSE model that strives for a predictive understanding of long term effects on landscape evolution (Pelletier et al., *in review*).

Nested locations within the larger CZO watershed (e.g., vegetation stands, hillslopes, ZOBs) represent narrow windows in geologic time and EEMT space. These are ideal locations for detailed studies of coupled processes as they occur at the current phase of CZ evolution. Coupled surface Earth processes are being probed through sensor and sampler installations. To expand the EEMT and geologic parameter space that might otherwise not be explored, we are focusing our installations on small basins that occur

along a gradient in climate or disturbance (with/without recent fire). By focusing on ZOBs situated in a range of climates within a common larger river basin, we seek to (i) quantify climate effects on CZO process coupling (via collocation of measurements of EHP, SSB, SWD and LSE), and (ii) scale up process-level understanding to resolve the dynamics of catchment aggregates and larger watershed systems (e.g., Santa Cruz and Jemez River Basins). These river basins – that capture essential water resources for growing human populations in the Southwest and that are expected to become hotter and drier with climate change – are likely to be dramatically affected by up-gradient changes in climate forcing.

## 2.1 *Activities:* Ecohydrology and Hydrologic Partitioning (EHP) Theme

The EHP group works closely with the other thematic groups (LSE, SWD, SSB), via weekly meetings, to address the following **three hypotheses**:

**Energy**: Hydrologic partitioning is uniquely related to effective energy;
**Water**: Vegetation controls pedon-scale water transit time; geomorphology controls catchment-scale water transit time;
**Carbon**: Hydrologic partitioning and water transit time control NEE, DOC and DIC input to subsurface, and biogeochemical export in streamflow.

EHP research efforts are focused on **two overarching questions** that guide installations and observations.

*(i)* *How do **temporal changes in vegetation structure and activity (e.g., mortality, phenology, seasonality**) affect hydrologic partitioning and the resultant transfer of water and carbon to subsurface and streamflow?*
*(ii)* *How does spatial variability in **vegetation composition and structure** reflect or control patterns in **hydrologic partitioning** over the last 1 – 100 yrs?*

Major new efforts in the current reporting year include observations designed to capture the ecohydrological response of CZ structure and function to the Las Conchas fire that burned a large area in the Jemez Mountains. These targeted efforts are in addition to the long-term observation strategies initiated over the last three years. Specific activities during the current project years to address these questions include:

- LiDAR derived snow depth products were combined with multiple years of snow surveys to quantify how elevation, aspect, vegetation structure and EEMT interact to control spatial variability in the fraction of winter snowfall that remains in the snowpack at maximum accumulation.

- Working jointly with the SWD and SSB themes, we developed a database of water chemistry and hydrological measurements in the Jemez River Basin. A simple mixing model was used to quantify how carbon and nutrient cycling varies across catchments draining different aspects on Redondo.

- Heavily burned areas on Rabbit Mountain in the Jemez were instrumented for energy, water and biogeochemical fluxes between land and atmosphere and in catchment runoff.

- An extensive vegetation survey was conducted at the Mixed Conifer ZOB (MC ZOB) at Jemez, NM and at the Schist and Granite ZOB at the Marshall Gulch watershed at Santa Catalina Mountains CZO. As part of our exercise in up-scaling transpiration from tree to stand to landscape level, sapwood cross-sectional areas were determined based on 5-mm diameter increment cores collected from tree

samples from each of the four plots where we have sap stations. The size of the plots was 30 m by 60 m at the Schist and Granite site at Marshall Gulch and 30 m by 30 m at the SE and SW facing aspect at MC ZOB. Apart from collecting tree cores, we also measured tree height, canopy diameter and diameter at breast height (dbh).

- Installation and data processing was competed on the CZO phenocams (16 total, with hourly images) and meteorological stations (6 total) in both JRB and SCM. This includes using MATLAB for obtaining snow depth and greenness indices from the phenocam images.

- Remote sensing vegetation products were combined with eddy covariance to quantify the contribution of understory vegetation to ecosystem scale carbon fluxes. Specifically, we ask the following questions: (1) how big is the contribution of the understory to ecosystem carbon uptake?; (2) at what times of year is the understory contribution important?; (3) does the eddy covariance carbon uptake signal (NEE-) reflect the greening up dynamics of the understory?; (4) are the greening up dynamics of the understory captured in our remotely-sensed products?; and (5) can remotely-sensed vegetation products such as MODIS-derived NDVI and EVI accurately reflect ecosystem-scale carbon uptake dynamics?

- We compared patterns of infiltration along an elevational gradient that incorporates distinct ecosystems using simple mini ring infiltrometers. Infiltration was measured in the cardinal directions at multiple distances from the stem of three random examples of the dominant plants in each ecosystem. Additionally, to assess canopy/intercanopy patterns, infiltration was measured every 50 cm along three 10 m transects in each ecosystem. To examine vegetation-infiltration relationships along this elevational gradient, we address three main hypotheses: (1) infiltration rates are highest nearest the plant stem regardless of ecosystem, (2) vegetation-infiltration relationships decrease with elevation; and (3) the difference between canopy and intercanopy infiltration rates is more complex in higher elevation ecosystems.

- Working within the Landscape Evolution Observatory at B2, we quantified how radiant energy fluxes and surface reflectance (albedo) affect energy available for critical zone processes. The albedo of a surface can change, e.g. by vegetation growth or soil wetting, which can further influence available energy. Here, we examined the soil moisture and albedo response of LEO soil to a 10 mm rainfall event, and compared the results to those found using traditional potting and native desert soils that differ in color and texture. We hypothesized that: 1) increased soil moisture would decrease albedo for all soil types; 2) a smaller wetting front would maximize any decrease in albedo, and 3) albedo will reach a minimum within hours of a rainstorm, returning to a maximum albedo value within the day.

- In the SCM sites we monitored soil evaporation and respiration to evaluate how snow accumulation and duration of snow cover affected these effluxes. Our study took place within a mixed-conifer ecosystem in the Santa Catalina Mountains about 10 km north of Tucson, Arizona. Here, three understory time-lapse digital cameras have monitored snow cover within the footprint of an eddy covariance tower for nearly two years. Using these cameras, we identified locations with short and long snow duration.

- In related work, we completed a two-year study to quantify the interactions between climate and soil type on soil respiration at sites in both the SCM and JRB.

- We installed a sap flow system within two mixed-conifer study sites of the Jemez River Basin – Santa Catalina Mountains Critical Zone Observatory (JRB – SCM CZO) to better understand the direct

role of vegetation in modulating transpiration in these water limited systems. At both sites, we identified the dominant tree species and installed sap flow sensors on healthy representatives for each of those species. At the JRB CZO site, sap sensors were installed in fir (4) and spruce (4) trees; at the SCM CZO site, sap sensors were installed at white fir (4) and maple (4) and one dead tree.

- We collected tree-ring data from the dominant tree species at the MC ZOB (SE and SW facing aspect) and at the low-elevation ZOB (Table 1). Per site and per species, we cored 15 trees (2 cores per tree) and GPS coordinates of individual trees were recorded. Furthermore, we collected additional cores for isotopic analysis from three trees of each dominant tree species. All tree cores were mounted and sanded and the majority of the cores from the MC ZOB has been cross-dated (Table 1). All cores intended for stable isotope analysis have been cross-dated and prepared for analysis.

- Extensive snow surveys were conducted in paired burned and unburned forested catchments on Rabbit Mountain to quantify changes in net snow water inputs following fire. These are among the first direct observations of stand and watershed-scale snowpack processes following high-intensity fire. Specifically, we are testing two hypotheses with potentially competing effects on net snowpack accumulation in unburned and post-burned forests: (1) reduced interception losses result in greater inputs to the snowpack; and (2) increased winter-season ablation from the snowpack surface results in reduced peak accumulation. To evaluate these processes we use three data sets from paired burned and unburned forests: (1) spatially distributed manual observations of new snow fall; (2) spatially distributed manual observations of total snow depth and SWE at maximum accumulation; and (3) catchment-wide LiDAR snow depth observations obtained in the paired catchments the year before the fire.

- We initiated seasonal measures of carbon and water flux with the overstory vegetation within the upper SCM CZO sites, including the Mt. Bigelow eddy covariance tower. Quantifying rates of photosynthetic uptake and transpirational water loss within numerous species and across multiple seasons both (1) yielded insights into the influence of community composition on seasonal NEE and ET dynamics and (2) aided in partitioning among vegetative and soil components of the vertical fluxes of water and carbon.

- In preparation of applying a widely used ecosystem model to the upper SCM CZO sites, we began seasonal measures of multiple vegetation-based parameters. Within all species, we quantified light use efficiency, light saturation point, carboxylation efficiency, rates of electron transport within the leaves, relative stomatal limitation to carbon uptake, leaf water potential, and water use efficiency. We will continue these measurements within the post-monsoon, fall, and winter seasons, and then we will begin parameterizing the SIPNET (Simple Photosynthesis Evapo-Transpiration) process-based model to boost performance in this snow *and* summer rain driven ecosystem. Ultimately, model development will enable us to (1) better estimate ecosystem fluxes in other upper elevation CZO sites that have climate forcing monitoring but lack eddy covariance measurements and (2) forward-cast ecosystem fluxes for these systems under various projected climate scenarios.

- Having developed a better understanding of the temperature dependence (or lack thereof) of soil respiratory and evaporative fluxes across the upper SCM CZO sites, we have begun quantifying the thermal sensitivity of overstory vegetation under periods of low and high water availability. We hypothesize that (1) there is substantial interspecific variation within each ecosystem, which may buffer against short-term periods of anomalously cold or warm temperatures, (2) species at the more southern extent of their range are likely more sensitive to high temperatures than species more adapted to warmer conditions, and (3) monsoon moisture modulates these temperature constraints on productivity.

- Water use by plant species is dependent on their phenophase. Phenological information was compiled on 222 species of plants that occur in Arizona and the Southwest. These plants were categorized into hydrological habitats (Obligate Wetland, Facultative Wetland, Facultative, Facultative Upland, Obligate Upland) and their approximate flowering time and, where available, the period of vegetative growth was recorded. These species include many of the dominant species in Arizona and are comprised of 90% of the species recorded in the USA NPN database for Arizona. A table listing the likely phenophase for each species throughout the year was compiled from a range of sources including - previous observations at the Santa Rita Experimental Range, field guides, online databases and herbarium specimens. We uncovered a large amount of non-digitized sources which will now be input into digital form and made available. A list of potential mathematical models to predict phenophase transitions was compiled from available literature.

## 2.2 *Activities:* Subsurface Biogeochemistry (SSB) Theme

The SSB group works closely with the other thematic groups via weekly meetings to address the following **three hypotheses**:

**Energy**: Mineral weathering rate/transformation increases with EEMT resulting in concurrent changes in soil C stabilization.

**Water**: Ratio of inorganic carbon to organic carbon flux increases with increasing water transit time.

**Carbon**: Wet/dry cycles promote $CO_2$ production, enhancing mineral weathering and thereby promoting greater soil C stabilization.

The SSB research efforts focus on **two overarching questions**:

*(i) How does the critical zone partition total rock weathering into components of:*
*(a) chemical denudation (elemental mass loss at pedon/hillslope scales);*
*(b) primary to secondary mineral transformation (element retention in thermodynamically stable forms).*
(ii) *In the subsurface, how is net ecosystem exchange partitioned into:*
*(i) DOC/POC, DIC export;*
*(ii) stable soil C pools;*
*(iii) physical erosion of soil C.*

Recent activities in the SSB theme include:

- Experimental assessment of the suitability of passive capillary wick sampler (PCaps) for DOM sampling in CZ research and comparison with aqueous soil extracts. In column experiments fiberglass wicks were infiltrated with Oa-horizon extract and effluent was monitored for changes in DOC, TDN, UVvis absorbance, Fluorescence spectra (quantified with PARAFAC) and FTIR spectra.

- Suitability of fiberglass wick-based PCaps for weathering fluxes. Release and sorption of cations, trace metals and REE as well as anions was assessed in column experiments where B-horizon extract was percolated through fiberglass wicks.

- Aqueous soil extracts (ASE) of severely burned soils as endmember for stream water DOM signature after wildfires (collaboration with SWD). ASE of mildly to severely burned areas of the burned ZOB were analyzed for DOC, DIC, TDN, UVvis and fluorescence spectroscopy.

- Quantifying how water and carbon fluxes (EEMT) control chemical denudation (collaboration with SWD theme). Water and carbon fluxes were translated into the currency of EEMT (overall CZ EEMT influx based on net ecosystem exchange, effective precipitation, and ambient temperature) and correlated with annual solute export in streams, as a direct test of the EEMT hypothesis.

- Quantification of bulk elemental chemistry and mineralogy and microscale weathering patterns of soils from convergent and divergent landscape positions from five ecosystems across the SCM gradient.

- Quantifying the physical distribution and mean residence time organic carbon across the various ecosystems and landscape positions in the SCM.

- High resolution sampling design and collection to characterize the subsurface structure of the high elevation mixed conifer ZOB in the SCM.

- Characterization of potential carbon mineralization for surface soils and soil depth profiles for granitic soils in the high elevation mixed conifer ZOB in the SCM.

- Testing of the utility of trace element signatures to provide insights into (bio-)weathering processes from pedon to watershed scales.

- Four sets (3 different depths: 15, 30, 64 cm) of soil gas samplers were installed in the MCZOB on two hillslopes (east and west facing) in open and covered canopy areas, near established soil lysimeters (Pits 1 and 3), to enable sampling of soil gases for concentration and isotopes to better constrain CZ carbon cycling. Similar soil gas samplers will be installed this fall in the burned ZOB and the SCM CZO sites.

- Sampled soils under different burn intensity and vegetation 3 weeks, 3 months, 10 months, and 12 months after the fire for soil moisture, soil pH, soil organic matter, soil nitrogen (N) pools and processes, and total C and N and isotopes as well as extractable dissolved organic carbon (DOC) in 3 week sampling.

- Analyzed soil profiles in burned ZOB for nutrients and process rates.

- Analyzed 3 month samples for microbial diversity using ION Torrent sequencer (first time this has been done).

## 2.3 *Activities:* Surface Water Dynamics (SWD) Theme

The SWD group works closely with the other thematic groups (LSE, EHP, SSB), via weekly meetings, to address the following set of research questions as part of our CZO efforts:

*(i) How does carbon and nutrient cycling vary as a function of EEMT, bedrock lithology, and water transit times?*

*(ii) How do chemical denudation rates vary as a function of EEMT, bedrock lithology, and water transit times?*

- Stream water samples were collected at the seven flumes (where continuous discharge is measured) surrounding Redondo Peak and the newly installed burned catchment in the Valles Caldera Preserve on a daily to weekly basis during snowmelt, and bi-weekly to monthly during the summer, fall and winter. Spring samples from each catchment were collected periodically throughout the year. Water samples were analyzed for major ion and trace metal chemistry, nutrients (N, P), stable isotopes ($^{18}O$,$^{2}H$,$^{13}C$), and rare earth elements. Carbon characteristics, including DOC, DIC, UVvis absorbance, and PARAFAC-quantified fluorescence spectra, were also analyzed. Select samples were analyzed for Ge/Si, Sr and uranium isotopes, and tritium.

- A third JRB CZO snow survey was conducted in mid-March (2012) to measure snow water equivalence (to couple with recent LiDAR data), in addition to solute and isotope chemistry (to couple with stream water and soil water data). Daily snowmelt samples were also collected for isotope and solute chemistry from two autosamplers (ISCOs) installed on west and east facing slopes in the MCZOB.

- Two ISCO auto samplers were installed during the summer at the La Jara and Upper Jaramillo flumes to collect stream flow samples for isotopes and chemistry analysis during the monsoon season. Rainfall samples were collected using two ISCO auto samplers at the lower La Jara and lower Upper Jaramillo catchments. In addition six bulk samplers (3 with and 3 without mineral oil) were installed in lower La Jara, Upper La Jara (MCZOB) and Upper Jaramillo catchments for rainfall chemistry and isotope analysis.

- After the high intensity Las Conchas wildfire, a small (13.1 ha) headwater catchment was selected in October 2011 as an intensive study site to investigate the impacts of fire on CZ processes. The Burned ZOB was instrumented with similar instrumentation as the La Jara MC ZOB (15.1 ha). Six soil pit locations were chosen to cover different soil and vegetation burn severities (unburned, low to high severity). Subsurface installations included soil temperature and moisture probes (3 per location), potentiometers (2 per location), suction cup lysimeters (4 per location), and passive capillary wick samplers (PCaps, 3 per location). Additionally, 3 piezometers were installed to allow for monitoring of groundwater table elevation changes. No flume was installed in the Burned ZOB due to the only poorly developed channel but a culvert guiding discharge under Highway 4, at the outlet of the catchment, into the Valle Grande was equipped with a pressure transducer.

- Stream water and soil water samples have been collected on a weekly basis from two ZOBs at high elevation (Marshall Gulch) and one ZOB at mid-elevation (Oracle Ridge) in the SCM CZO, starting in 2006 and 2011, respectively. Snowmelt samples were collected in snowmelt lysimeters in the two high elevation ZOBs during April-May, and rainfall samples were collected with and without mineral oil for isotopes and chemistry. Water samples were collected from the low-elevation B2 Desert site when water was present. Water samples from the SCM CZO sites were analyzed for similar parameters as the JRB CZO sites, including major and trace metal chemistry, rare earth elements, nutrients and water stable isotopes. In both high elevation ZOBs two snow depth sensors, a net radiometer, and temperature and relative humidity sensors were installed prior to winter. An additional ISCO was installed in Marshall Gulch to sample rainwater during

the monsoon season for isotope analysis. In June, an automated pumping system was installed at Oracle Ridge used to turn mechanical pumps on and off for the Prenarts (**Fig. 4**).

**Figure 4.** New battery operated pump system for Prenart sampling developed by Nate Abramson (SCM-CZO field scientist) has significantly improved pore water sample recoveries from the vadose zone.

## 2.4 *Activities:* Landscape Evolution (LSE) Theme

Students and faculty in the landscape evolution theme are focused primarily on quantifying flooding and erosion in fire-prone, semi-arid landscapes including the JRB and SCM. We are also taking a regional perspective to test the applicability of ideas and models developed in the JRB and SCM landscapes to other landscapes in the western U.S. at a range of spatial scales. EEMT and slope aspect/gradient play a major role in controlling erosion through the vegetation cover of the landscape, which depends strongly on slope aspect and gradient. The LSE group also serves the other three themes. For example, PI Pelletier is working to quantify variations in soil thickness above bedrock around Redondo Mountain in JRB in order to help determine the controls on water residence times.

Principal LSE theme activities in the third year of the CZO project included:

- Modeling study and seismic refraction survey of soil thickness around Redondo Mountain in the JRB to assess the role of aspect on soil thickness above bedrock.
- Terrestrial laser scans (ground-based LiDAR) measurements of post (Los Conchas) wildfire erosion in the JRB.
- Assessment of EEMT and aspect controls on fire severity.
- Quantifying the shapes of first-order valleys and its adjacent hillslopes undergoing steady headward growth.
- Development of a new method for distinguishing hillslopes from valleys in high resolution (e.g., LiDAR) digital elevation maps that enables drainage network extraction.
- Quantification of flood probabilities using NEXRAD radar data.

## *3. Findings in each of the JRB-SCM Science Themes.*

### 3.1 *Findings*: Ecohydrology and Hydrologic Partitioning (EHP) Theme

- **We have a better understanding of snowpack processes following severe forest canopy disturbance by fire.** Our work showed that despite increased new snowfall due to less interception in the burned forest, there was less peak snowpack following fire (**Fig. 5**). These results suggest that increased winter season sublimation due to increases in radiation or turbulence compensated for reduced interception. Our results have important implications for water availability following severe forest disturbance.

- **We have quantified how climate and topography interact to determine the stream chemistry of the catchments around Redondo.** The more solar exposed catchments are subject to much more variability in streamflow and hydrochemistry during years with smaller snowpacks. The results suggest that catchments around Redondo will vary in their susceptibility to climate change based on interactions between groundwater storage controlling baseflow and solar exposure controlling net snow water inputs.

- **Analysis of sap flux rate ($J_s$) within the Jemez River Basin – Santa Catalina Mountains Critical Zone Observatory (JRB – SCM CZ) in 2011 has revealed different environmental factors regulating the transpiration rate of co-occurring tree species at different times of the growing season.** In the Mixed Conifer zero order basin (MC ZOB) at Jemez, NM while soil temperature ($T_s$) ($R^2$ = 0.63, p< 0.05) at 10cm depth was the primary driver of the sap flux rate of fir during the snowmelt period (DOY 71 – 136), a combination of net radiation ($R_n$) and vapor pressure deficit ($D$) were weak regulators of the flux rate during the summer (DOY 137 – 181) and monsoon season (DOY 182 – 302). In case of spruce, $T_s$ at 10 cm depth ($R^2$ = 0.61, p<

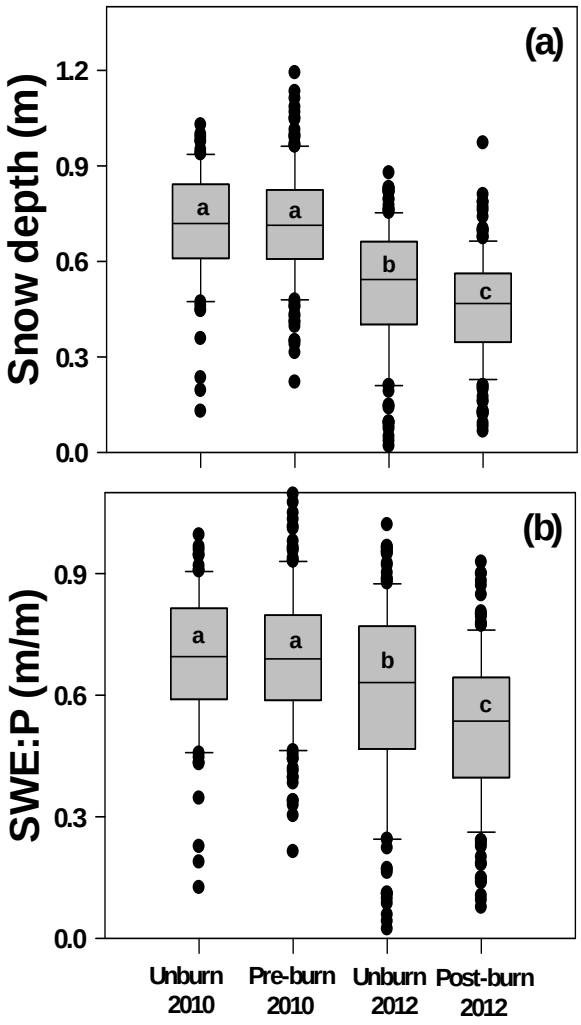


**Figure 5**. Snow surveys in 2012 demonstrate that the amount of snow depth (SWE is similar but not shown) and the fraction of winter precipitation in the snowpack at maximum accumulation are lower following fire, presumably due to increased sublimation from the snowpack surface once the canopy has been removed by fire (P. Brooks et al.).

0.05) and air temperature ($T_a$) ($R^2$ = 0.62, p< 0.05) were the dominant drivers of sap flux rate during the snowmelt period while $R_n$ ($R^2$ = 0.44, p< 0.05) was the dominant driver during the monsoon period.

- **Soil moisture at 10 ($R^2$ ~ 0.8, p< 0.05), 30 ($R^2$ ~ 0.85, p< 0.05) and 50 cm ($R^2$ ~ 0.83, p< 0.05) depths were the primary drivers of the sap flux rate for maple during the summer period** (DOY 114 – 181), the strength of the correlation at all three depths ($R^2$ ~ 0.2, p< 0.05) drastically reduced during the monsoon period (DOY 182 – 302). In case of evergreen white fir, soil moisture was weakly correlated ($R^2$ ~ 0.4, p< 0.05) with the flux rate during the summer and monsoon period.

- **We demonstrated that infiltration rates are higher next to a plant and decrease as distance from the plant increases (Fig. 6).** Even in the higher elevation ecosystems, infiltration rates tend to be higher in canopy patches than in intercanopy patches. However, important variations in these vegetation-infiltration relationships emerge along the elevation gradient.

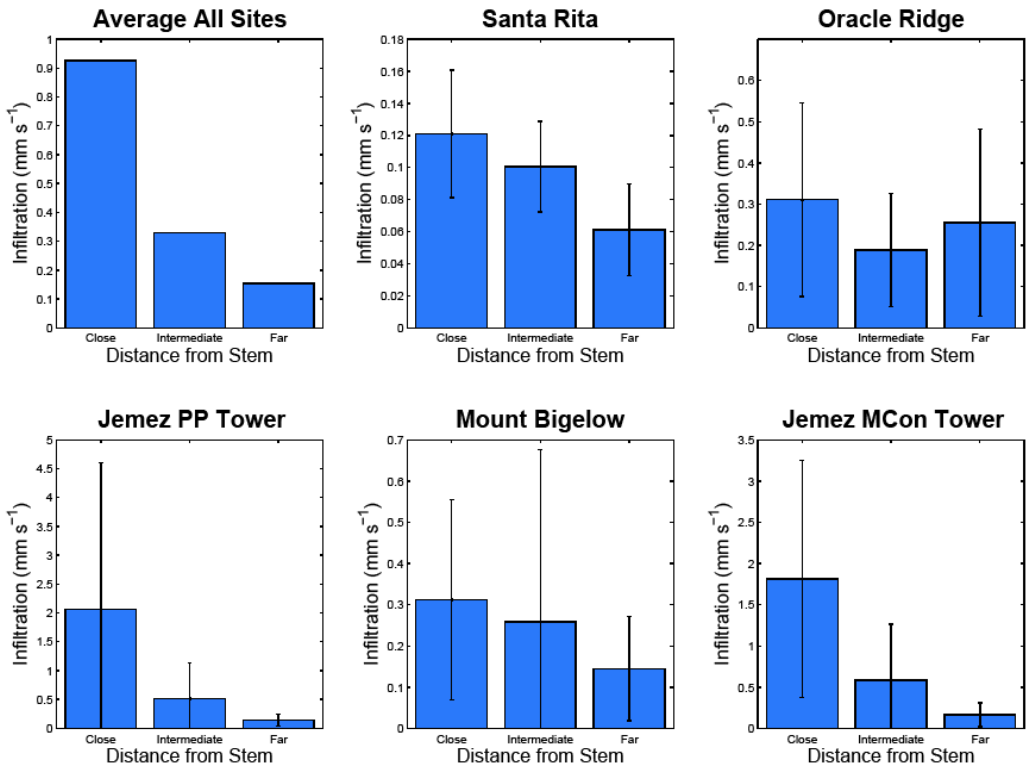


**Figure 6.** Variability in infiltration associated with distance from stem for sites across the elevation and climate gradient from SCM and JRB sites reveals a consistent pattern of high infiltration close to stems irrespective of ecosystem type (S. Papuga et al.).

- **In the LEO soils the wet albedo is significantly lower than dry albedo following a 10 mm wetting event for all three soil types.** The homogeneous dark LEO soil experiences the largest and most significant decrease in albedo following the wetting event. Decreases in albedo are thought to be due to the darkening of the soil following the wetting event. The LEO soil seems to darken more for the same amount of water (**Fig. 7**).

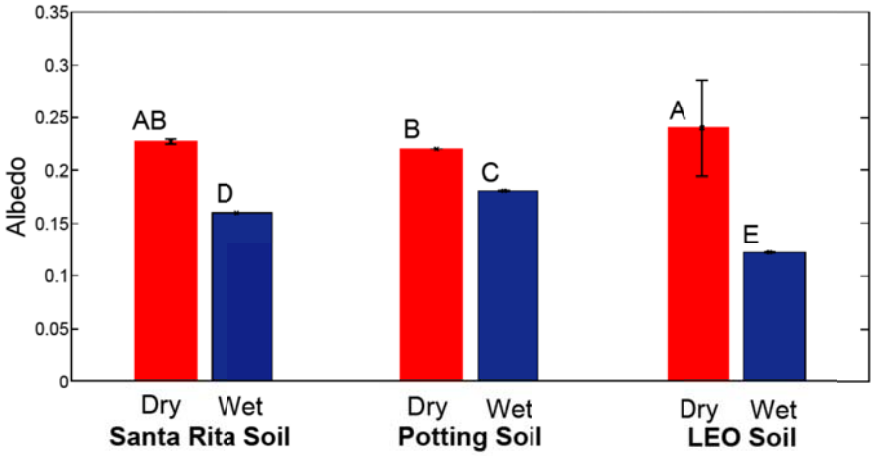


**Figure 7.** Change in albedo associated with wetting events in the Landscape Evolution Observatory soils (S. Papuga et al).

- **Our findings suggest that rates of evaporative water loss will not be strongly influenced by changes in length of snow season, but that $CO_2$ fluxes will be significantly influenced by these environmental changes such that we might expect greater carbon losses to the atmosphere.** Since July 2010, evaporation and soil respiration data have shown that (**Fig. 8**): (1) evaporation fluxes do not vary drastically between long and short snow season sites, (2) evaporation fluxes for both short and long snow seasons have a strong relationship with soil moisture and a poor relationship with soil temperature, (3) $CO_2$ fluxes vary noticeably between long and short snow season sites throughout the year, with short snow season fluxes typically higher than those of long snow season sites, and (4) $CO_2$ fluxes for short and long snow seasons have a strong relationship with soil temperature and a poor relationship with soil moisture

- **Evaporation dynamics generally followed precipitation dynamics at both short snow season (SSS) and long snow season (LSS) sites (Fig. 8)**. Evaporation was high in the summer with the onset of summer precipitation in both 2010 and 2011. However, in summer 2011, *E* was much lower than 2010, which is consistent with lower summer precipitation inputs in 2011 than 2010. Evaporation rates began to decline as soil temperatures declined, reaching minimum rates in December. A spring peak in *E* appeared to be associated with a combination of snowmelt, a small precipitation event in late February, and an increase in soil temperature. Overall, SSS sites tended to show slightly higher *E* rates than LSS sites, especially when *E* rates were at their maximums. However, the opposite was occasionally true (e.g. in 2010, DOY 188, 195, 253; in 2011, DOY 39, 130, 147, 193, 224).

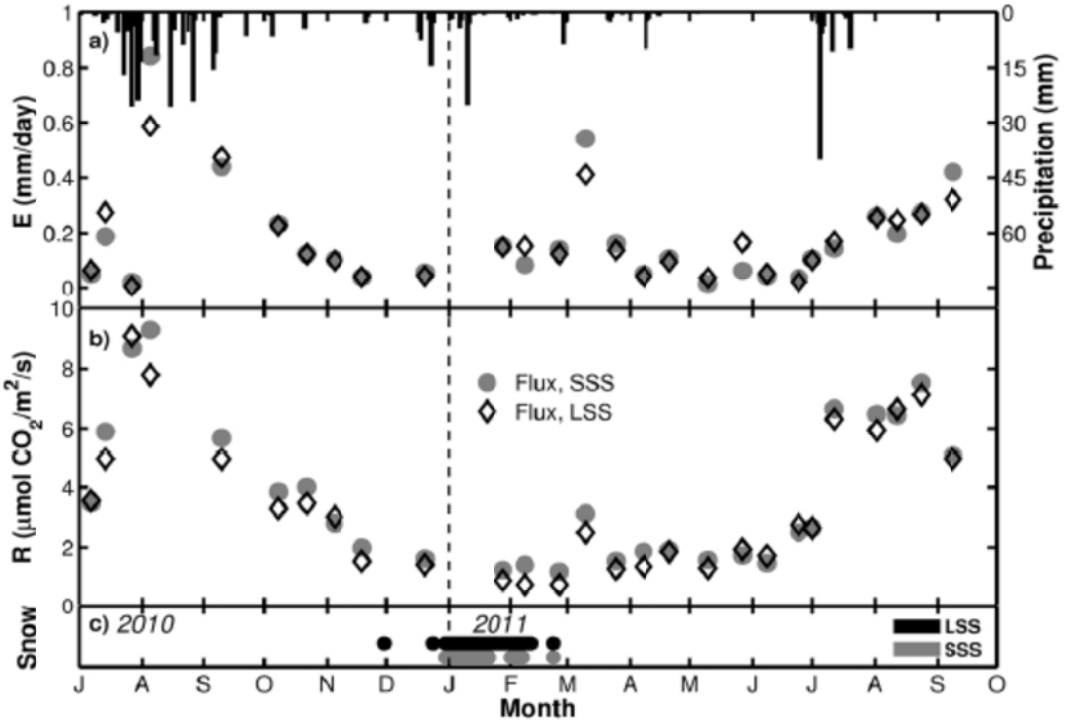


**Figure 8.** Time series of respiration and evaporation response to precipitation inputs from the SCM forest sites demonstrates pulsed nature of respiration in response to water inputs as either rain or snowmelt (Papuga et al).

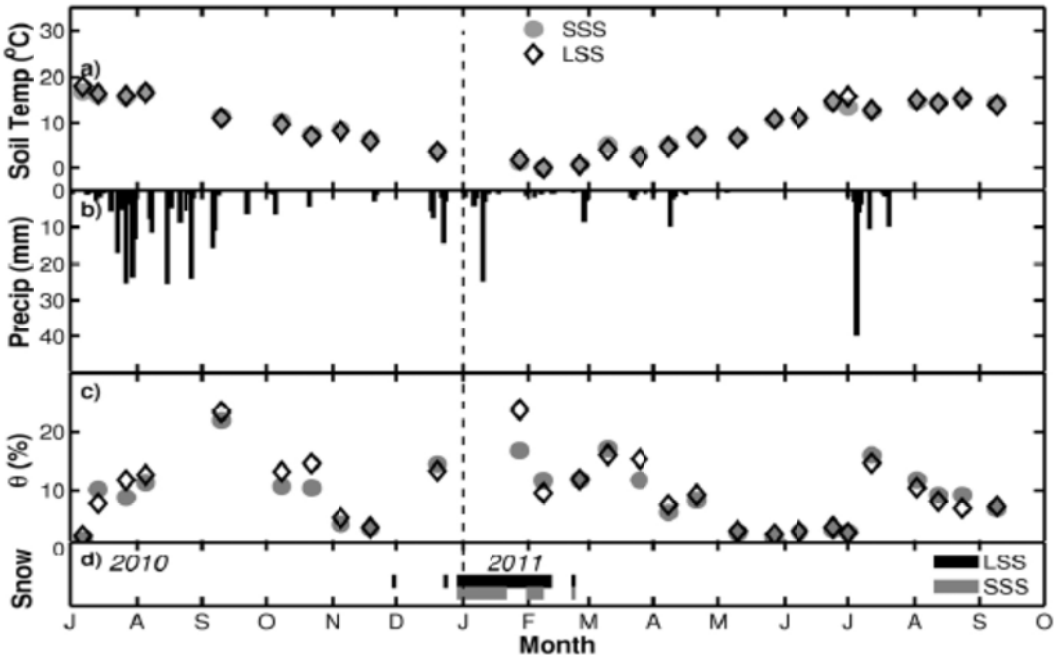


**Figure 9.** Time series of Temperature and soil moisture response to precipitation inputs in the SCM forest sites (Papuga et al.).

- **oil respiration dynamics were similar to *E* dynamics throughout the study period (Fig. 8), though we observed interesting advanced differences between the two fluxes.** Soil respiration was highest in the summer in both years, associated with the onset of summer precipitation and increased soil moisture. As opposed to *E*, however, the magnitude of *R* was not much lower in 2011 than in 2010 despite the difference in summer precipitation inputs between the years. Similar to the response seen for *E*, the summer increases in *R* happened quickly (over 1 month) but *R* decreased to the minimum values more slowly (over 3 months). Respiration also exhibited a small, quick peak in May 2011 shortly after snowmelt, but otherwise *R* remained low for the remainder of the spring and into the early summer. Throughout the study period, respiration rates at SSS sites were predominantly higher than at LSS sites, with only a few exceptions.

- **On an annual basis, *E* had almost identical values between SSS and LSS sites (48.4 and 47.7 mm, respectively), which accounted for approximately 20% of the total precipitation for that time.** Additionally, *E* between SSS and LSS sites tended to be almost identical except during the spring, when SSS sites had higher *E* rates for about 3 months (**Fig. 8**). At the end of this time, however, LSS fluxes increased while SSS fluxes leveled off, resulting in almost matching values once again. Contrary to the *E* results, cumulative *R* shows a notable difference between SSS and LSS sites throughout the course of the year. The difference between the SSS and LSS fluxes increased slightly through the spring and summer, then decreased slightly in the spring, but SSS sites saw consistently higher values. By the end of the water year, SSS sites had released 3782 $g/m^2$ of $CO_2$, while LSS sites had only released 3440 $g/m^2$ of $CO_2$.

- **The relationship between *R* and *E* was strong for both SSS and LSS sites (Fig. 10). However, LSS sites had a higher *WUEsoil* than SSS sites, i.e. the slope of regression between *R* and *E* was significantly greater for LSS sites than for SSS sites ( $p<0.01$).** Interestingly, SSS sites had higher *WUEsoil* when soil moisture was low than LSS sites ($p<0.01$), suggesting that SSS sites became more efficient at carbon loss (i.e. used less water for their carbon release) as the soil dried than LSS sites. While not as strong as for soil moisture, the case was similar for soil temperature: SSS sites had slightly higher *WUEsoil* than LSS sites when soil temperature was high, though this was not statistically significant ($p>=0.1$). This suggests that SSS sites became slightly more efficient at carbon loss as the soil warmed than LSS sites.

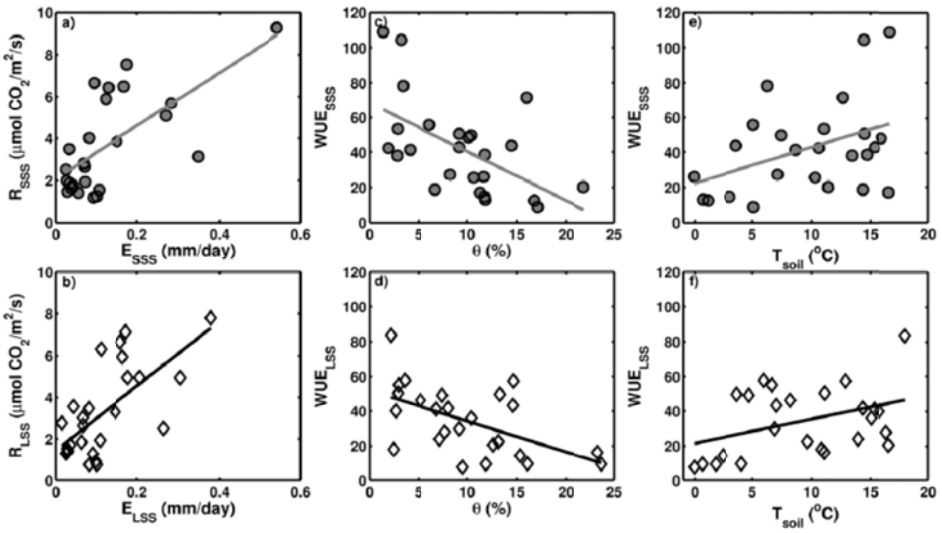


**Figure 10**. Relationships between soil moisture, temperature, evaporation, and water use efficiency, and respiration in SCM forested sites (Papuga et al.).

- **Differences in water use strategy were observed between fir and spruce at the JRB MC ZOB (Fig. 11).** In April and May, fir had a higher flux rate than spruce which corresponded to the snow melt period even though from June onwards, overall diurnal flux rates of both fir and spruce were nearly equal but higher in magnitude. In contrast, at the Schist ZOB site of the SCM, growing season duration significantly influenced the difference in the water use strategy between evergreen white fir and deciduous maple (**Fig. 12**). White fir had higher sap flux rate than maple in April which corresponded to the time period when maple was leafless. From June onwards, flux rate of maple was significantly higher than white fir which corresponded to the leaf expansion stage. Unlike maple, while fir was conservative with regard to water use. Diurnal flux rates of both the species were however nearly equal in October which corresponded to the period leaves of maple had started to senesce.

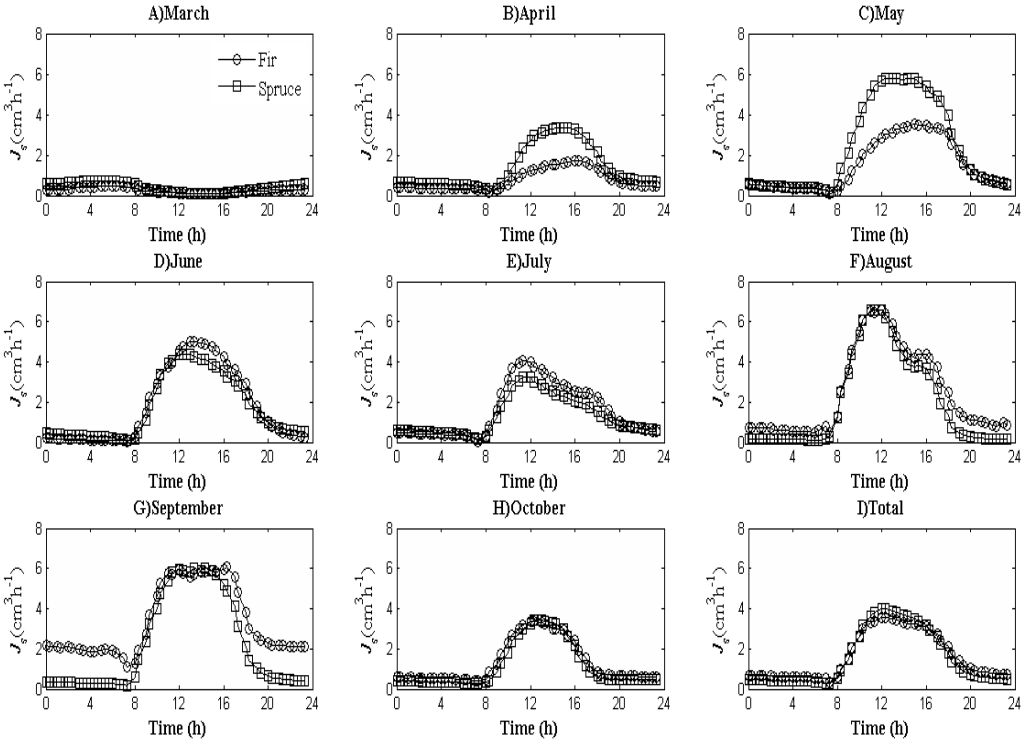


**Figure 11.** Average diurnal sap flow rate ($J_s$) of fir and spruce for each month for 2011 as well as the average diurnal pattern for the study period in MC ZOB, JRB (Total (DOY 71 – 302)) (Papuga et al.).

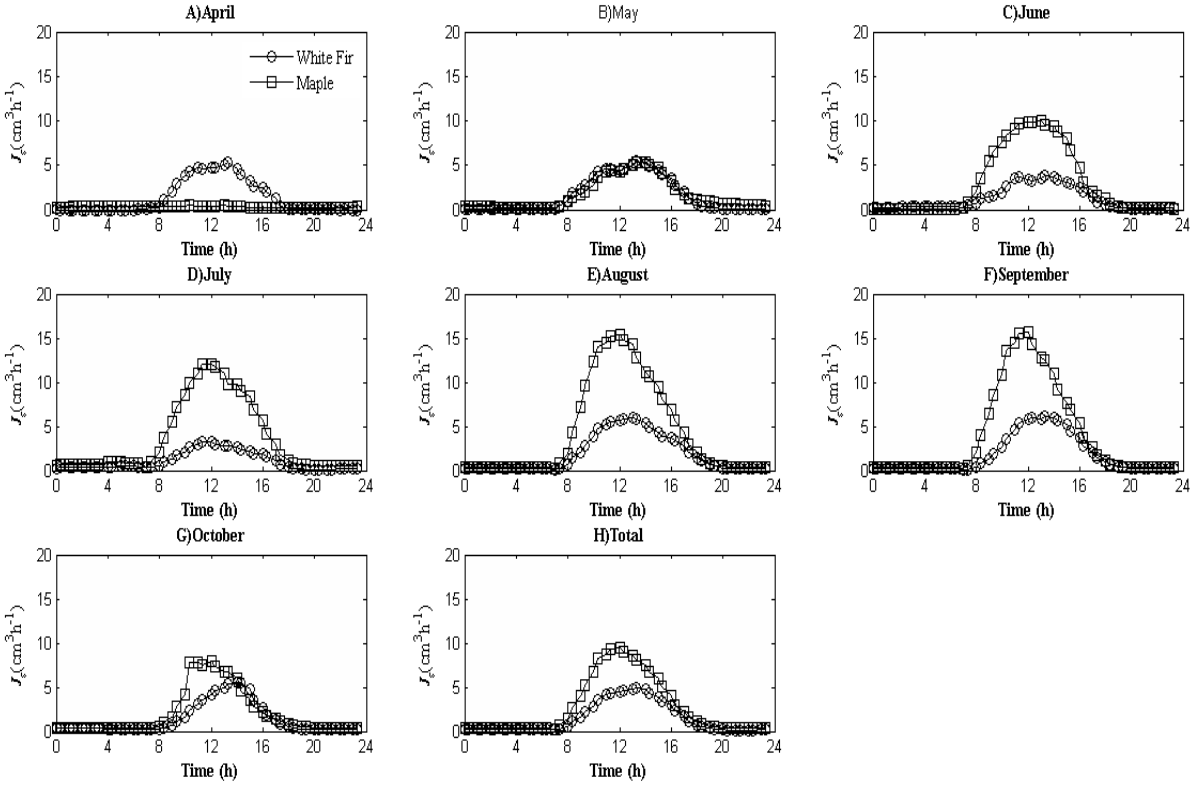


**Figure 12**. Average diurnal sap flow rate ($J_s$) of white fir and maple for each month for 2011 as well as the average diurnal pattern for the entire year (Schist site ZOB, SCM) (Papuga et al.).

- **Two years of distributed soil respiration measurements demonstrated that soil moisture was a stronger control on soil $CO_2$ fluxes than temperature in forested, seasonally snow covered sites in both SCM and JRB.** This was true both for winter and summer fluxes, and perhaps most interestingly, respiration rates were always higher in schist derived soils than granitic soils, presumably due to the greater water holding capacity of the fine grained schist soils that remained significantly wetter over the course of the study (**Fig. 13**).

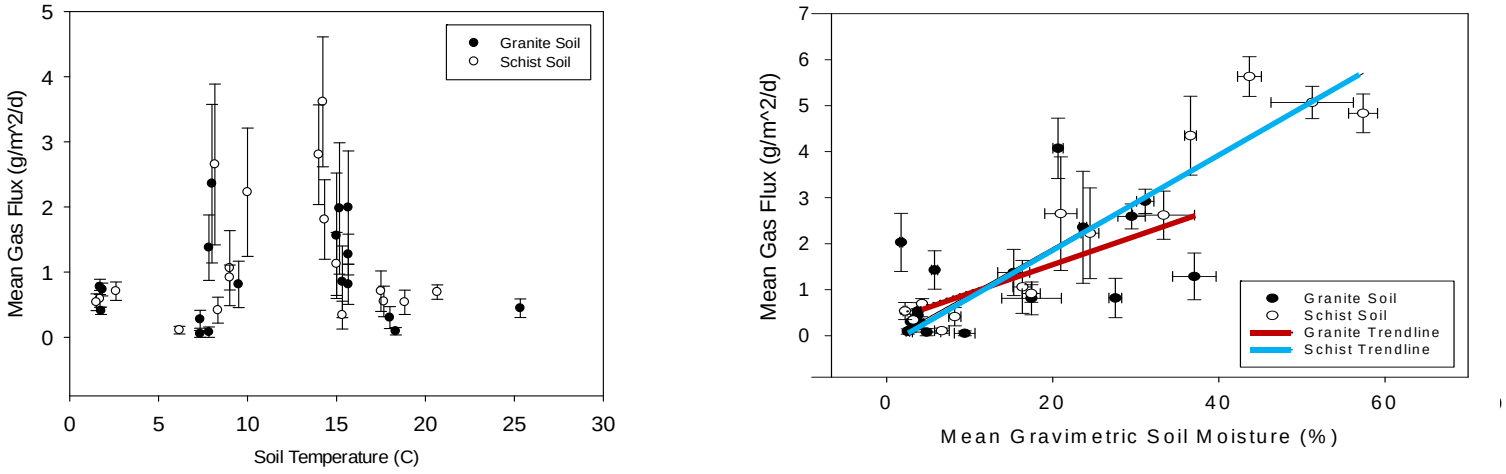


**Figure 13**. Relationship between soil temperature and mean gas flux for fine schist soils and coarse granitic soils during the growing season demonstrates that maximum fluxes occur at intermediate temperatures (top). The relationship between soil temperature and mean gas flux for fine schist and coarse granitic soils during the growing season indicates that moisture is a better predictor for respiration than temperature in these mixed forest sites (Stielstra et al.).

- **Rates of transpirational water loss (*E*) and net photosynthesis (*A*) were species specific and varied significantly in response to available moisture (Fig. 14-15).** All species had higher *E* rates during the wet monsoon than the dry pre-monsoon. *P. menziesiii* maintained low rates of *E* during the dry pre-monsoon, yielding the greatest *WUE* (**Fig. 14**). However, once the soil water was more consistently available during the monsoon, *E* rates increased 4.5 fold, decreasing water use efficiency (*WUE*). Other *Pinus* species experienced marked increases in *E*, but *WUE* remained unchanged, indicating that increases in rates of water loss were tightly coupled with increased photosynthetic uptake (**Fig. 15**).

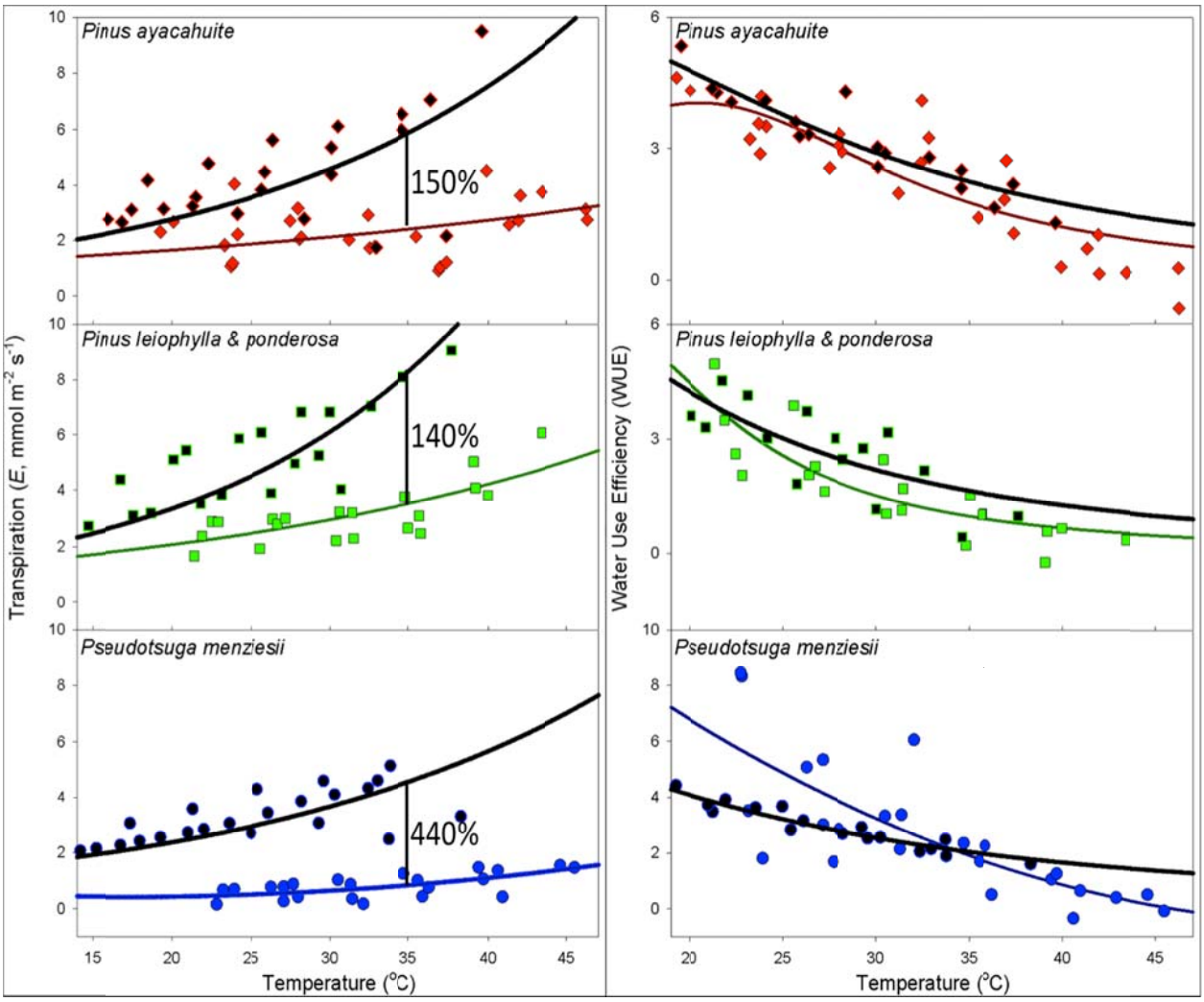


**Figure 14**. Leaf-level rates of transpirational water loss (left panels) and the resulting water use efficiency (photosynthesis/transpiration; right panels) within the dry pre-monsoon (light lines) and wet monsoon (dark lines) (Bigelow Tower, SCM) (Barron-Gafford et al.).

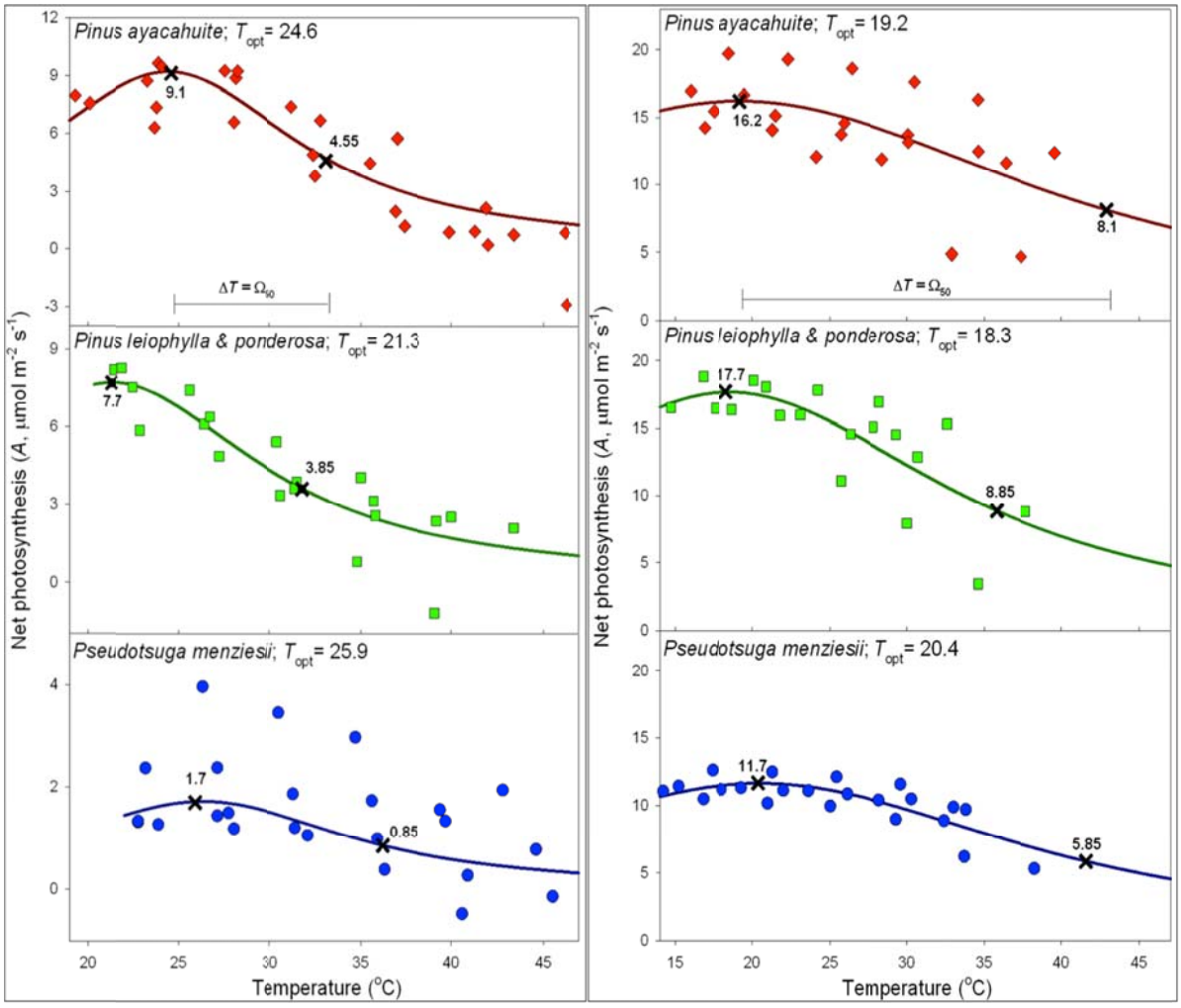


**Figure 15.** Rates of leaf level photosynthesis (*A*) among dominant, overstory species across a range of measurement temperatures within the dry pre-monsoon (left panels) and wet monsoon (right panels). We used a measure of the range of temperatures across which a plant could conduct rates of *A* at 50% of maximum ($\Omega_{50}$) as a metric of thermal sensitivity. The numbers indicated within each plot highlight the peak *A* and the point along each temperature response curve when rates dropped below 50% of this peak; the range of temperatures between these points constitute the $\Omega_{50}$ for that species during that season (Barron-Gafford et al.).

- **Both eddy covariance measurements and remotely sensed products can provide ecosystem-scale estimates of trace gas and energy flux, and the contribution of the understory to these estimates appears significant (Fig. 16).** We use three years of eddy covariance data from two similar subalpine mixed-conifer ecosystems within the Jemez River Basin – Santa Catalina Mountain Critical Zone Observatory (JRB-SCM CZO). The mixed-conifer site at the JRB is at roughly 3000 m and has substantial understory, while the mixed-conifer ecosystem of the SCM is at roughly 2500 m has very minimal understory. Within the footprint of the eddy covariance towers at both sites, three time-lapse digital cameras (phenocams) take hourly images of the understory from which a greenness index (Ig) is calculated. We show that daily NEE- and Ig are generally synchronized, suggesting that the understory may substantially contribute to ecosystem-

scale carbon uptake. However, while remotely-sensed vegetation indices and Ig are synched at certain times throughout the study period, often they are not. For instance, in 2010 NDVI remains higher for a longer period than does Ig. This suggests that relying solely on remotely-sensed products may lead to an overestimation of carbon sequestration by these ecosystems. We argue the contribution of the understory to ecosystem-scale carbon, water, and energy exchange with the atmosphere is important and therefore critical to understanding how climate change will alter their feedback with the climate system.

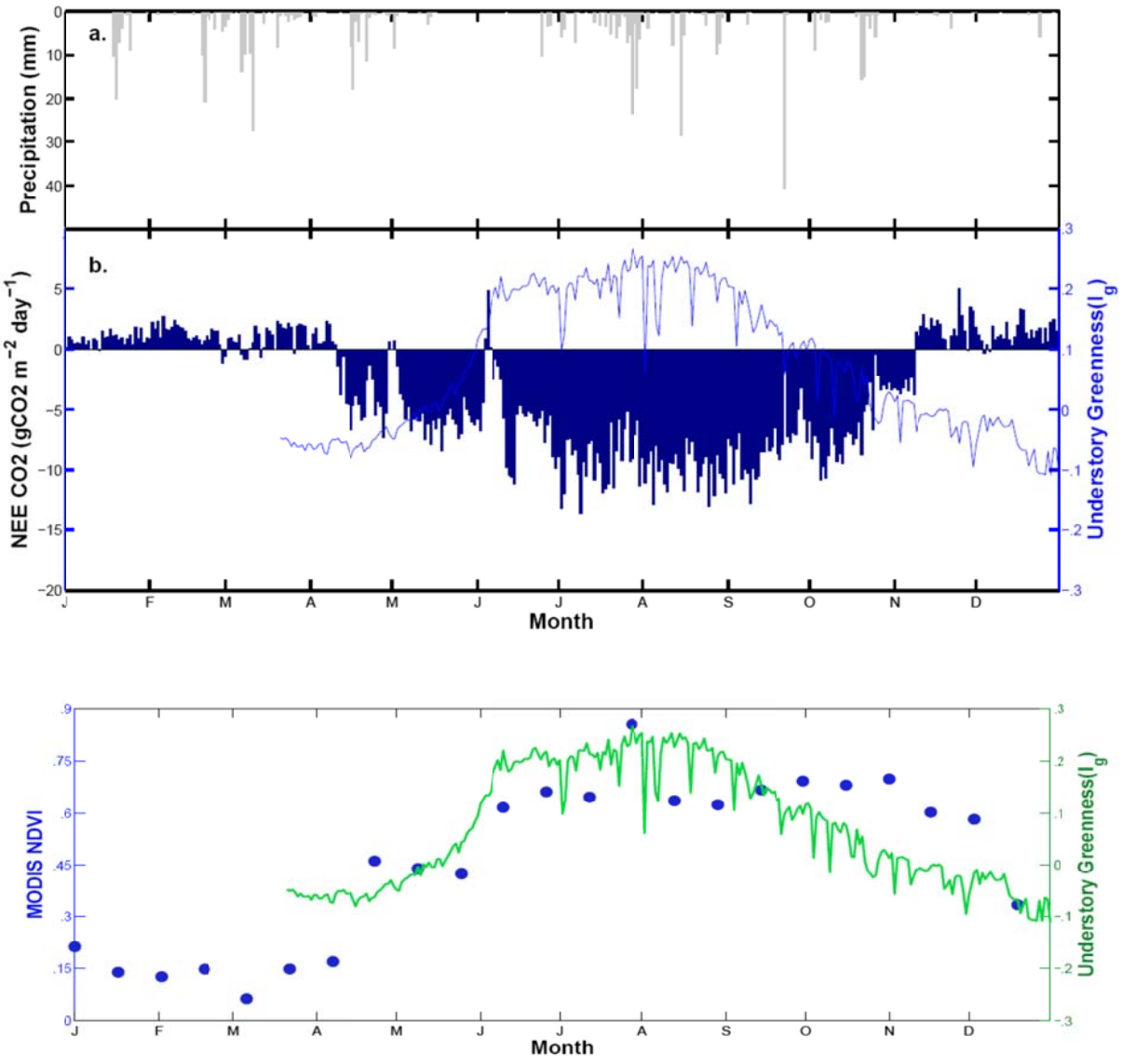


**Figure 16**. Relationships between tower derived NEE and understory greenness (top) and MODIS NDVI and understory greenness (bottom) show close correspondence between remotely sensed imagery, understory growth, and tower NEE (MC tower JRB) (Barron-Gafford et al.).

## 3.2 *Findings*: Subsurface Biogeochemistry (SSB) Theme

- **Soil nitrogen ammonium pools were significantly elevated in high intensity burn sites relative to controls, and patterns differed for mixed conifer, aspen, and ponderosa pine (Fig. 17).** Nitrate pools were low initially and have increased with increased rates of nitrification over time.

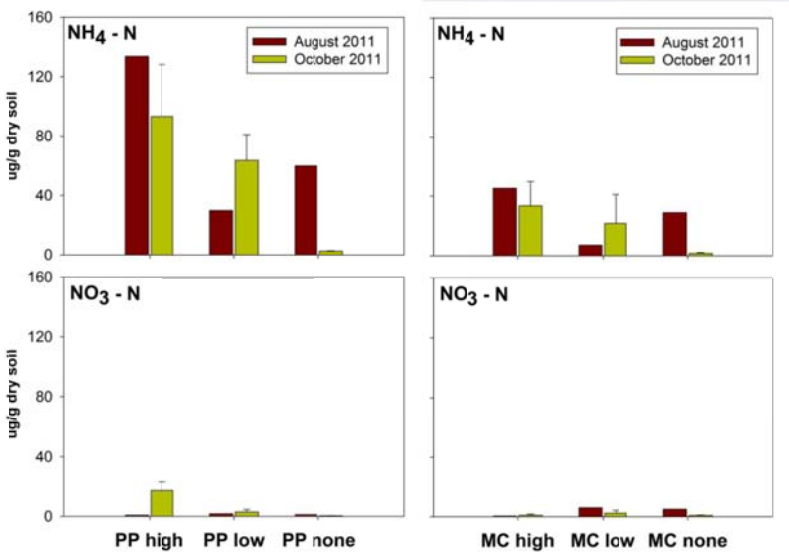


**Figure 17.** $NH_4^+$ pools were substantially higher in the Ponderosa Pine (PP) compared to Mixed Conifer (MC) forest soils, and $NH_4^+$ and $NO_3^-$ pools tended to decrease with burn intensity. $NH_4^+$ pools decreased from three weeks to three months after the burn whereas $NO_3^-$ pools increased in PP and decreased in MC forest soils (K. Lohse et al.).

- **Strong moisture controls were apparent in the burned ZOB with lower toe-slope position having higher rates of mineralization and nitrification and thus nitrate pools compared to backslope positions.**

- **Preliminary sequencing results show striking contrasts in microbial diversity as a function of burn intensity but also vegetation type.**

- **Fire severity strongly affected aqueous soil extracts (ASEs) in recently burned areas in the JRB.** The ASE from severely burned areas indicated that DOC concentrations increased with depth and DIC concentrations (highest in surface horizon) decreased with depth (**Fig. 18**). PARAFAC analyses of fluorescence spectra showed a decrease in fluorescence attributable to reduced quinone-like constituents coupled to an increase of oxidized quinone-like fluorescence in the severely burned upper portion of the pedon. This signature was translated into the streams as well.

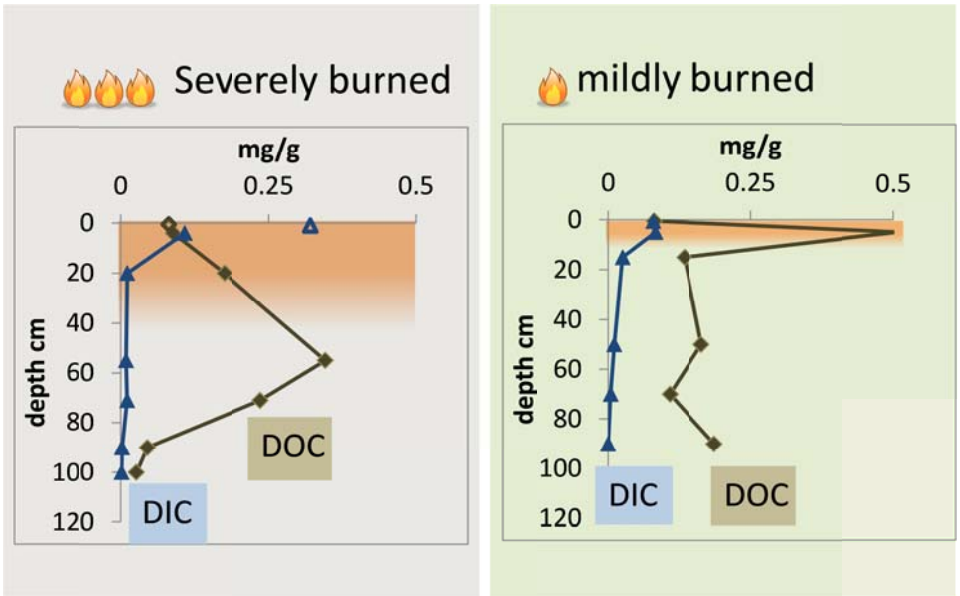


**Figure 18.** Aqueous soil extracts (ASE) from severely burned soils show decreased amount of water extractable organic matter (WEOM) but increased DIC. Mildly burned soil ASE show burn effect only in upper cm of the profile (J. Perdrial et al.).

- **The suitability of capillary wick samplers for quantifying DOM and weathering fluxes was assessed by experiment.** It was determined that PCap's using fiberglass wicks are suitable for DOM sampling. Wicks do not sorb, release or fractionate DOM when sampling (**Fig. 19**). Thus PCap samples can be assumed to yield representative mobile DOM samples (no soil physical changes during installation assumed) (Perdrial et al., 2012).

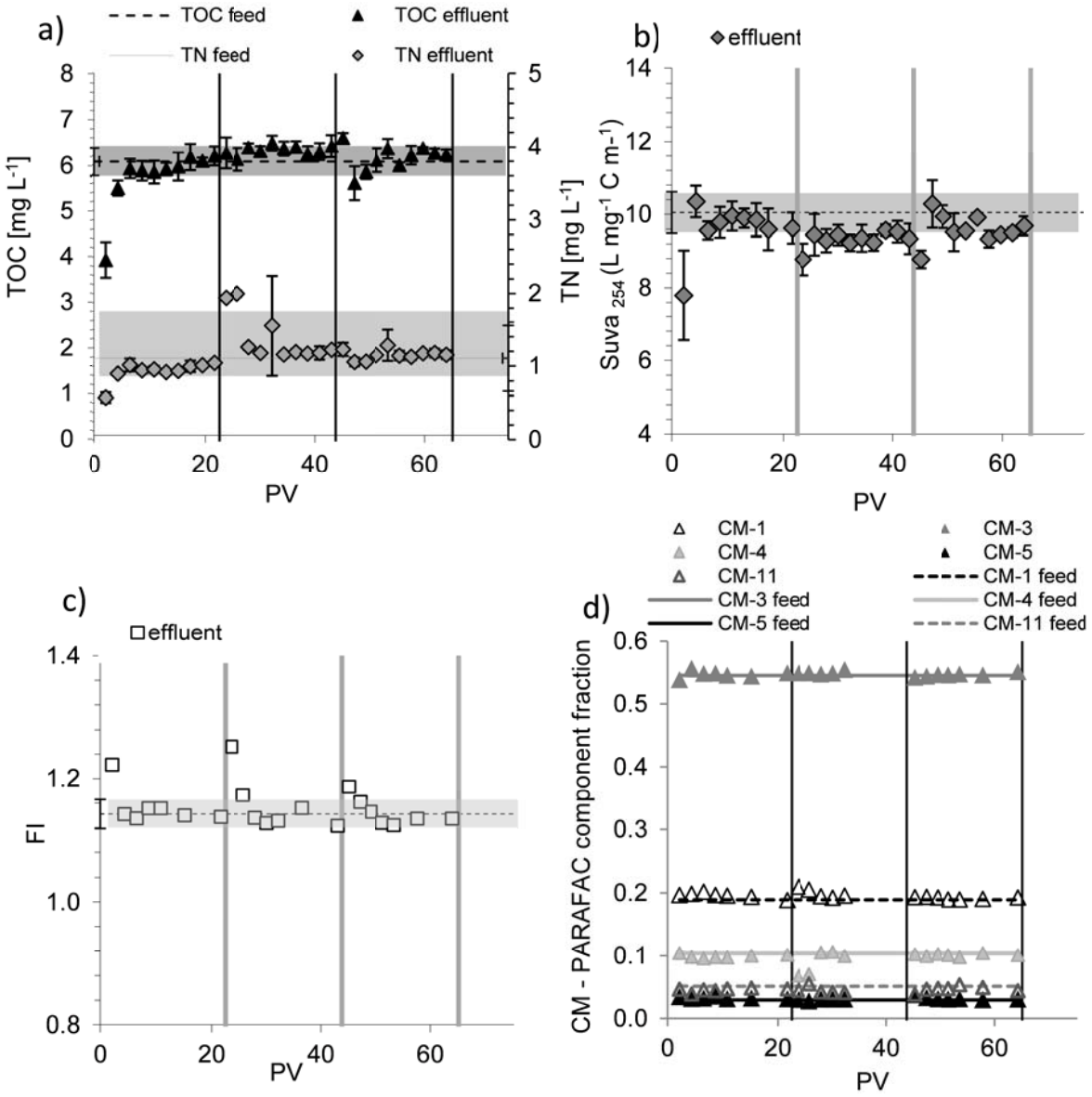


**Figure 19.** Results of DOM solution-wick interaction experiment. Feed and effluent values for a) TOC and TN, b) SUVA254, c) fluorescence index (FI) and d) PARAFAC component abundances. Mean values of feed solutions are indicated by dotted horizontal lines and respective standard deviations are highlighted in grey. Vertical lines indicate 24 h of stop flow (J. Perdrial et al.).

- **The impact of PCaps on solution chemistry measurements was quantified by laboratrory experiment** to evaluate their utility in CZ studies, and to assess their suitability for use in

quantifying weathering fluxes. Our results indicate that fiberglass wicks release to varying extent (via glass dissolution) DIC, and some major cations (Si, Na, Mg, and Ca), but for many metals, including Fe and Mn as well as all rare earth elements (REE's), the PCaps appear very suitable with limited sorption or release. Sr and Ba are strongly sorbed (or exchanged for Ca). Boron (also released from wicks) can be used to back out released amount of Si based on an empirical relationship (**Fig. 20**).

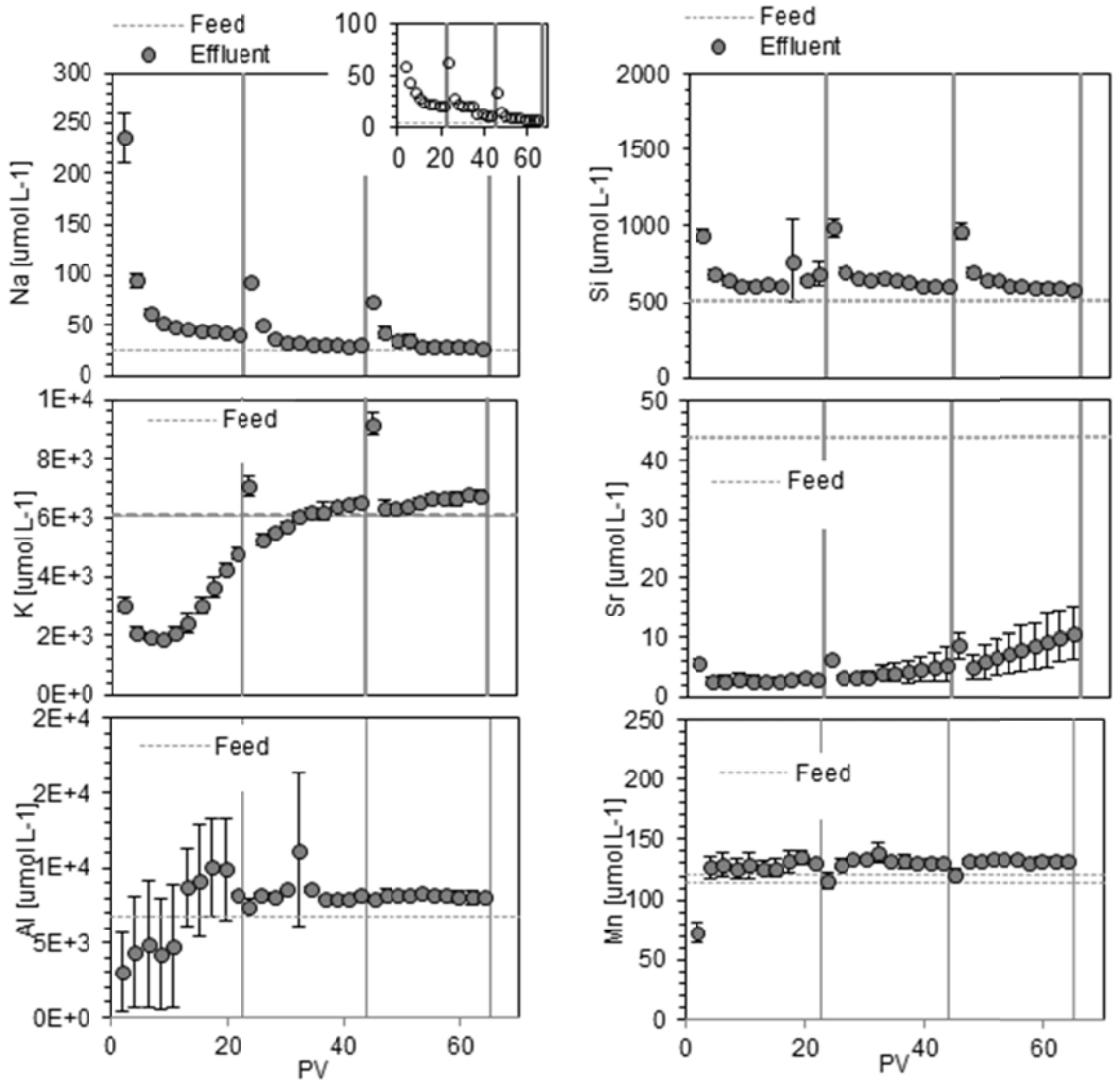


**Figure 20**. Experimental data demonstrate the suitability of PCaps for quantifying weathering fluxes. Na and Si are released, K and Sr sorbed by the wicks. Most metals are unaffected by the presence of wicks (J. Perdrial et al.).

- **Rare earth elements (REE) are potential tracers of biogeochemical weathering across scales during snowmelt in the JRB.** Time series of REE patterns in precipitation, soil pore water, ground water, and stream water are related to REE composition of contributing soil, rock and atmospheric dust.

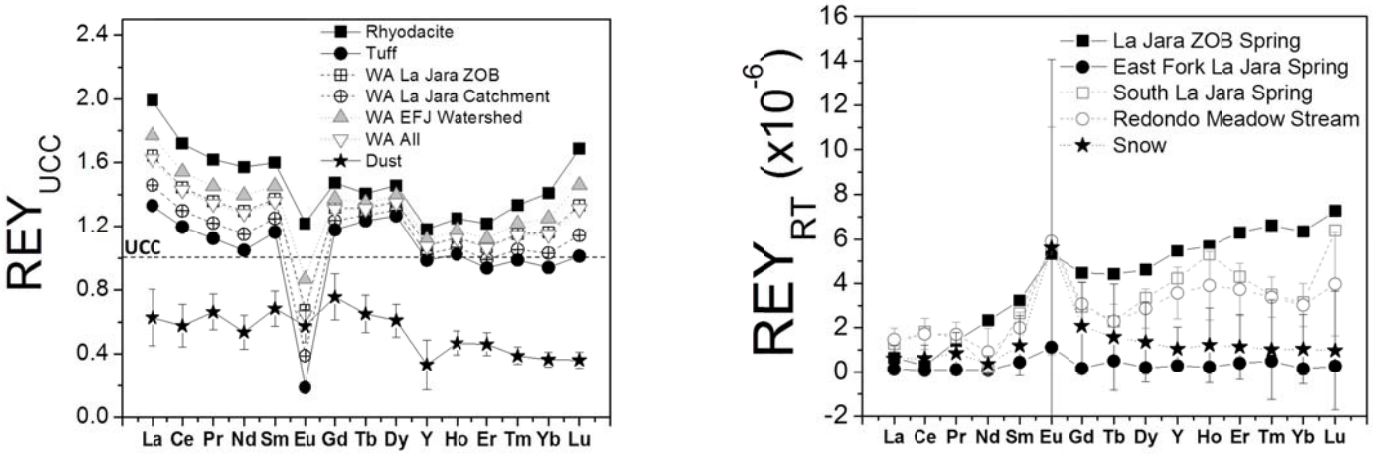


**Figure 21.** Mean rare earth element (and yttrium) patterns in parent materials (left) and aqueous solutions (right) in several Jemez River Basin sites where weathering studies are underway (A. Vazquez-Ortega et al.).

- **Rare earth element (REE) and dissolved organic carbon concentrations (DOC) were positively correlated during snowmelt, consistent with REE complexation and mobilization in association with organic ligands during the period of shallow subsurface flow.** Most annual (bio)chemical denudation of REE occurs during the snowmelt-derived DOC pulse.

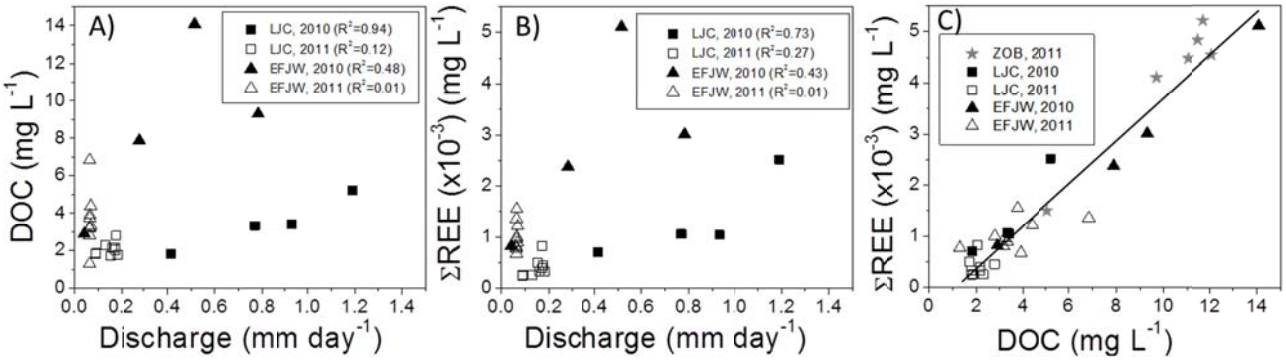


**Figure 22.** Comparison between (A) discharge versus DOC, (B) discharge versus ∑REE, and (C) DOC versus ∑REE for surface waters at the outlet of the La Jara MC ZOB, La Jara catchment, and EFJ watershed during the snowmelt period for water years 2010 and 2011. The coefficient of determination ($R^2$) for the entire data set presented in part C is 0.94. REE are in mg $L^{-1}$. (A. Vazquez-Ortega et al.)

- **The climate gradient on granitic lithology of the SCM is being used to understand how climate and landscape structure control soil chemical denudation, mineral transformation, and its coupling to short and long-term soil carbon sequestration across a wide range of ecosystems in the southwestern United States (Fig. 23a).** Soil profiles were sampled from divergent-convergent landscape unit pairs within five vegetation communities ranging from desert scrub to mixed conifer forest (**Fig. 23b**). In total, 130 soil and rock samples were collected in convergent-divergent landscape unit pairs from north-facing zero order catchments for a total of 4 soil pedons per ecosystem.

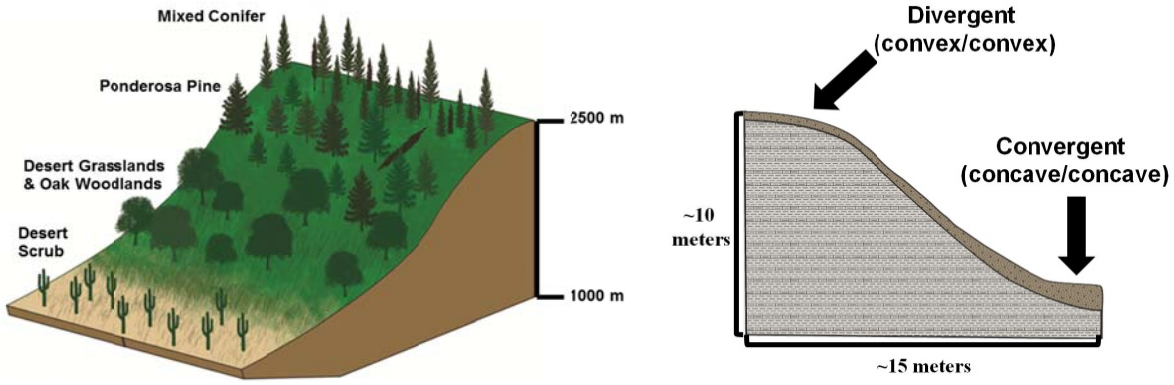


**Figure 23.** a) General broad scale depiction of vegetation zones encompassing the environmental gradient of the Santa Catalina Mountains, Arizona and b) Local scale representation of divergent and convergent landscape positions sampled in the current study (R. Lybrand et al.).

Soil primary and secondary mineral compositions were determined using electron microprobe, and quantitative and semi-quantitative x-ray diffraction (XRD). Quartz/Plagioclase (Q/P) ratios, used as a proxy of chemical weathering in bulk soils, were lowest in desert scrub and higher in mixed conifer systems, consistent with increased chemical weathering at high elevation sites (**Fig. 24**). Secondary mineral assemblage of desert scrub and grassland sites was dominated by smectite and partially dehydrated halloysite whereas vermiculite, chlorite and kaolinite were predominate in the mixed conifer systems (**Fig. 25**).

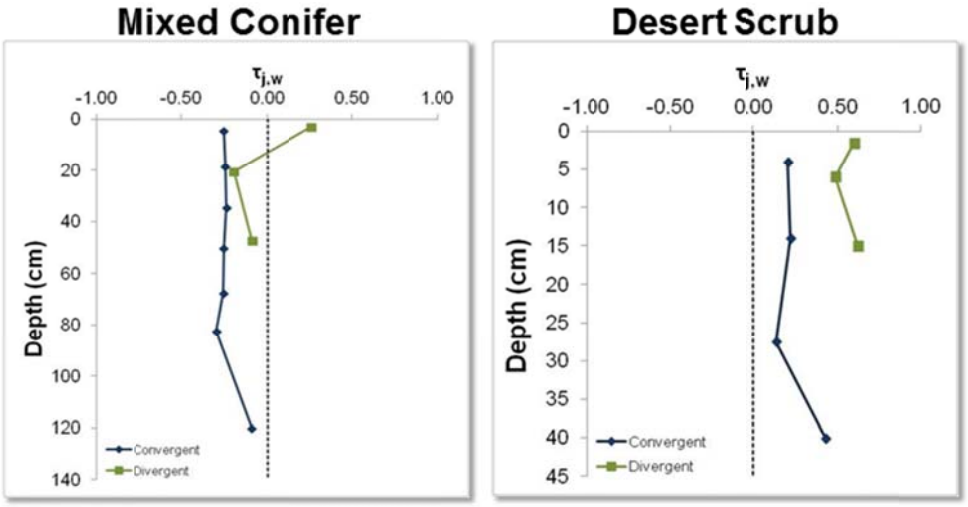


**Figure 24.** a) Quartz/Plagioclase ratios for convergent and divergent landscape positions in the a) the Mixed Conifer and b) Desert Scrub ecosystems in the SCM CZO (R. Lybrand et al.).

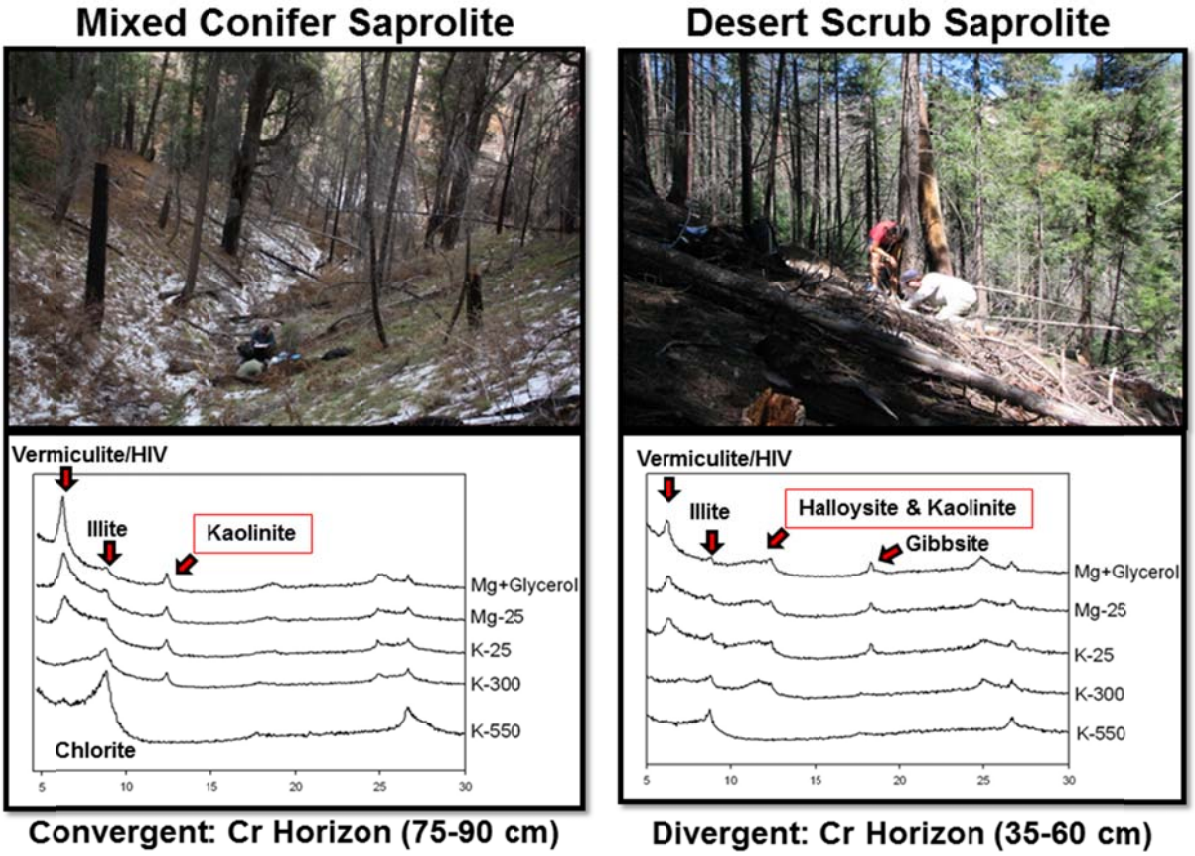


**Figure 25.** Multi-treatment X-ray diffraction patterns of the clay fraction were used to assess secondary mineral compositions for saprolite samples from the a) mixed conifer and b) desert scrub ecosystems in the SCM-CZO (R. Lybrand et al.).

- **Bulk elemental chemistry, including major, minor, and trace elemental constituents, was determined by x-ray fluorescence (XRF) for all samples and microscale weathering patterns were quantified using electron microprobe analyses.** From these data, elemental mass-transfer percentages were calculated and normalized to the parent rock materials using Na and Zr as mobile and immobile elements, respectively. Chemical depletions of Na, a proxy for plagioclase feldspar weathering, were observed in both the desert scrub and mixed conifer ecosystems. Electron microprobe analyses of surface and subsurface soils at the mixed conifer site revealed a significant decrease in Na mass percent from the unaltered regions of the grains (Na of ~7-8%) to fully transformed areas of the grains (Na of ~0.2-0.3%) located in joint fractures and at grain edges. In contrast, electron microprobe analyses of desert scrub soils indicated incomplete mineral transformation where Na mass percent spanned ~7% in un-altered grain centers to ~4% in grain fractures and edges. Backscattered electron (BSE) images support these patterns where more completely transformed minerals were observed in the mixed conifer soils compared to incomplete transformations in soils at the desert scrub site (**Fig. 26**).

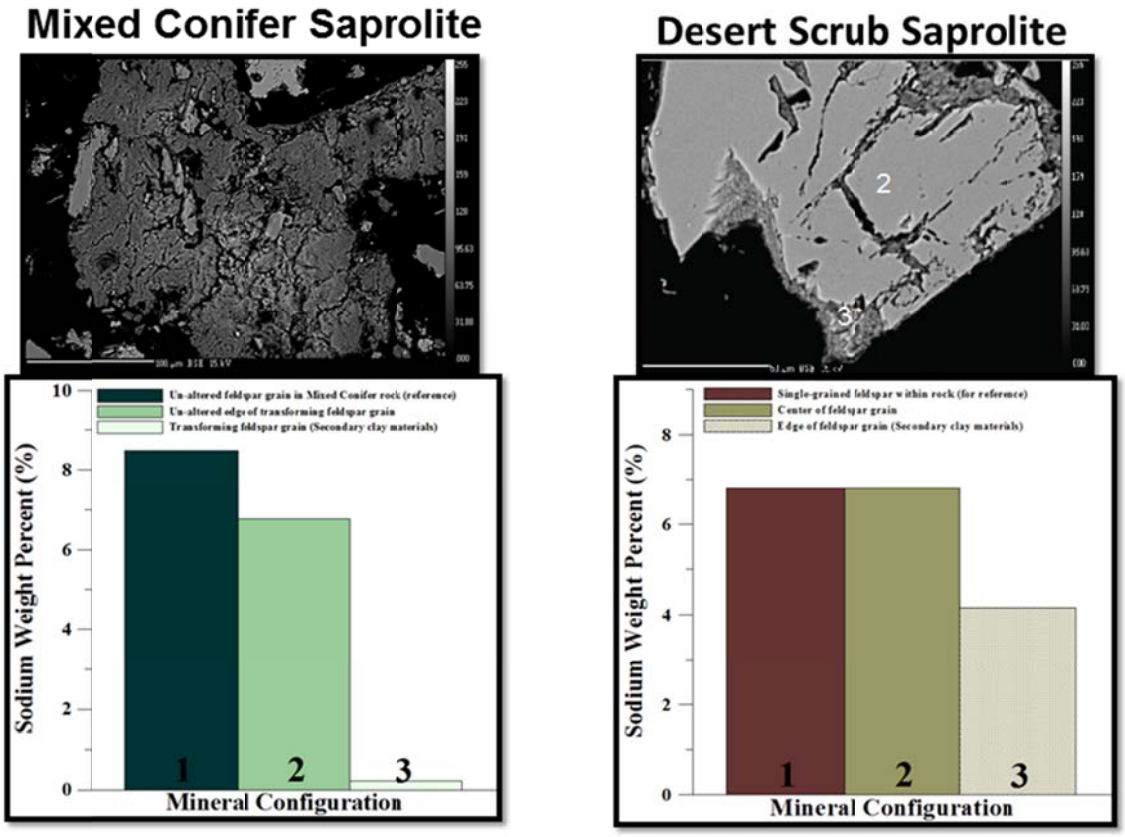


**Figure 26.** Backscattered electron images and sodium elemental loss plots for reference rocks, un-altered feldspar grains, and transformed feldspar grains containing secondary clay materials for the a) mixed conifer and b) desert scrub saprolite samples (R. Lybrand et al.)

• **Climate and landscape position affect soil organic carbon distribution and its mean residence time. Soil incubation experiments quantified the potentially mineralizable carbon fraction in fresh surface soils from the SCM-CZO.** Soil C, stable C isotopes and soil respiration data show that differences exist in total C stock and its susceptibility to microbial degradation across the gradient. Variation in short-term C turnover times however need to be coupled with measures of physical C partitioning in the soil matrix and long-term carbon constraint of C-cycling using radiocarbon analysis. SOC distribution is being examined using density and aggregate separations to obtain the free, occluded and mineral soil C pools for convergent and divergent surface and subsurface soils at the Desert Scrub, Mid-Ponderosa Pine and Mixed Conifer SCM-CZO sites (**Fig. 27**).

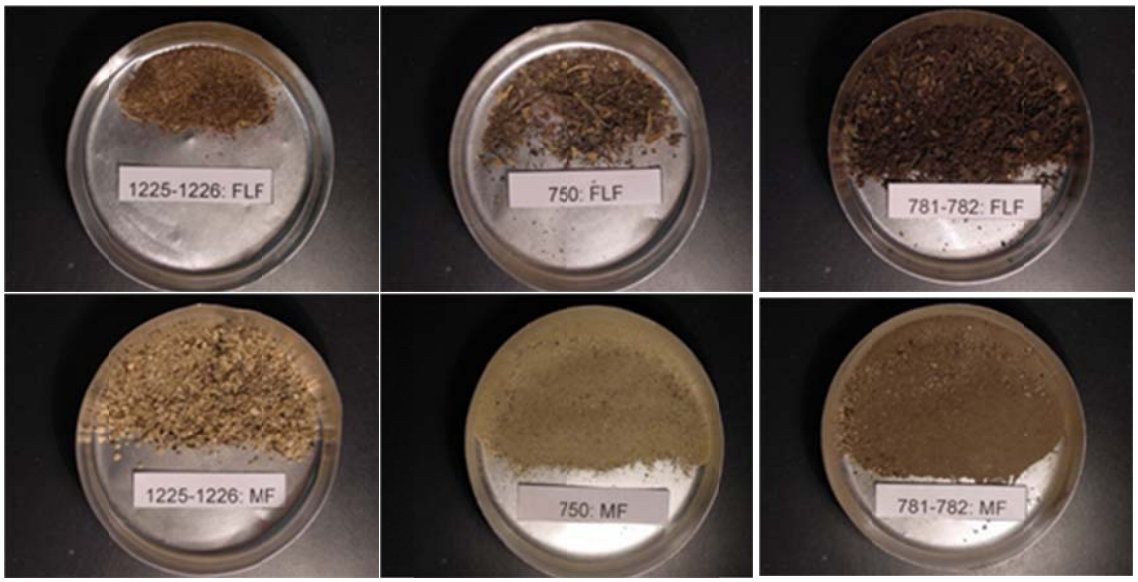


**Figure 27**. Photographs of the free light fraction (FLF) and mineral fractions (MF) for surface soils from the a) Desert Scrub, b) Mid-Ponderosa-Pine and c) Mixed Conifer ecosystems (Rasmussen et al.).

• **It was determined through multiple iterations that input layers of soil depth, slope, solar radiation, wetness index, NDVI and NAIP bands 3/2 are the variables needed to capture 95% of the landscape soil variability of the Marshall Gulch catchment.** A stratified random model was then used to determine optimal sampling locations. At each of 20 sample sites a soil pit was dug to refusal (paralithic contact) described and sampled according to genetic horizon (**Fig. 28**). Catchment soil depth was found to be highly variable, with shallow soils (32-45 cm) on the ridges and steep slopes, and deeper soils (72-111 cm) in open swale areas that have higher frequency of water flow and saturation. Samples were analyzed for bulk chemistry (XRF), bulk mineralogy (XRD), particle size, color, pH, EC, loss on ignition (LOI) to characterize chemical and physical properties. By quantifying chemical denudation and mineralogical variability of the collected soils, we establish a proxy for regolith weathering both on the profile scale ($1m^2$) as well as the catchment scale ($50k\ m^2$).

• **For three selected profiles, samples from surface to bedrock were incubated. Stepwise multiple linear regression indicated that soil C mineralization and k values were correlated with slope and topographic wetness index, and slope and vegetation cover, respectively (Fig. 29).** Biosphere 2 REU

student, Chase Martin, conducted a study of catchment-scale carbon mineralization in SCM-CZO soils as a function of depth for selected pedons by coupling extensive field sampling with laboratory incubations. The upper 20 cm of the A horizons of 20 soil profiles were incubated at 60% water holding capacity and 20° C for 35 d. Using these models to interpolate mineralization parameters across the catchment indicated the greatest C mineralization occurring on the steep slopes and minor drainages of the basin. In contrast, the highest k-values were found on the ridgelines and southern aspects of the catchment (**Fig. 29**).

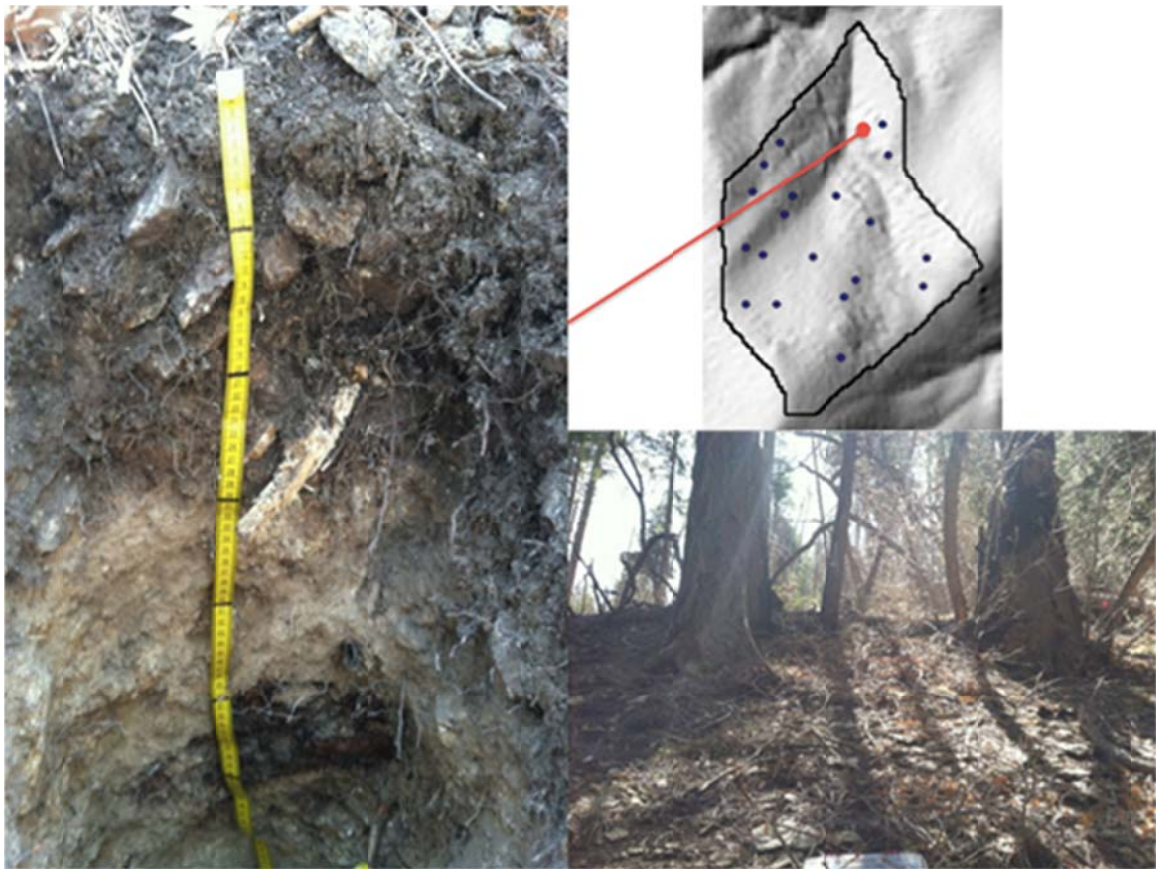

**Figure 28.** Final 20 sample locations in the granite mixed conifer ZOB (upper right). Typical granite profile in the granite Marshall Gulch ZOB. At 29 cm the sharp transition from the dark (10YR 3/2) organic rich soil is observed in contrast to the underlying highly weathered saprolite (7.5YR 3/2)(left) and represents the boundary between colluvial and residual materials (Holleran et al.).

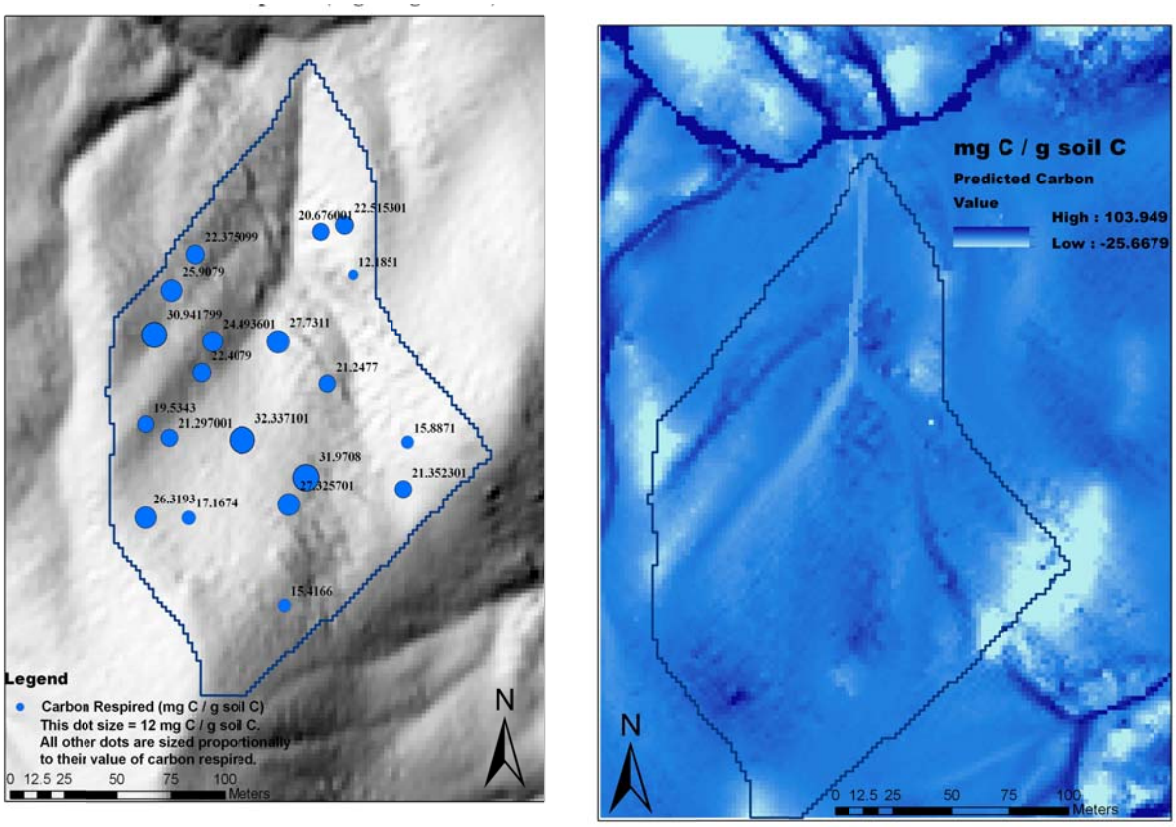


**Figure 29.** Spatial variation in measured surface soil C mineralization and predicted using regression techniques and landscape attributes (Martin et al.).

## 3.3 *Findings*: Surface Water Dynamics (SWD) Theme

Prior work by Broxton et al. (2008, 2009) indicates that terrain aspect affects the hydrologic response of forested catchments in the JRB. North-facing terrains in the Valles Caldera (JRB, **Fig. 30**): accumulate thicker snow packs, maintain longer snow cover duration, comprise higher soil moisture content, and exhibit longer hillslope water transit times.

This suggests that catchments with predominantly north-facing aspects should have more water availability and consequently a different hydrologic response than catchments with a different land orientation. To test this hypothesis, four years of hydrologic and meteorological data were compiled from the instrumented network in the JRB CZO, focusing on three perennial catchments (La Jara (LJ),

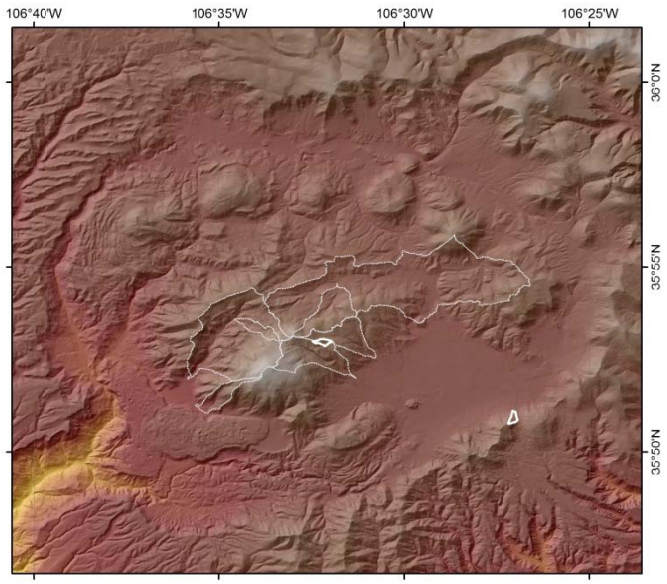


ɜ various
Caldera
ɨ Burned
ınndo and

History Grove (HG), Upper Jaramillo (UJ)) with similar topographic characteristics, climate, vegetation and geology, but different aspects. UJ is the most north-facing catchment, while HG and LJ are predominantly east facing. **For water years (WY) 2008 and 2011, annual precipitation (PPT) was 86% and 71% below the mean (711.5 mm), and during WY 2009 and 2010, it was 4% and 1% above the mean, respectively (Fig. 31).**

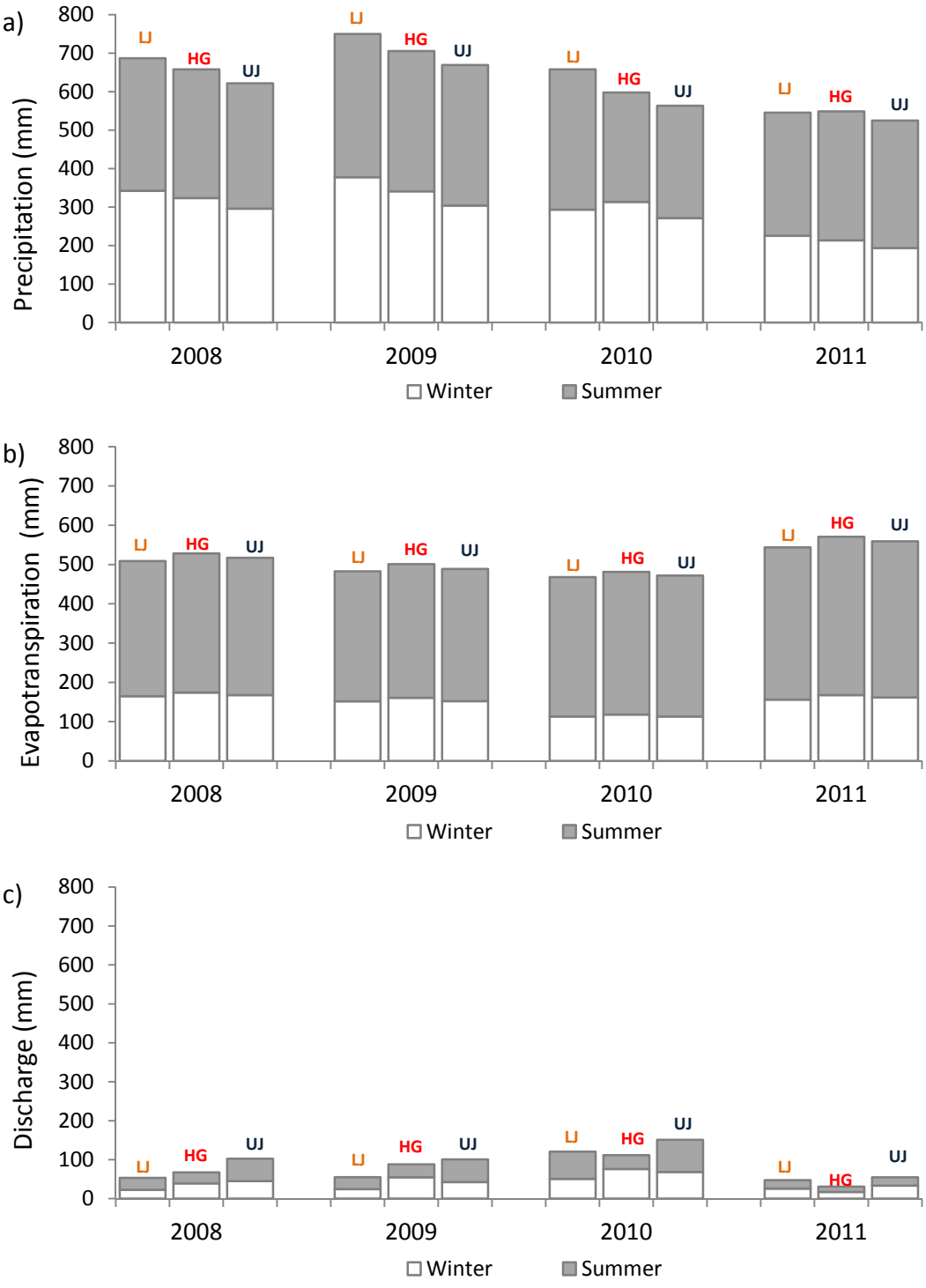


**Figure 31.** Annual precipitation, evapotranspiration and discharge for La Jara (LJ), History Grove (HG) and Upper Jaramillo (UJ) in JRB CZO from 2008 to 2011 (Zapata et al.).

• **The ratio of winter to annual PPT varied from 59.4 to 39.4%; the maximum snow water equivalent (SWE) was equal to 303 mm and 53 mm during 2010 and 2011.** The north-facing catchment (UJ) had the highest annual discharge during the 4 years. Water yield (Q/P) for UJ was the highest and ranged from 0.10 during the driest year (2011) to 0.27 for the wettest year (2010). UJ also shows the highest peak of specific discharge, which happens within a few days delay with respect to the other catchments (**Fig. 32**). UJ retains water for a longer time and it shows during dry and wet years the lowest variability between the flow percentiles Q15 and Q90 suggesting that north-facing catchments are less susceptible to climate variability.

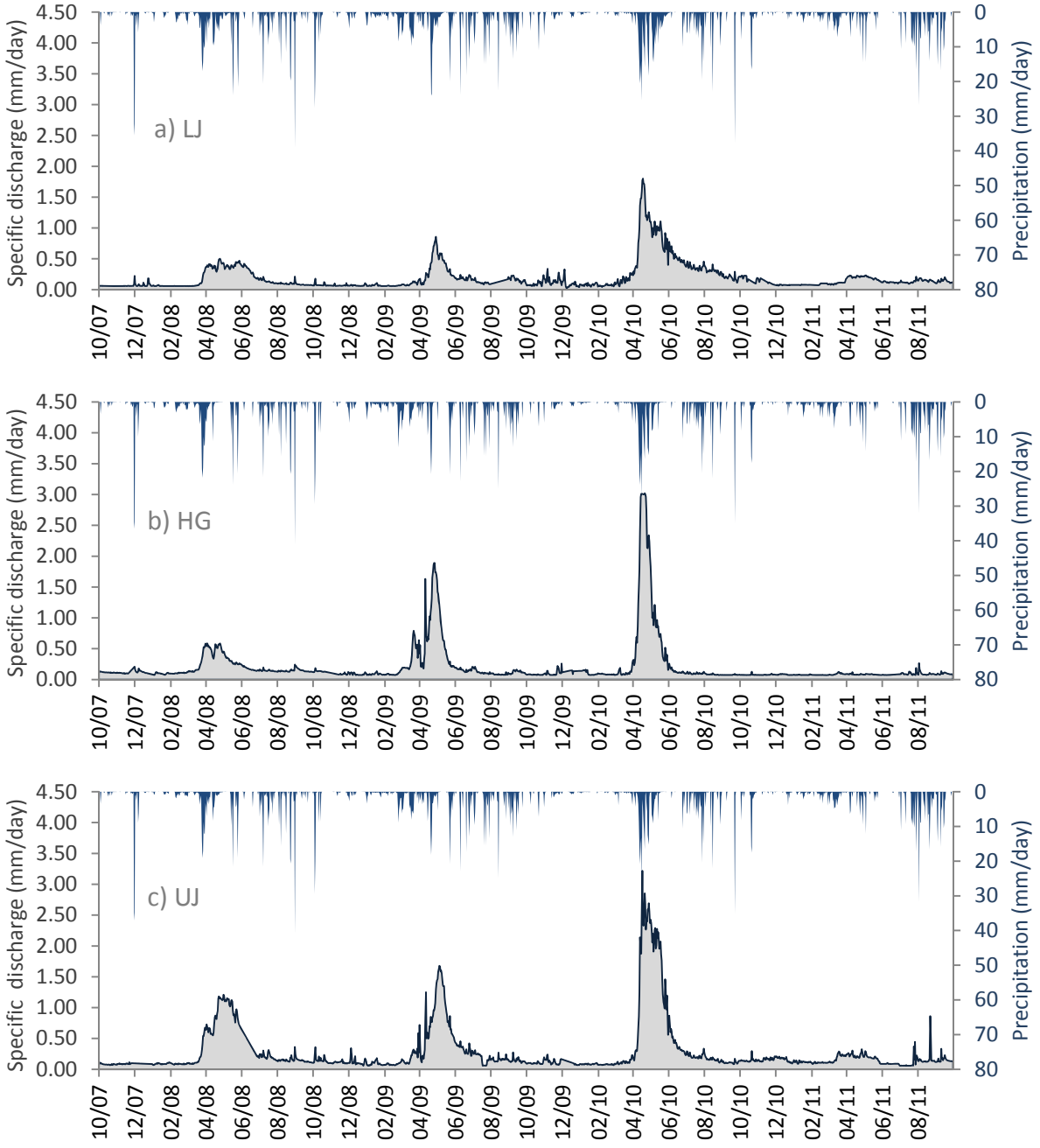


**Figure 32.** Stream hydrographs and precipitation for La Jara (LJ), History Grove (HG) and Upper Jaramillo (UJ) for Water years 2008 to 2011 (Zapata et al.).

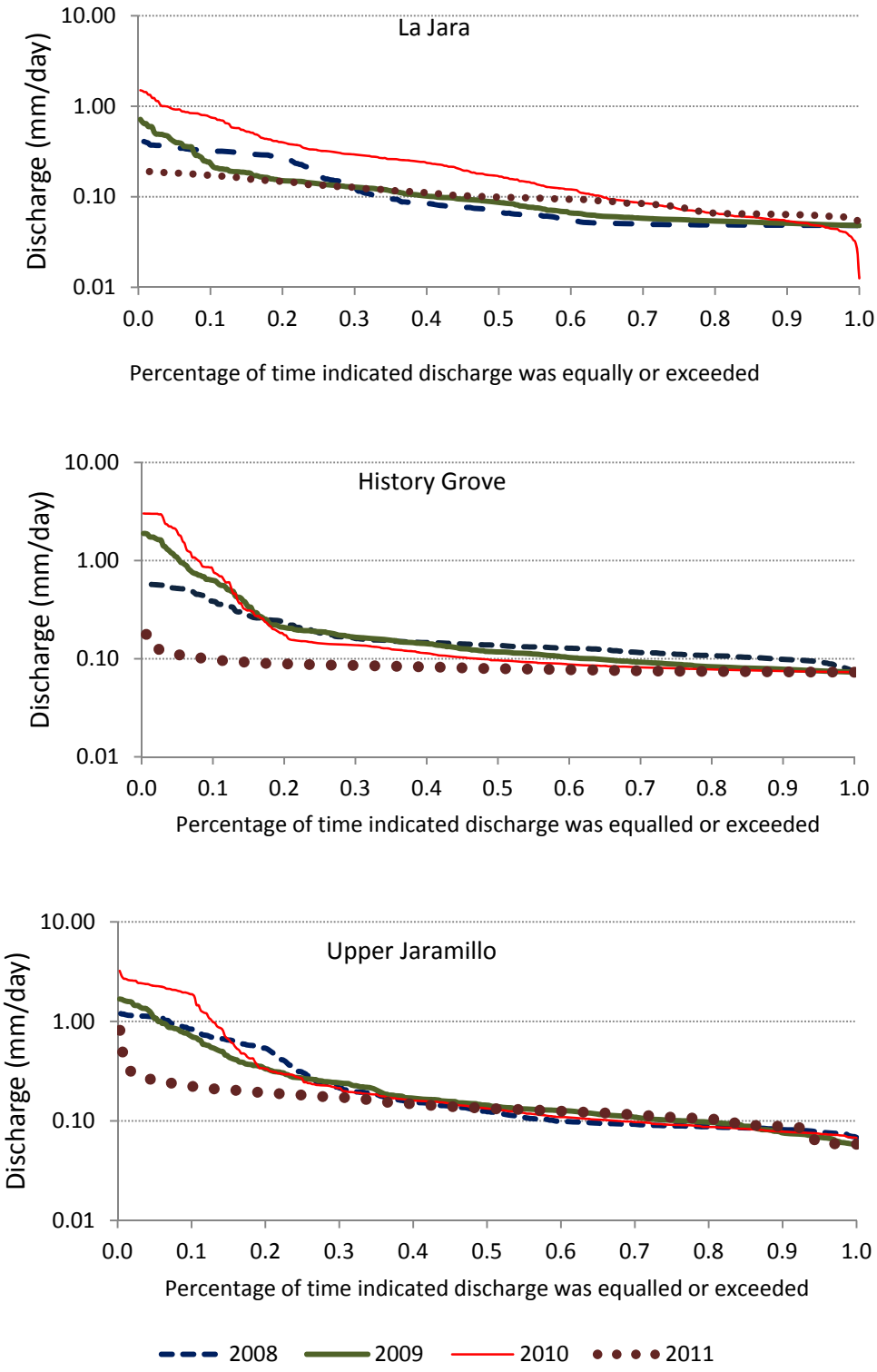


**Figure 33.** Flow duration curves for La Jara (LJ), History Grove (HG) and Upper Jaramillo (UJ) during water years 2008-2011 (Zapata et al.).

Hydrometric, chemical and isotopic data over 2 variable water years (2010 and 2011) from 3 catchments (La Jara, Upper Jaramillo, History Grove) within the JRB CZO were used to address the question: how does catchment aspect interact with climatic variability to alter streamflow generation and stream chemistry?

• **Results suggest that north-facing catchments with more topographical shading and a deeper groundwater system are less likely to have changes in carbon and nutrient chemistry as a consequence of winter climatic variability.** Stable water isotopes, Si and Cl provided good constraints on endmember water (precipitation, shallow soil water [SSW], deeper groundwater [DGW]) contributions to stream flow (**Fig. 34**). Springs located at the base of Redondo Peak (e.g. Redondo Meadow) are most representative of the regional deep groundwater source to stream flow. Springs located at higher elevation in La Jara catchment are most similar to shallow soil waters, likely representing perched aquifers. Si-Cl models show that DGW contributed 65% of stream flow during 2010 snowmelt (with significant soil water inputs) and decreased during the post-melt season, with the exception of UJ where DGW contributions were more than 80%.

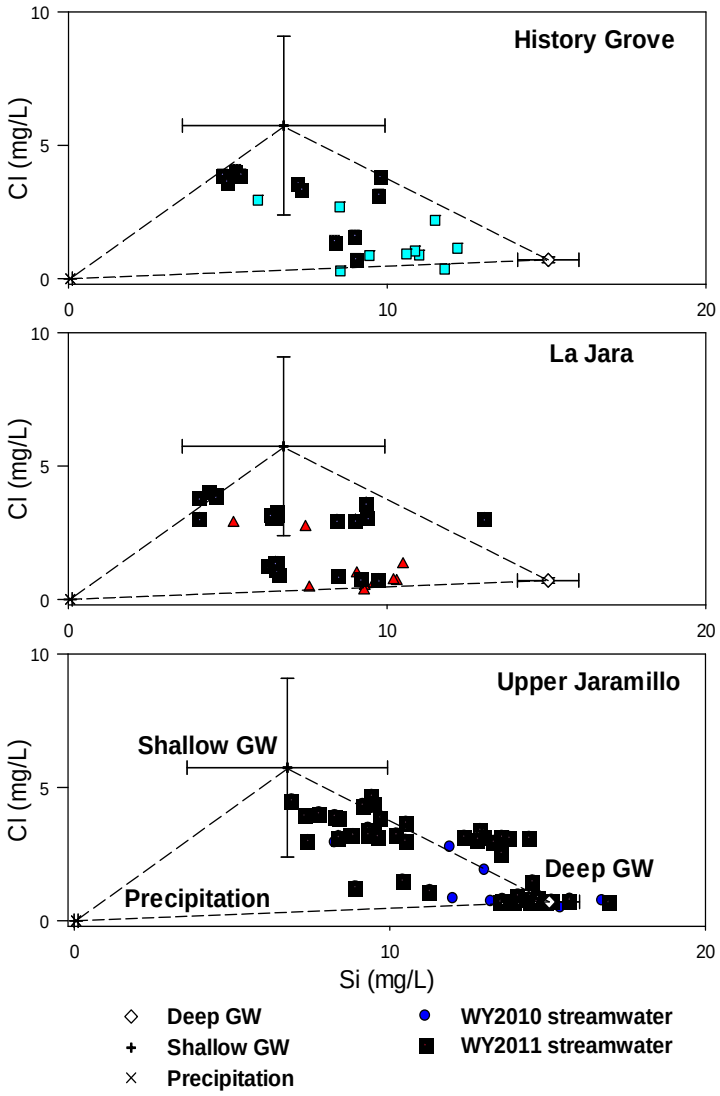


**Figure 34.** Streamwater Si and Cl concentrations for three headwater JRB CZO catchments and mixing spaced formed by the three end-members: deep groundwater, shallow groundwater, and precipitation. Closed symbols refer to WY2010 and open symbols to WY2011 (Harpold et al, in prep.).

• **Proportions of DGW in stream flow declined in 2011, and upland spring contributions made up more of the stream discharge likely due to the lack of a significant snowpack to recharge the regional groundwater table.** DGW and SSW have $\delta^{18}O$ values within the range of snowmelt, with no indication of monsoon rainwater contributions suggesting infiltration of snowmelt is the dominant source of recharge to regional groundwater, consistent with other evidence, such as the timing of peak flow and the end of snow cover and differences in water yields between years in relation to maximum SWE. Observed versus predicted relationships with stream nutrient chemistry shows that high DGW contributions to stream flow are indicative of periods when the upland hillslopes are hydrologically connected to the stream channel and biogeochemical cycling along flowpaths is reduced (**Fig. 35**; Harpold et al., manuscript in prep).

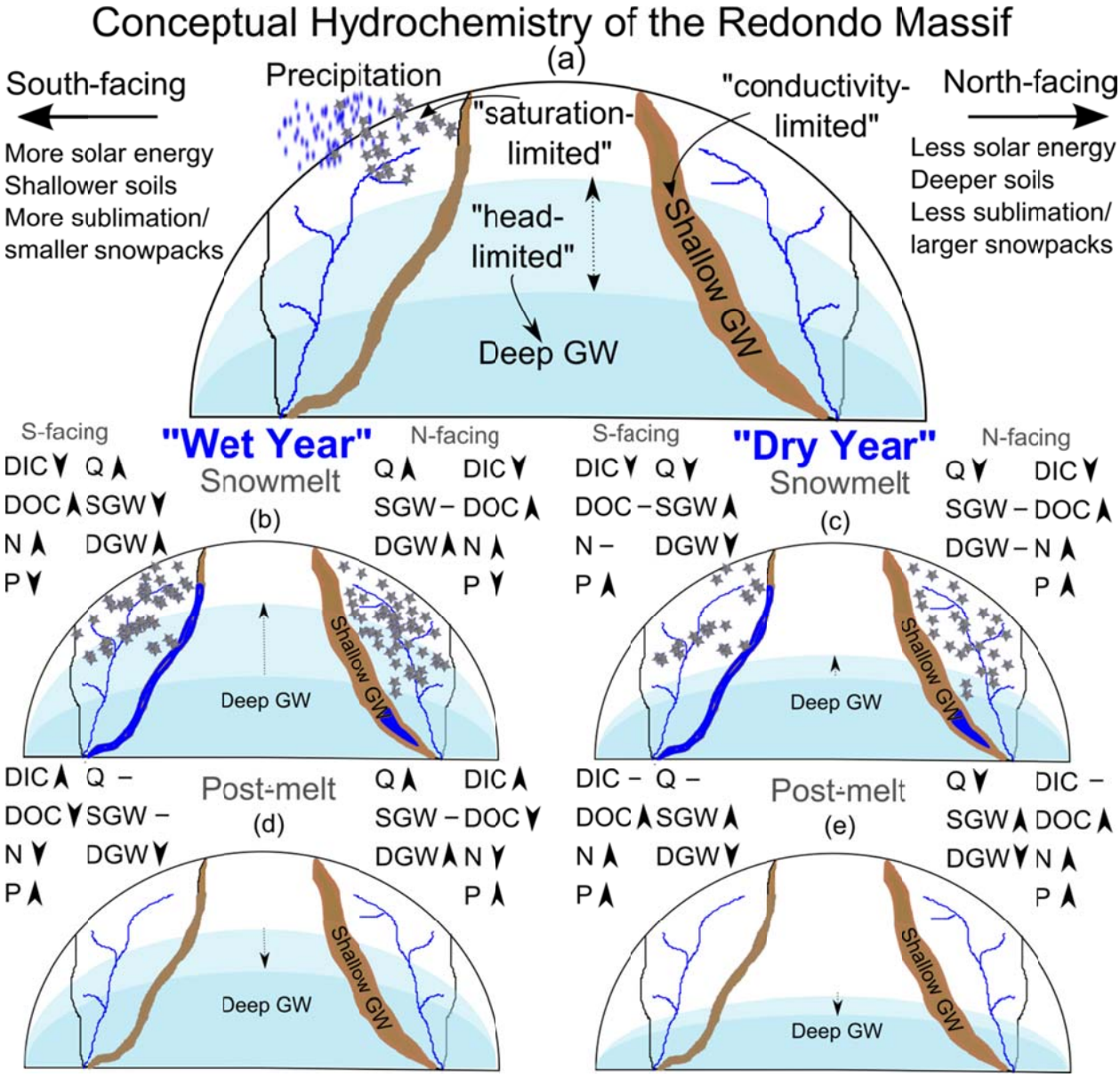


**Figure 35.** Conceptual model of runoff and solute generation across seasons and climatic conditions in the Valles Caldera (Harpold et al., in prep.).

• **Determination of solute sources to streams is facilitated by using multiple geochemical tracers.** Changes in seasonal and interannual hydrologic conditions, as observed over the past 4 water years in the JRB CZO, may alter subsurface flowpaths, influencing mineral weathering contributions to streams. Elemental and trace metal chemistry were coupled to Sr isotopes and Germanium-Silica (Ge/Si) ratios to constrain weathering processes from soils to streams in La Jara catchment over 3 variable water years. Little variation (chemostatic behavior) was observed in major cation chemistry throughout water years 2010 to 2012, despite large variations in discharge (**Fig. 36**), suggesting a dominant source water (DGW) contributes to stream flow, and water flux controls solute transport to the stream. These results are consistent with mixing model results described above (Harpold et al., manuscript in prep).

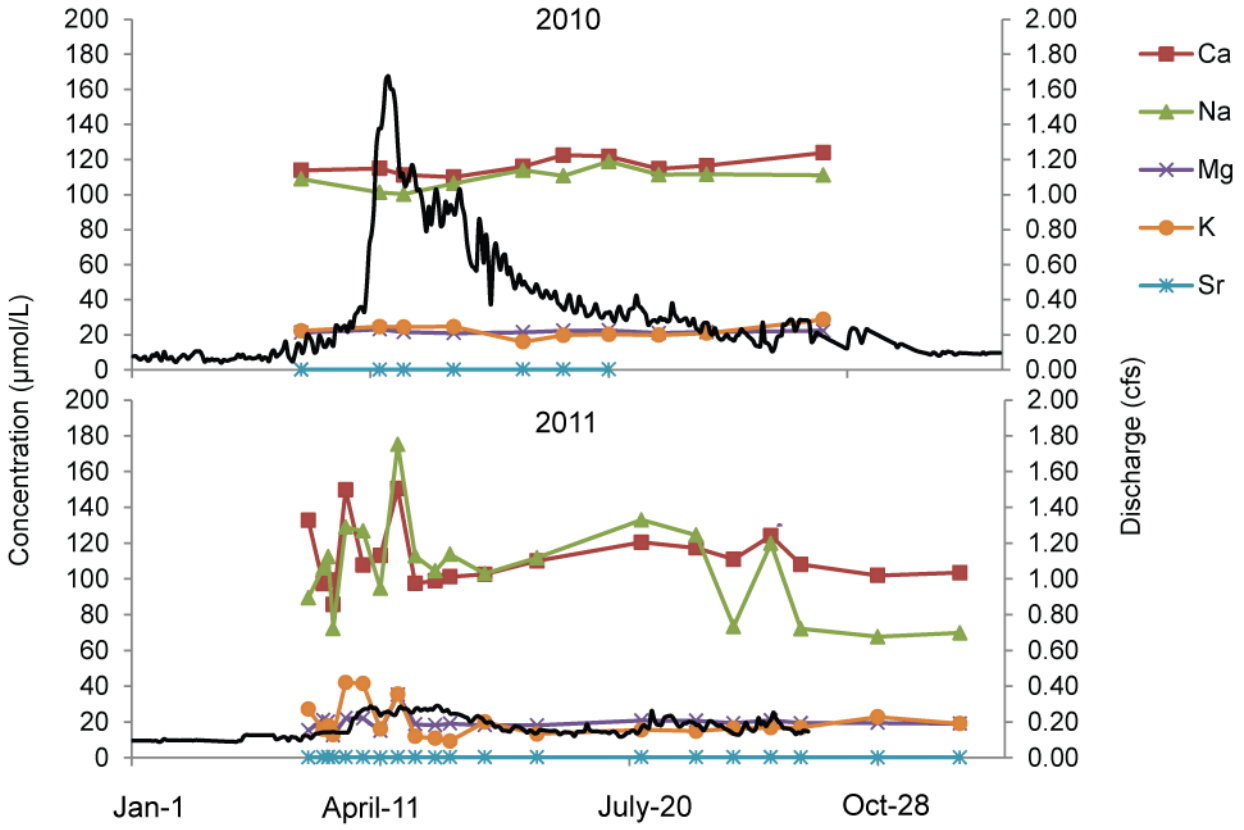


**Figure 36.** La Jara Creek base cation concentrations are relatively constant despite large differences in stream discharge, indicating a consistent source of solutes to stream water throughout the year. More variation in concentration is observed in 2011, likely due to the increase in sampling frequency during snowmelt (C. Porter et al).

• **Minor contributions of shallow groundwater (SGW, similar composition to soil water and upland springs) to stream flow were observed in 2010 (relatively wet year) during spring snowmelt, as seen in elevated DOC, Fe, and Al concentrations, Ge/Si ratios, and Sr isotopes in stream waters (Figs. 37-38).** Soil water signatures were minimal in stream flow in 2011, likely due to the lack of snow cover resulting in frozen soils and limited hydrologic connection between the hillslope and stream **(**Porter et al., 2011 AGU abstract; 2012 AGU abstract submitted; manuscript in prep**)**.

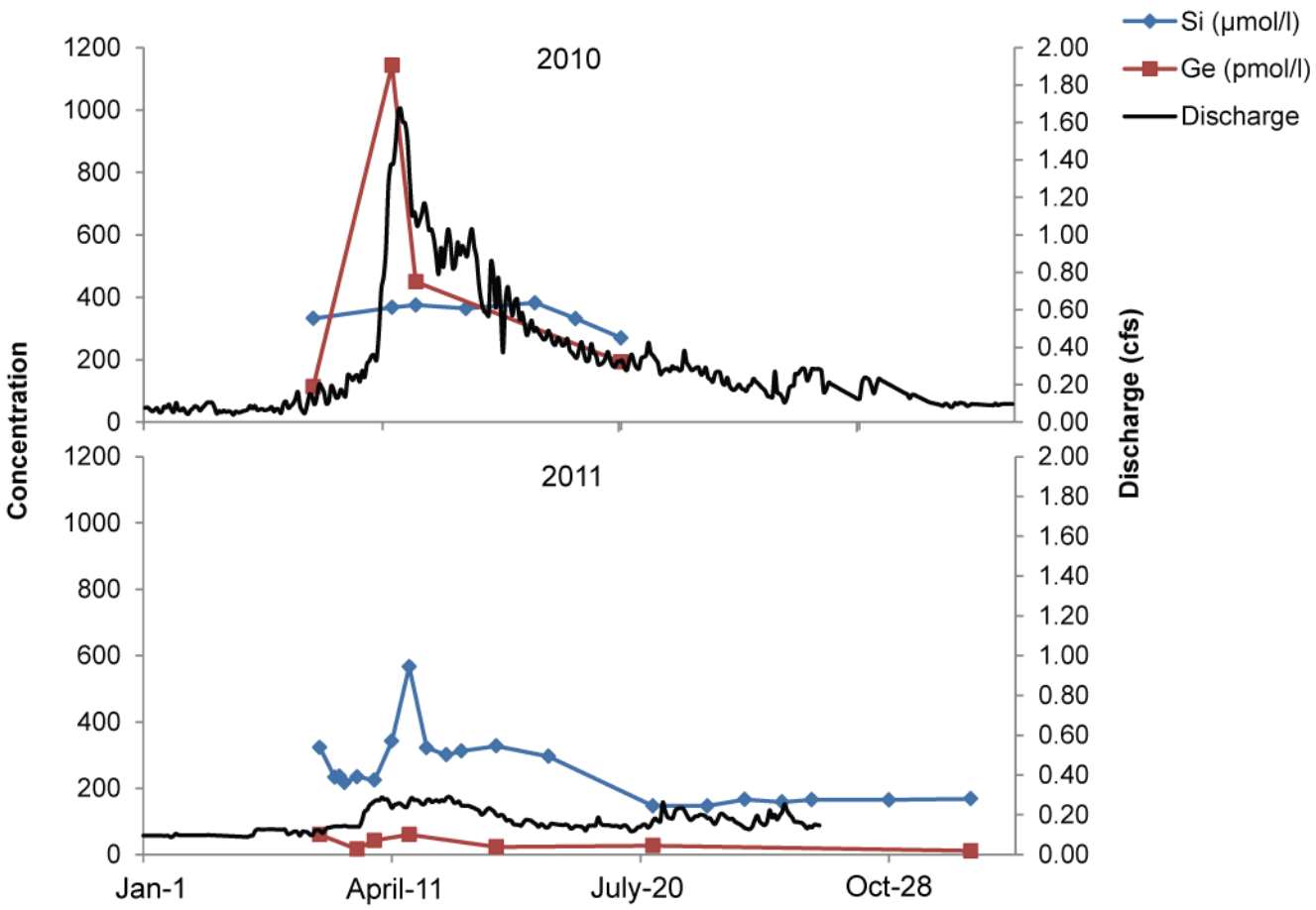


**Figure 37.** Si and Ge concentrations in La Jara stream flow. Spikes in Ge values correspond to elevated Fe, Al, and DOC concentrations, indicating inputs of shallow soil waters to the stream, during wet snowmelt years (2010) when the hillslopes are hydrologically-connected to the stream. Si concentrations remain stable between years, similar to base cations, reflecting export of primary mineral weathering products along deeper, longer residence time flowpaths to the stream (C. Porter et al., in prep.).

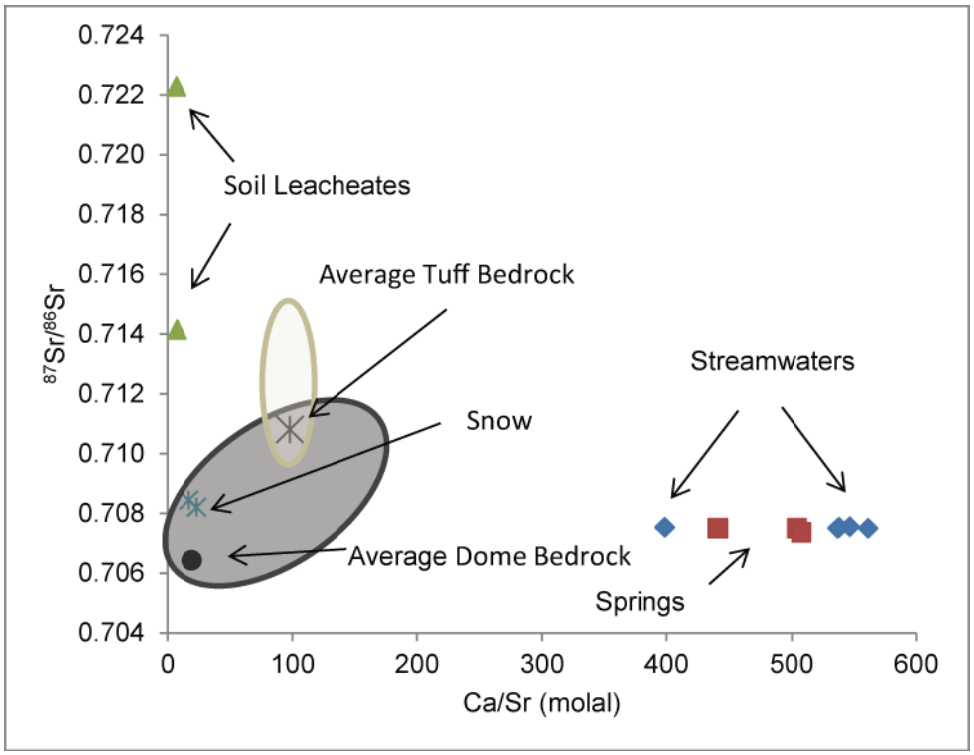


**Figure 38.** Sr-isotopes plotted versus Ca/Sr ratios for various waters and solid samples in the JRB CZO. Stream waters have similar Sr isotope values as local bedrock and upland springs, with high Ca/Sr ratios suggesting preferential export of Ca relative to Sr (C. Porter et al., in prep).

• **The carbon budget was calculated for several headwater catchments surrounding Redondo Peak in the JRB CZO for both wet (2010) and dry (2011) water years.** Annual carbon inputs (NEE) are 2-3 orders of magnitude higher than dissolved carbon (DIC and DOC) effluxes in the streams (**Fig. 39**). In dry years, both NEE and DOC fluxes decrease. The substantial carbon store could be related to biomass accumulation following repeated logging (in the 1970s) in all catchments. With an approach to steady state biomass, future carbon uptake may decrease **(**Perdrial et al., manuscript in prep**)**.

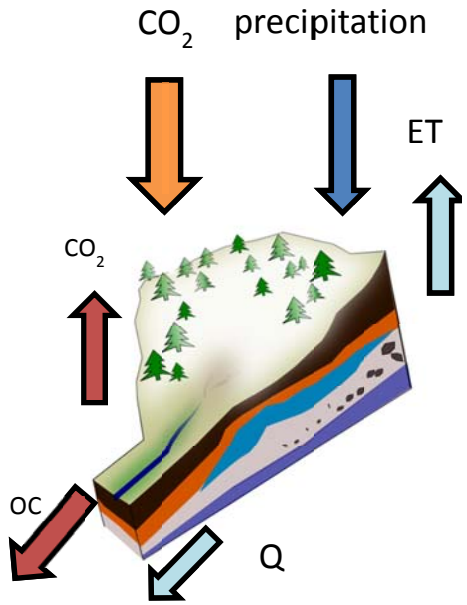


**Figure 39.** Summary diagram of mean calculated carbon fluxes for headwater catchments in the JRB CZO (Perdrial et al., in prep).

• **Winter climate and aspect affect stream water carbon fluxes.** Stream water carbon characteristics (DOC, DIC, TDN, UVvis absorbance, PARAFAC-quantified fluorescence spectra) were compared for two climatically distinct water years (WY). WY 2010 was characterized by an early, thick and consistent snowpack, whereas in WY2011, snowpack was established later, and was thin and inconsistent. Due to soil freezing and decreased water yield, snowmelt carbon fluxes of WY2011 were 10% those for WY2010 (**Fig. 40**). Summer $P_{CO2}$ exceeded atmospheric values in both years (up to 12 times). North-facing streams exported more DOC during snowmelt and less $CO_2$ in the summer than south and east-facing slopes **(Fig. 41)** (Perdrial et al., in review).

**Figure 40.** Stream water fluxes for the snowmelt period (defined as the period between 03/15 and 05/15) for WY2010 and WY2011 for upper Jaramillo (JO) and LaJara (LJ) for DOC (a) and TDN (b). Differences between the two years are significant at the 95% confidence level (J. Perdrial et al., in review).

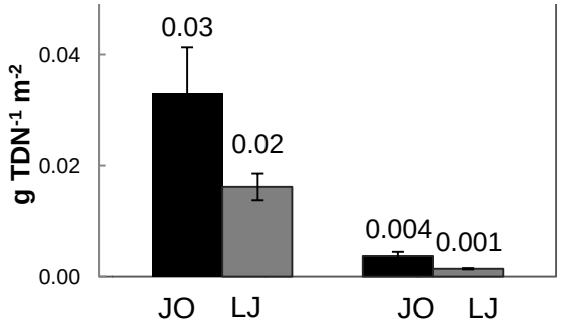


**Figure 41.** Schematic of winter and snowmelt processes WYs 2010 and 2011 for the S facing LJ and N-facing JO catchments. Winter 2010 is characterized by a thick snow pack, unfrozen soils and winter microbial activity (conceptualized by yellow circles). Winter 2011 is characterized by a thin snow pack, soil freezing and reduced winter microbial activity. Snowmelt 2010 is characterized by intensive soil flushing (flow paths conceptualized by white arrows). Snowmelt 2011 is characterized by reduced soil flushing (J. Perdrial et al., in review).

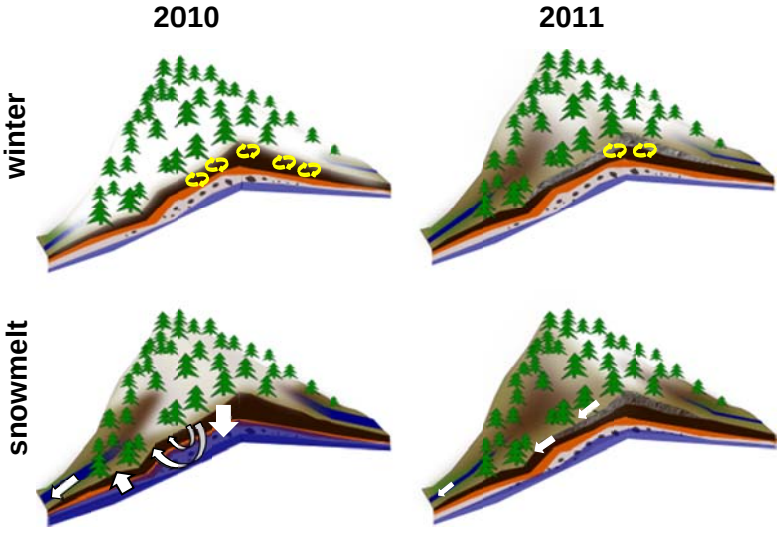

• **Water and carbon fluxes (combining measurements from SWD, EHP, SSB CZO science themes) were translated into the currency of EEMT (overall CZ EEM influx based on NEE, $P_{eff}$, ambient T) and correlated with annual solute export in streams.** Positive correlations (e.g. $R^2$=0.6 for Si, 0.9 for REE; **Fig. 42**) between annual EEMT and stream water solute fluxes support the hypothesis that CZ water and carbon can be used to predict chemical denudation fluxes; the greatest chemical denudation being observed in north-facing catchments **(**Perdrial et al., manuscript in prep; AGU abstract submitted**).**

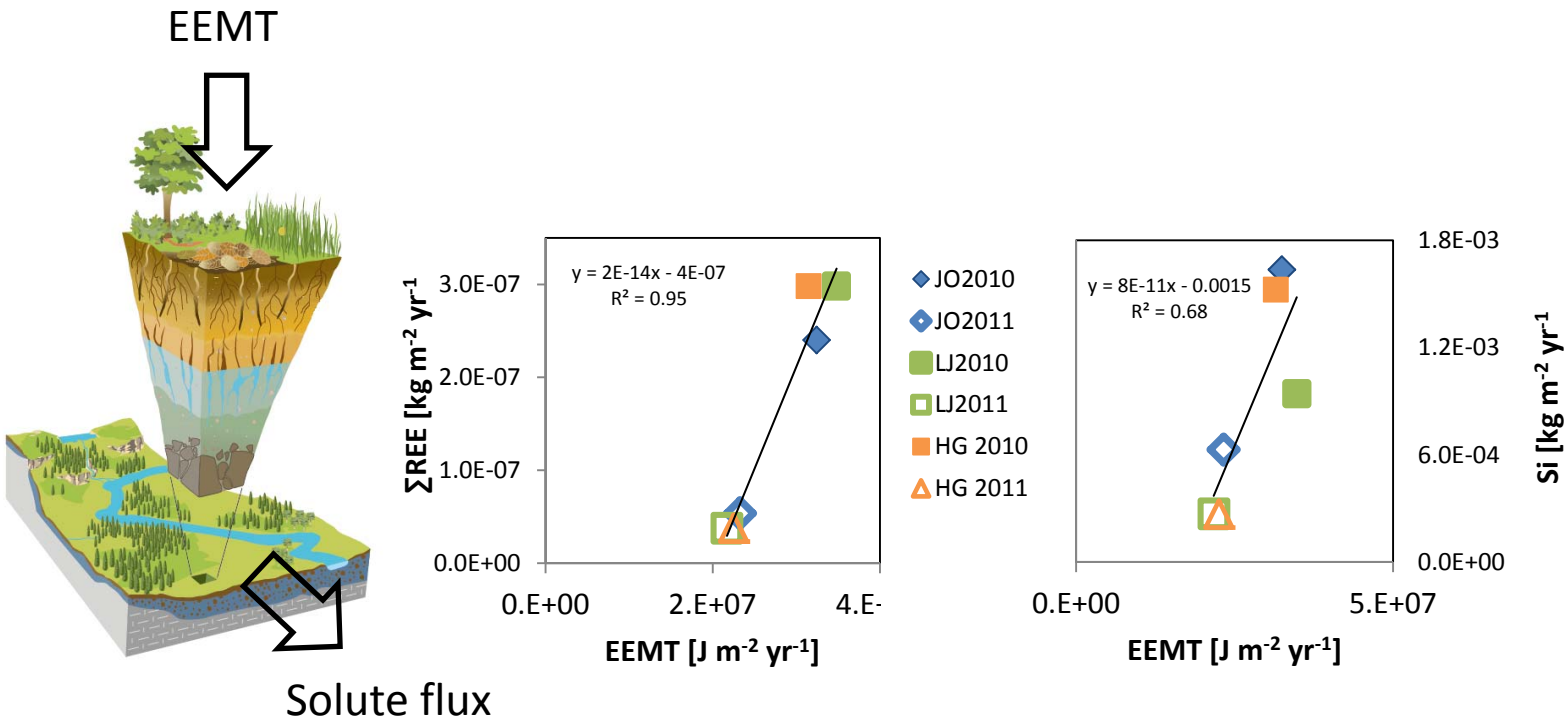


**Figure 42.** EEMT calculation include i) NEE that is estimated for each catchment based on an empirical relationship between NEE ant winter precipitation (Brooks et al., Harpold et al.),ii) effective precipitation and iii) ambient temperature (J. Perdrial et al., in prep.).

## 3.4 Landscape Evolution (LSE) Theme

• **Topographic slope controls soil thickness and hence water residence time around Redondo Mountain** A long-standing question for the JRB-SCM CZO is: why do water residence times vary around Redondo Mountain? Do these variations relate to solar insolation/EEMT, or do they relate to topographic and geologic differences between the north-facing and south-facing sides of the mountain. Using the modeling framework of Pelletier and Rasmussen (2009), PI Pelletier is currently working with Professor Roy Johnson of the UA geosciences department to analyze shallow seismic refraction surveys conducted in May, 2012. Over 8 d, a team consisting of Pelletier, Johnson, and 5 students acquired seismic reflection/refraction data along 7 seismic lines with 2.5 m horizontal resolution. We acquired 2 cross-valley profiles each in La Jara, History Grove, and Upper Jaramillo, plus 1 in Banco Bonito for calibration (because many soil pits have been dug there coinciding with the seismic transects). The work

was logistically challenging, e.g. carrying truckloads of gear, by ATV, for more than a mile along logging roads strewn with downed trees to reach Upper Jaramillo catchment.

LSE modeling results (**Fig. 43**) indicate that average soil thickness correlates reasonably well with mean transit time (from tritium decay), with History Grove the shortest and Upper Jaramillo the longest. There is also a good correlation with valley bottom area, which relates to average soil thickness and could be considered a more appropriate measure of soil thicknesses if hillslope drainage is fast and the water spends most of its time percolating down through the valley bottom. This analysis was based on a uniform EEMT model that does not include microclimate effects associated with aspect (that are discussed in section 3.5 of this report). Rather, it reflects the way soil thickness is inversely related to topographic slope (consistent with the partial inverse correlation of slope and MTT shown in Broxton et al. 2008), with Upper Jaramillo having a lower slope than the south-facing catchments simply because it drains to a higher base level. This effect is ultimately related to the drainage structure of the caldera, since Lower Jaramillo creek has to drain around the northeast side of Redondo Mountain before it meets the East Fork of Jemez River, and it is not because Jaramillo catchment receives less radiation. These data, together with the inability of EEMT/net radiation to explain differences in MTT in VCNP, suggest that differences in topography, ultimately related to the caldera structure/drainage organization, are more important than differences in microclimate in controlling MTT in VCNP.

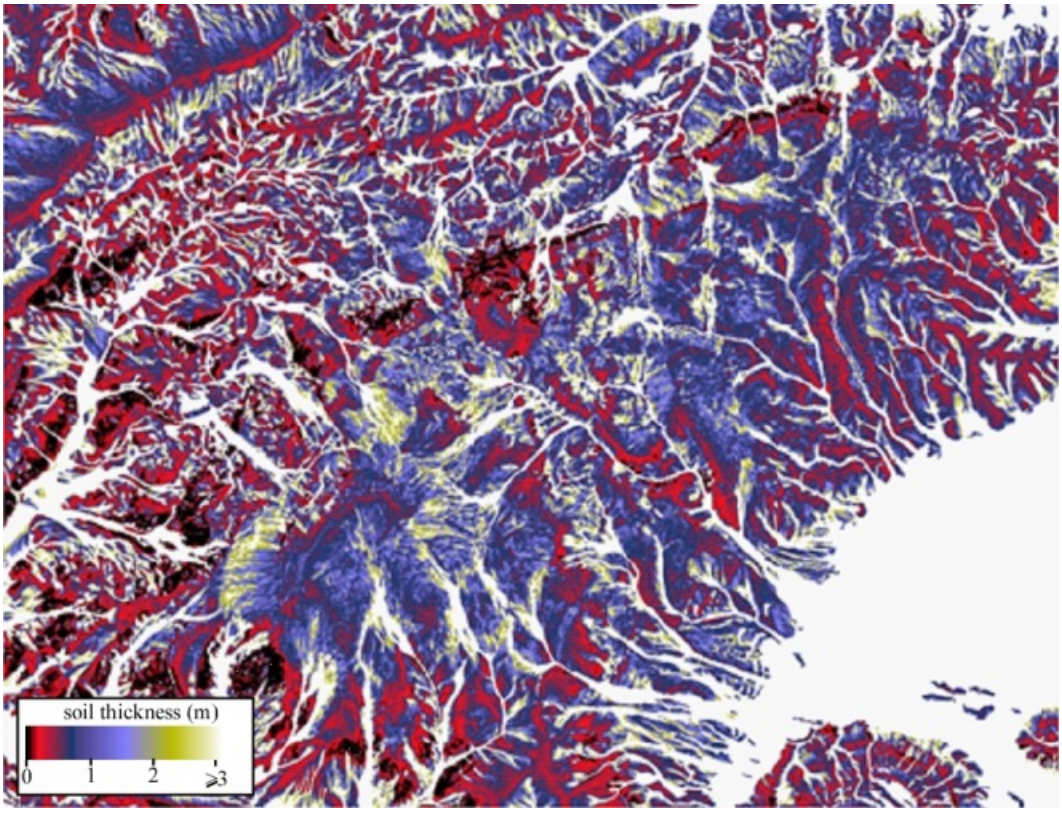


**Figure 43.** Color map of model results for soil thickness around Redondo Mountain assuming a uniform soil production rate (i.e. soil thickness controlled by topography alone, not by slope aspect/microclimate). This dataset is currently being validated against seismic refraction surveys of soil thickness. Average soil thicknesses correlate with mean travel times (MTT) of water, suggesting that MTTs are controlled by topographic variations in soil thickness (J. Pelletier et al.).

**• Post-fire erosion in JRB-CZO headwater catchments swamps background levels.**

The Jemez River basin (location of the University of Arizona CZO project) was recently the site of the largest wildfire in New Mexico state history (until Summer 2012, when it was surpassed by another event). This event presented a unique opportunity to quantify and understand the geomorphic, hydrologic, and ecological response to a major perturbation using high-resolution mapping, field measurement/data collection, and numerical modeling.

Student Caitlin Orem and PI Jon Pelletier are taking the lead in studying the geomorphic effects of this fire. Caitlin has been monitoring erosion in non-fire affected regions and she has found that the amount of erosion that has occurred in one year following the fire is orders of magnitude larger than the "background" erosion rate of non-fire-affected catchments. This raises the possibility that the vast majority of all the erosion that occurs in forested landscapes occurs in the few years following a high severity fire.

We are acquiring terrestrial laser scans (ground-based LiDAR) over time in order to quantify how sediment yields change through time as the landscape "recovers." Conceptual models for the landscape adjustment to fire predict that landscapes return to a state similar to pre-burn conditions following an exponential decrease from an initial post-fire peak to a new quasi-equilibrium condition over a time scale of several years to decades. Our CZO project aims to calibrate that recovery graph and its ecologic, hydrologic, and geomorphic controls. Ground-based LiDAR will play an important role in that effort but it is important to emphasize that ground-based LiDAR cannot possibly measure geomorphic change in even a fraction of the total fire-affected area. As such, airborne LiDAR data is needed. NSF generously funded an airborne LiDAR survey of the burned area in May 2012. On the day of this writing, that dataset was received from NCALM and we have begun working on comparing the pre-fire and post-fire datasets.

**• EEMT and aspect control fire severity.**

Is there a slope-aspect control to fire severity or is the slope aspect control primarily in the geomorphic response following the fire? To examine this question, we analyzed satellite-image-derived measures of fire severity and related those to topography. This work was conducted with the broader goal of understanding how fire behavior exhibits scaling laws and deviations from scaling laws. The frequency-size distribution of forest fires in the conterminous western U.S. is approximately a power law with an exponent of –1. However, the frequency of fires with areas larger than $\sim 10^2$ $km^2$ is lower than that predicted by an extrapolation of the power-law trend for smaller fires. Previously proposed cellular automata (CA) models for forest fire cycles do not reproduce the observed departure from scaling unless the frequency of fire initiation is set to be unrealistically high. CA models of forest fire cycles are also limited in that they do not include known controls on forest fires. Pelletier et al. (2012) proposed a modification of the classic CA model for forest fires that maintains the simplicity of the classic model but is more consistent with observed data. Fuel in the model grows at a rate dependent on topographic northness. In the model, more fuel is available to burn on north-facing slopes in water-limited environments in the Northern Hemisphere due to lower solar insolation, lower evaporation, and higher soil water availability. Some south-facing slopes, with less available fuel, act as geographic barriers to the spread of high-severity forest fires. The resulting model matches 1) the observed frequency-size distribution of forest fires in the conterminous western U.S., including the observed departure from scaling, 2) the observed slope and aspect control of burn severity in recent large forest fires of the western U.S. (e.g., **Fig. 44**), and 3) the scaling behavior of spatial variations in fuel availability and burn severity in forest fires (**Fig. 45**).

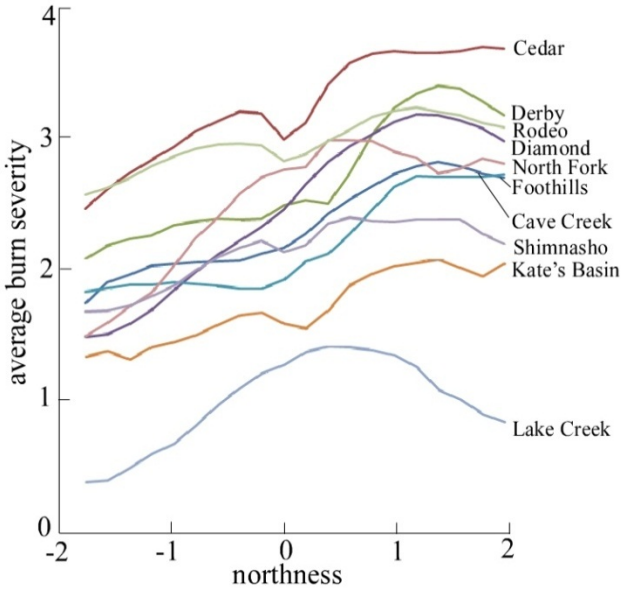


**Figure 44**. Plots of average burn severity versus northness for ten large fires in the western U.S. Nine of the ten fires show a systematic increase in burn severity with increasing northness. One of the ten fires (Lake Creek) shows a maximum burn severity for relatively flat topography (i.e. near zero northness). Burn severity values for this fire are plotted after subtracting the burn severity class by one in order to more easily distinguish this curve from those of the other nine fires (J. Pelletier et al).

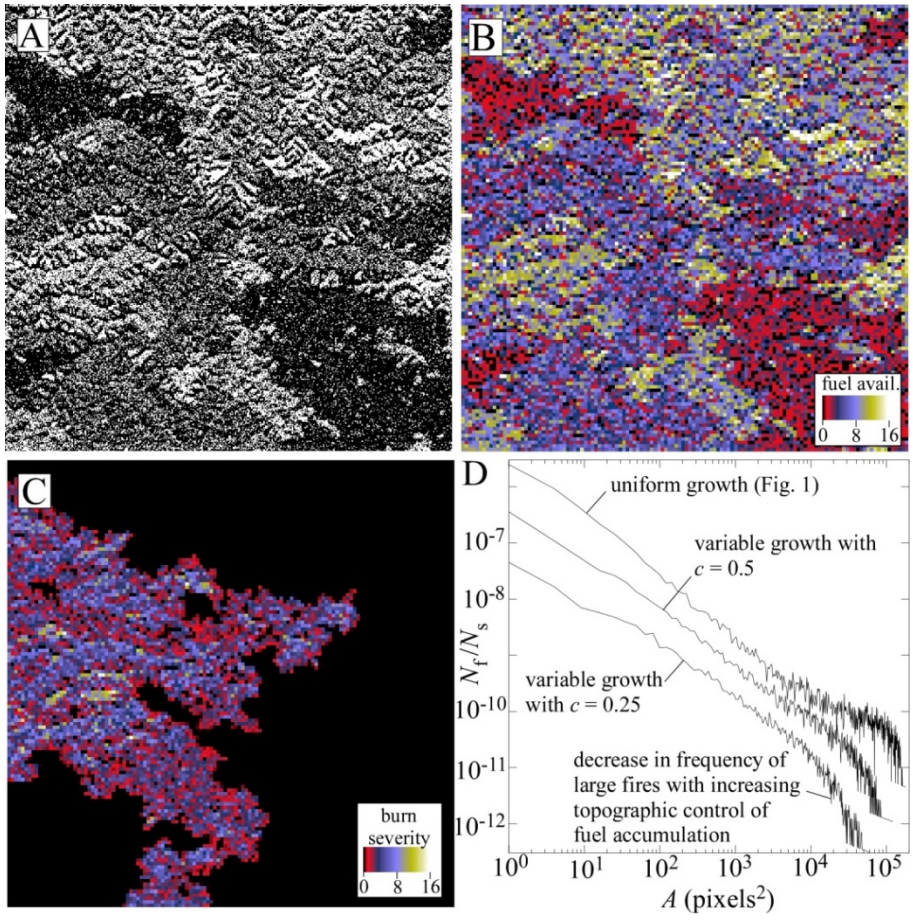


**Figure 45.** Example outputs of the topographically controlled forest fire model with N = 512, T = 0.04N2, and c = 0.5 (A) Occupied (white) and unoccupied (black) grid points at an example snapshot in time. (B) Color map of fuel availability obtained by averaging the data from (A) in 4x4 pixel boxes. (C) Map of burn severity, equal to the number of trees burned in each 4x4 pixel box during a representative large fire. (D) Frequency-size distribution of fires in the model with different degrees of topographic control on fuel growth rates, illustrating the roll off in power-law behavior of frequency versus area for large fires when topographic control of fuel availability is included. The curves for c = 0.5 and c = 0.25 are also shifted down by a factor of 5 and 25, respectively, so that the three plots can be more easily distinguished (J. Pelletier et al.).

• **Flood probabilities can be quantified using NEXRAD radar data**

This technique has applications to understanding the episodicity of erosion in the JRB and SCM landscapes, but is also important for constraining flood hazards regionally throughout the western U.S. Flood-envelope curves define the upper limit of flood discharges in drainage basins of different size within a given hydroclimatic region. Their usefulness, however, is limited by the lack of a well-defined recurrence interval for the maximum flood. We have found that frequency-magnitude-area relationships can be constructed for floods using Stage III Next-Generation Radar (NEXRAD) precipitation estimates and flood-routing algorithms. Our method retains the power of the flood-envelope curve approach in that drainage basins of similar size are grouped together to make maximum use of sparse and/or short-duration discharge data. Our method improves upon the flood-envelope curve approach by assigning a recurrence interval to each flood magnitude for a given drainage basin area. We used our method to quantify the frequency-magnitude-area distributions of flood discharges in the Upper and Lower Colorado River Basins as examples. Results show that average precipitation rates over a given area are power-law functions of drainage area with an exponent of approximately 0.75 for a wide range of recurrence intervals (**Fig. 46**). Flood-discharge frequency-magnitude-area curves are not power-law functions of area, however, but instead exhibit the concave-down shape characteristic of published flood-envelope curves. Our results suggest that this concave-down shape is due primarily to geomorphic dispersion of flood waves within drainage basins. Flood magnitudes calculated by our method are comparable to, but slightly higher than, those reported in the literature for our study regions, suggesting that previously published flood-envelope curves in these areas may underestimate the frequency of large, rare floods (Orem and Pelletier).

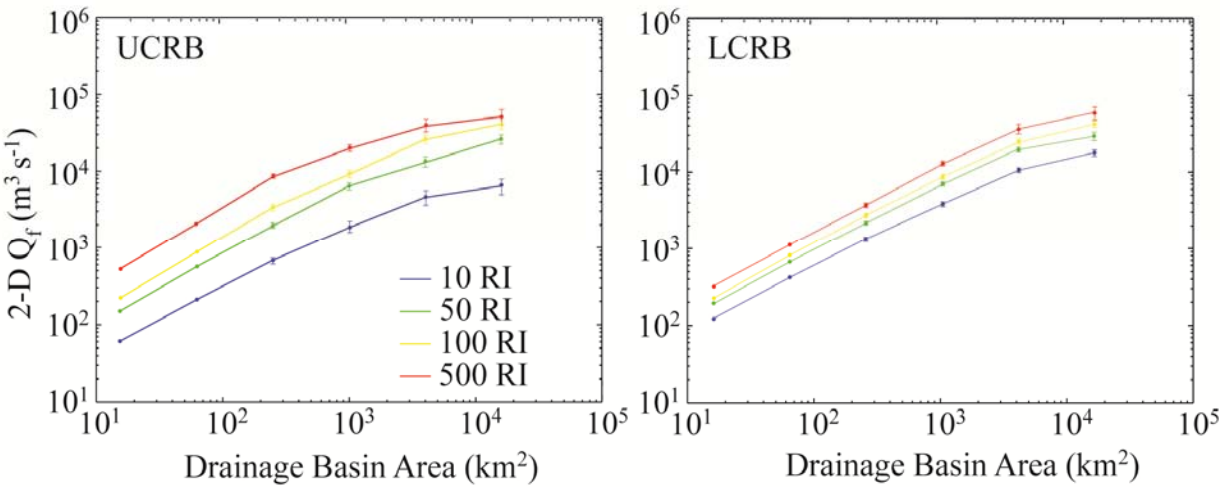


**Figure 46**. Frequency-magnitude-area graphs of modeled flood dicharges (calculated using Brutsaert flow routing method) versus drainage basin area for recurrence intervals of 10, 50, 100, and 500 years for the upper Colorado River basin (UCRB) and the lower Colorado River basin (LCRB) (Orem et al.).

• **Ivantsov solution provides an accurate prediction of valley morphology**

PI Pelletier, working with Taylor Perron of MIT, have used first-order valleys in southern Arizona to test a new theoretical model for the shapes of valley heads. In a recent paper in the *Journal of Geophysical Research* we presented an analytic solution for the morphology of a valley and its adjacent hillslopes undergoing steady headward growth. The mathematics of this problem was first solved by *Ivantsov*

[1947] in the context of heat flow near a parabolic solidification boundary. We tested whether the Ivantsov solution provides an accurate first-order prediction of the morphology of valley heads and their adjacent hillslopes by comparing the model predictions to survey data from two study sites in southeastern Arizona. The model predicts that elevation contours of valley heads are parabolas and that topographic transects normal to contour lines are error functions. High-resolution Digital Elevation Models (DEMs) were constructed for the two study sites using Real-Time Kinematic Global Positioning System (RTK-GPS) measurements and a Terrestrial Laser Scanner (TLS). Our analyses show that the model reproduces the first-order morphology of headward-growing valleys and their adjacent hillslopes (**Fig. 47-48**). We also show that by analyzing hillslope profiles at different distances from the valley head, the model framework can be used to infer likely changes in the valley head migration rate through time.

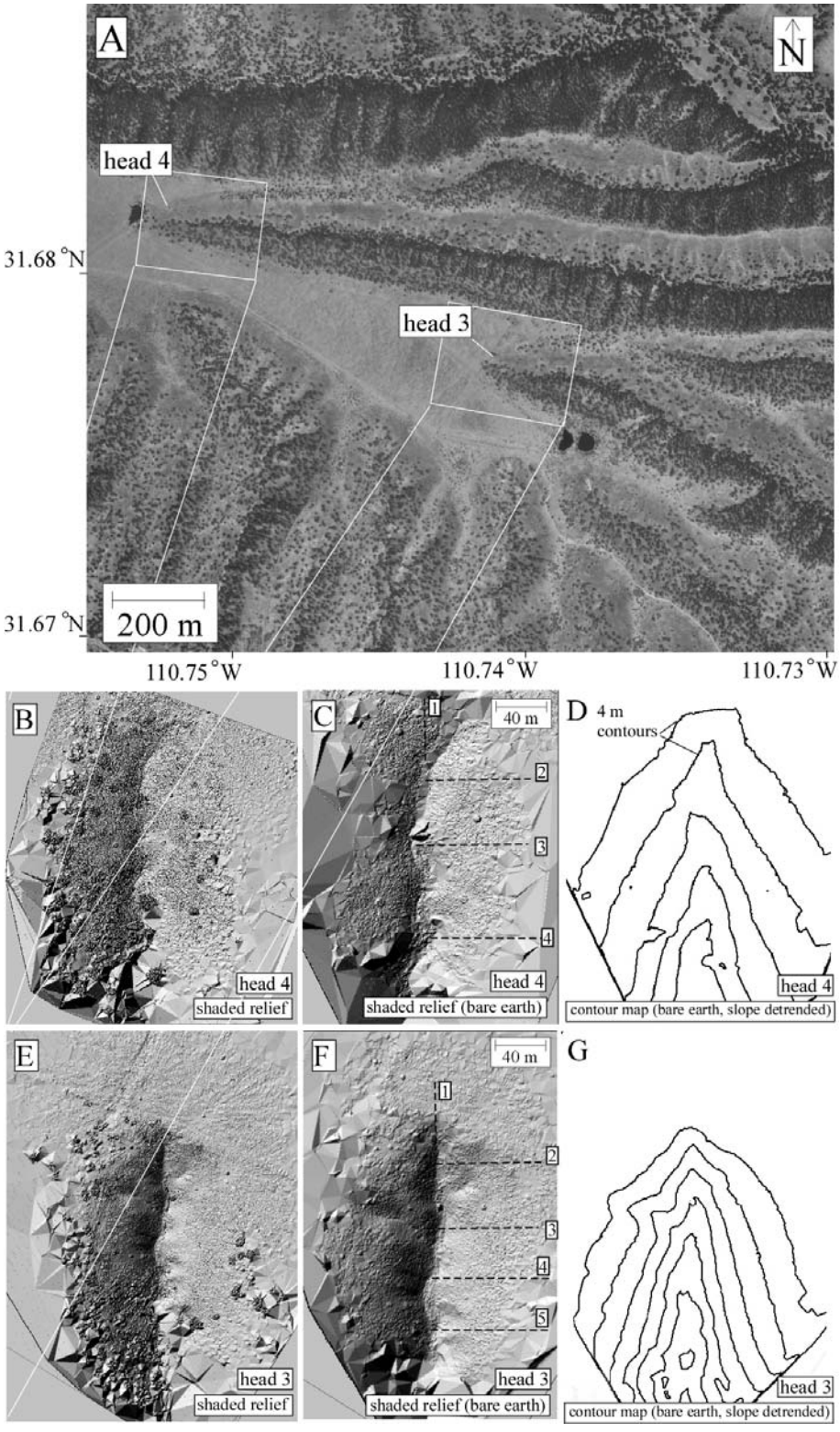


**Figure 47**. Maps of valley heads in one of our study sites in southern Arizona. (A) Portion of U.S.G.S. orthophotoquad that includes the two valley heads surveys (outlined in white rectangles). (B)&(E) Shaded relief images of DEMs made from TLS survey. (C)&(F) Shaded relief images of valley head DEMs with vegetation removed. (D)&(G) Contour maps of valley heads with regional/far-field slope removed (Pelletier et al.).

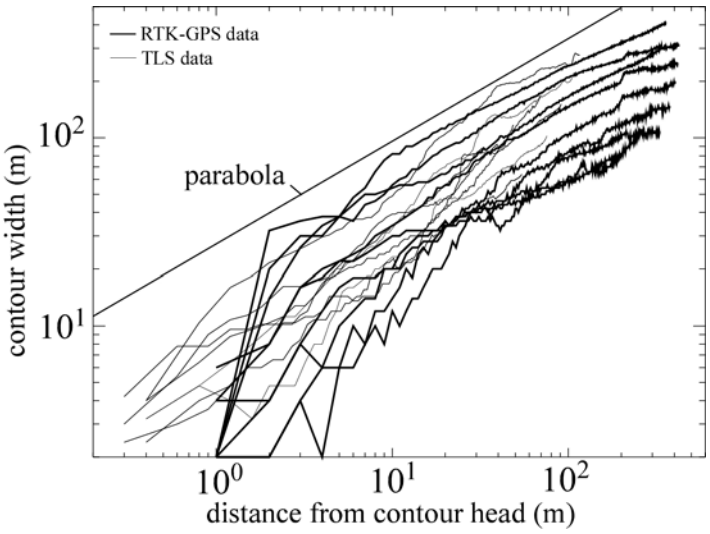


**Figure 48.** Test of the model prediction of parabolic contours. The graph plots the contour width versus the distance along the valley from the contour head, i.e. the point where the contour crosses the valley centerline. Data is shown for all valley heads studied. The parabolic model prediction (i.e. a slope of 1/2 on log-log scales) is shown for comparison. RTK-GPS data (thick lines) have limited resolution below scales of a few meters, while TLS data (thin lines) resolve variations in contour width down to sub-meter scales (Pelletier et al.).

**• A new method was developed for extracting drainage valleys from (e.g., LiDAR) digital elevation maps (DEMs).**

PI Pelletier has developed a new method of distinguishing hillslopes from valleys in high resolution (e.g. airborne LiDAR) DEMs. Distinguishing valleys from hillslopes is a fundamental step in many hydrological and geomorphic analyses. In hydrology, for example, many models require that different values of hydraulic roughness, infiltration, or other model parameters be applied to valleys and hillslopes in order for realistic results to be obtained. In geomorphology, the computation of valley or drainage density, defined as the ratio of the total length of valleys divided by the basin area, requires that the valley or drainage network first be defined. Drainage density, which varies over approximately two orders of magnitude in fluvially dominated terrain on Earth, i.e. from ~3 $km^{-1}$ to ~300 $km^{-1}$, is important because it defines the transition from predominantly colluvial to predominantly fluvial sediment transport in landscapes.

Existing methods for drainage network extraction rely on contributing area or length (and user-defined contributing-area or length thresholds that define the transition from hillslope to valley) to distinguish valleys from hillslopes in DEMs. Early methods of drainage network extraction from DEMs used contributing area only or a combination of contributing area, length, and slope. Using contributing area or length as a criterion for drainage network extraction is problematic for two reasons. First, since drainage density is inversely related to the average contributing area upstream from valleys, using contributing area as a criterion for drainage network extraction results in circular reasoning – the drainage density resulting from the analysis depends strongly on the contributing area threshold (or similar contributing-area-dependent parameter) used to identify the transition from hillslopes to valleys in the extraction procedure. Second, using contributing area as a mapping criterion is problematic because valleys are areas of localized, confined flow, not simply areas with large contributing area. As such, the topographic curvature or V-shapedness should be used to define valleys. In a forthcoming paper in *Water Resources Research*, Pelletier presents a method for drainage network extraction from high-resolution DEMs (e.g. those derived from Airborne Laser Swath Mapping) that requires just two user-defined parameters. This work illustrates the accuracy and robustness of the method using synthetic valley networks that mimic the complexities of real landscapes (i.e. microtopographic variability and discontinuous valley networks) and for which the true drainage network is known exactly, by construction. The method involves six principal steps: optimal Wiener filtering to remove microtopographic noise, mapping of the contour curvature,

identification of valley heads using a user-defined contour-curvature threshold criterion, routing of a unit discharge of water from each valley head using a multiple-flow-direction routing algorithm, removal of discontinuous reaches from the drainage network using a user-defined discharge-per-upstream-valley-head threshold criterion, and thinning of the valley network to a single pixel width. The method yields accurate results using the same user-defined parameters for the two CZO field sites considered in the paper (one from JRB and one from SCM), suggesting that it can produce accurate results using default parameter values.

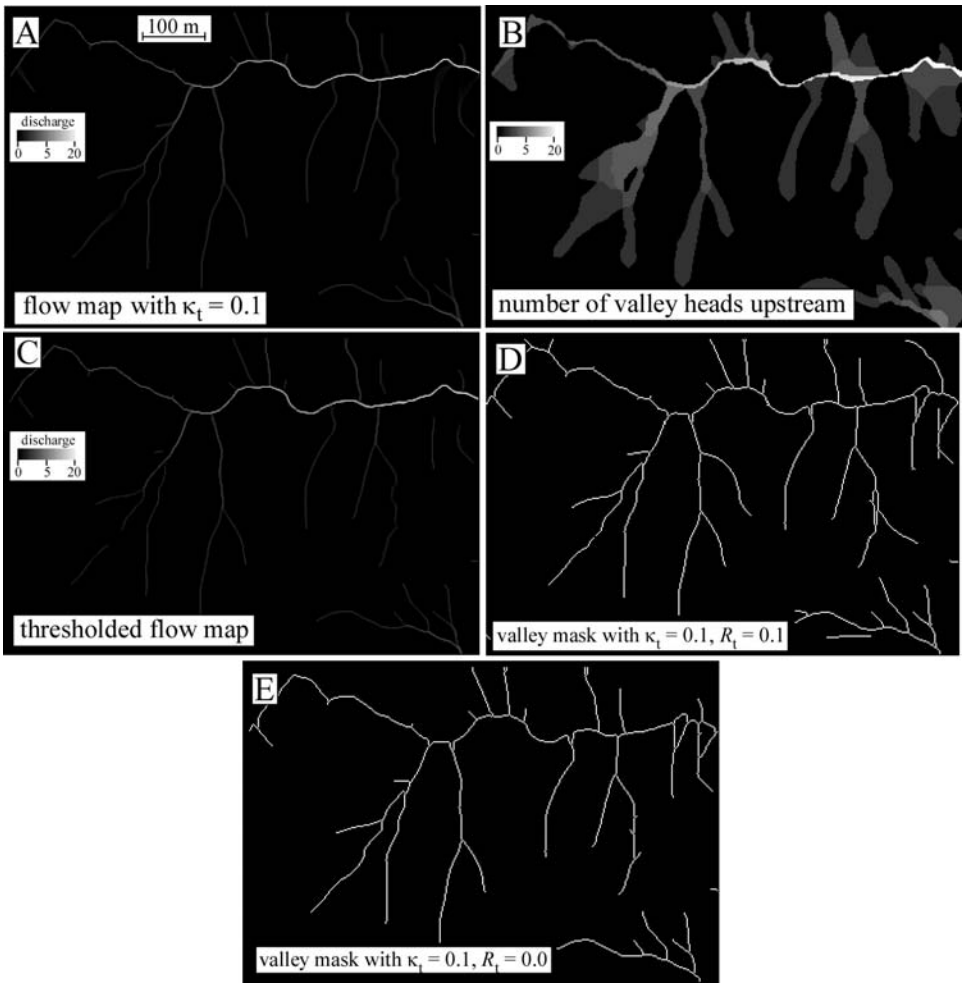


**Figure 49**. Results of the drainage network extraction method on the Marshall Gulch test case, Santa Catalina Mountains. (A) Grayscale map of discharge resulting from first identifying the valley heads using contour curvature with $\kappa_t$ = 0.1 $m^{-1}$ and then routing a unit of discharge from each valley head. (B) Grayscale map of the number of valley heads upstream from each pixel. (C) Grayscale map of discharge with discontinuous sections removed using $R_t$ = 0.1. (D) Binary map of the valley network predicted by the method with $\kappa_t$ = 0.1 $m^{-1}$ and $R_t$ = 0.1. (E) Binary map of the valley network predicted by the method with $\kappa_t$ = 0.1 $m^{-1}$ and $R_t$ = 0 (Pelletier et al.).

**• Soil-vegetation interactions affect sediment transport and nutrient transport in Desert Scrub hillslopes**

From August 2011 to July 2012 Dr Ciaran Harman worked as a Postdoc at UA, supervised primarily by Peter Troch. During this time, Dr Harman participated in a number of collaborative projects, but work on soil-vegetation interactions in the desert CZO sites (at the lowest elevation of the SCM-JRB climosequence) was the most fruitful. Those activities extended work that had been done as part of NSF grant EAR 0911205, leading to the submission of a manuscript to *JGR – Biogeosciences*. Other ongoing work is concerned with analyzing water storage dynamics in the JRB watersheds, and with investigating links between long-term geomorphic and soil development and hydrologic functions along the SCM-JRB climosequence.

The project on soil-vegetation interactions at the Sonoran Desert sites aimed to better understand the coupling between soils, vegetation and sediment transport on steep semi-arid hillslopes. Shrublands in semi-arid regions are heterogeneous landscapes consisting of infertile bare areas separated by nutrient-rich vegetated areas known as resource islands. Research has shown that this strong spatial patterning develops through feedbacks that include the transportation of water and nutrient resources from the intershrub space to areas below shrubs, and the retention of these resources to locally drive productivity and tight biogeochemical cycles. However this conceptual understanding of plant-soil feedbacks is based predominantly on research performed on stable or depositional geomorphic surfaces, and it is unclear whether the patterns of association between soils and vegetation, and the autogenic processes that create them, also occur on more steeply sloping terrain. The contrasting lithologies of the CZO hillslopes in the Sonoran Desert provide an idea laboratory to examine these issues. Dr Harman engaged in four main research activities over the last year to investigate them:

(i) Terrestrial LIDAR surveys of two desert hillslopes. LIDAR equipment was supplied by the Biosphere2 LEO facility and used in the field to acquire high-resolution scans of the above-ground vegetation and soil topography in 20m by 10m areas on each slope. These surveys provided detailed information about the spatial organization of vegetation and microtopography in the study areas (**Figs. 50-51**).

(ii) Soil sampling and analysis. Previous soil sampling campaigns in the study areas conducted as part of NSF grant EAR 0911205 were extended to provide greater coverage of the natural spatial variability in soil organic matter. Sample locations were mapped back to the LIDAR datasets, allowing the soil organic matter contents to be analyzed in relation to the microtopography and vegetation density at fine (~5cm) spatial scales. This was combined with data on soil composition and hydraulic properties from the previous soil sampling.

(iii) A numerical model of overland flow. A model of the full St Venant equations for shallow flow, coupled to a Green-Ampt infiltration equations, was developed. This model will be used to further investigate the effect of soil, vegetation density and microtopographic variations on surface runoff, infiltration and shear-stress.

The study found that contrasts in soil composition were significant on these steeper slopes, in contrast with the results of other studies. Moreover, there were patterns and process signatures apparent in the results that are perhaps unique to steeply sloping semi-arid hillslopes. The spatial patterns in soil organic matter observed suggested that soil organic matter under woody shrubs is re-distributed into the interspaces between the canopies in steeper hillslopes. This pattern was stronger in the granite site, which also had lower gradients, coarser soil texture and more pronounced rill and inter-rill structure. The association of the SOM with microtopography and the downslope asymmetry of the plumes suggested that they are controlled by slope dependent transport processes.

Slope dependent processes may be more important at the lower-gradient granite site (perhaps counter-intuitively), because there the lower overall gradient allows microtopography associated with vegetation to more effectively control concentrated flow paths, protecting areas downslope of vegetation from overland flow. This leads to the formation of clear `plumes' extending downslope 2-3 canopy radii, and significant asymmetry in organic matter content within the canopy of woody shrubs at the granite site. At the schist site these plumes are still evident, but their structure is not as clear and asymmetry within the canopy was not significant. This hypothesis requires testing with further field and modelling studies.

These results contrast a large body of work that has focused on spatial patterns of lower-gradient areas, such as alluvial fans. The transport that creates these plumes inverts the common conceptual model of redistribution of resources from the bare interspace to the vegetated patches. If slope-dependent transport processes (such as rainsplash) are significant, this also suggests that modelling based on fluvial transport alone is insufficient to capture carbon transport dynamics in these areas.

The co-evolved patterns discussed have significant implications for the connection between ecohydrologic dynamics of water-limited ecosystems the interactions between vegetation and erosion on hillslopes, and the coupling of geomorphic processes and the spatio-temporal dynamics of desert microbial communities.

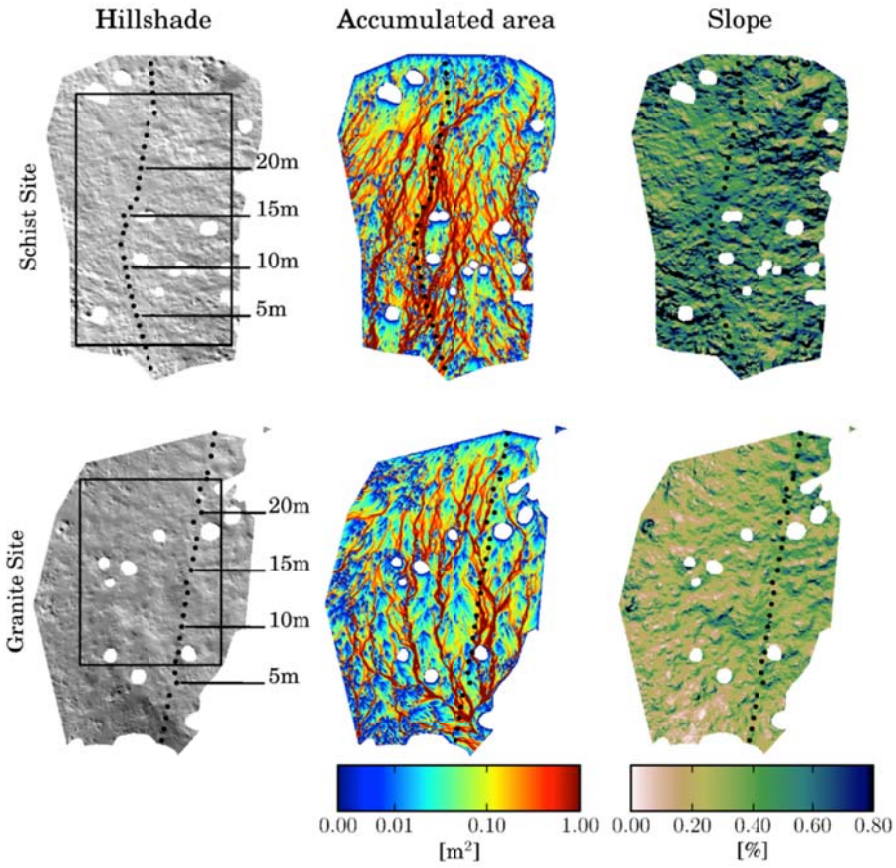


**Figure 50.** Surface topography of the Sonoran Desert CZO hillslopes, showing the different slope and surface drainage patterns that arise in each of the different lithologies (Harman et al., 2012).

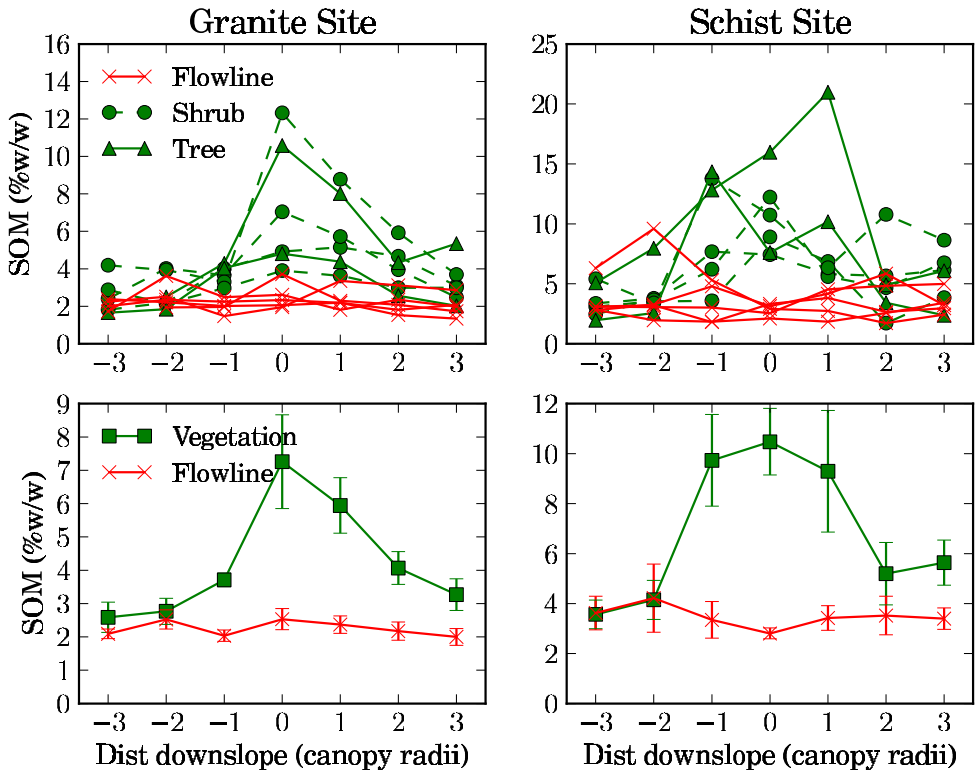


**Figure 51.** Asymmetry of soils altered by biota in the vicinity of vegetation on the hillslopes. On the granite site, organization of flow into rills (see Figure 1) preserves areas downslope from overland flow, leading to accumulation of soil organic matter in 'plumes' that extend downslope from woody shrubs on the order of 2-3 canopy radii. At the schist site this effect is present, but more muted (Harman et al., 2012).

## 3.5 Continued EEMT model development.

Understanding how water, energy and carbon are partitioned to primary production and effective precipitation is central to quantifying the limits on critical zone evolution. Recent work suggests quantifying energetic transfers to the critical zone in the form of effective precipitation and primary production provides a first order approximation of critical zone process and structural organization. However, explicit linkage of this effective energy and mass transfer (EEMT; W $m^{-2}$) to critical zone state variables and well defined physical limits remains to be developed. The objective of this work (Rasmussen, 2012) was to place EEMT in the context of thermodynamic state variables of temperature and vapor pressure deficit, with explicit definition of EEMT physical limits using a global climate dataset. The relation of EEMT to empirical measures of catchment function was also examined using a subset of the Model Parameter Estimation Experiment (MOPEX) catchments.

The data demonstrated three physical limits for EEMT: i) an absolute vapor pressure deficit threshold of 1,200 Pa above which EEMT is zero; ii) a temperature dependent vapor pressure deficit limit following the saturated vapor pressure function up to a temperature of 292 K; and iii) a minimum precipitation threshold required from EEMT production at temperatures greater than 292 K (**Fig. 52**). Within these limits, EEMT scales directly with precipitation, with increasing conversion of the precipitation to EEMT with increasing temperature. The state-space framework derived here presents a simplified framework

with well-defined physical limits that has the potential for directly integrating regional to pedon scale heterogeneity in effective energy and mass transfer relative to critical zone structure and function within a common thermodynamic framework.

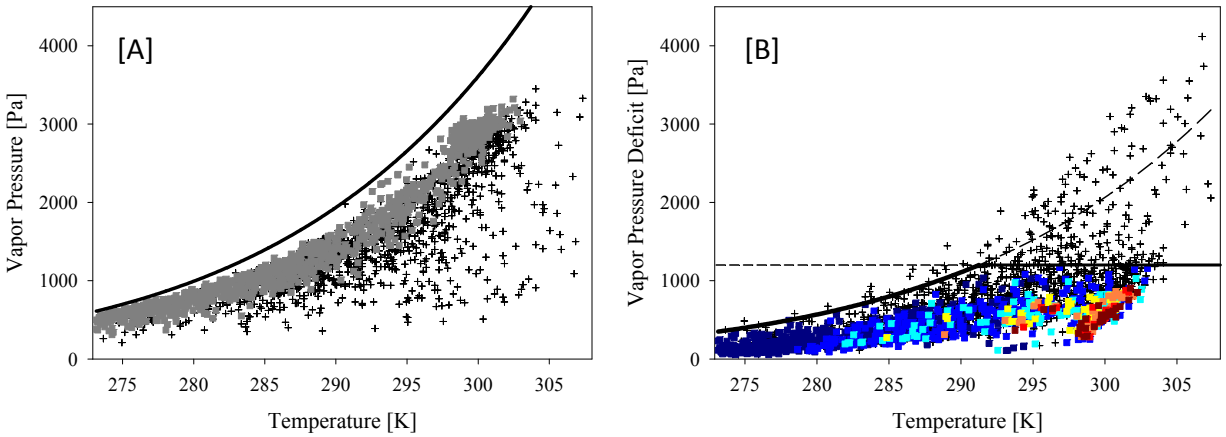


**Figure 52**. Climate data in (a) vapor pressure and temperature and (b) vapor pressure deficit and temperature state space. The solid line in (a) is the saturated vapor pressure line, the gray squares are locations of positive effective energy and mass transfer (EEMT), and cross hairs are locations of zero EEMT. In (b), the solid lines indicate the upper physical limit of EEMT as defined using a modified Clausius-Clapeyron equation for locations temperature < 292 K and set at 1,200 Pa for locations with temperature > 292 K; dashed lines indicate the extension of those limits beyond their point of intersection. The colored squares are locations of positive EEMT scaled with increasing EEMT, and cross hairs are locations of zero EEMT (Rasmussen et al.).

Additionally, we have further refined EEMT to account for local scale variation in topography and vegetation. Topographic variation was accounted for by implementing a full Penman-Monteith approach to modeling actual evapotranspiration that takes into consideration aspect effects on radiant and vapor pressure deficit evaporative forcing and vegetation control on surface resistance. Topographic redistribution of water was accounted for using a modified topographic wetness index. The updated model of EEMT has been applied at high resolution (1 to 10 m pixel resolution) for the Sabino Canyon watershed in the SCM that extends from the top of the SCM down to the base and includes the Marshall Gulch catchment (**Fig. 53**). The new model provides highly resolved prediction of EEMT that will be used to inform ongoing data collection and analyses.

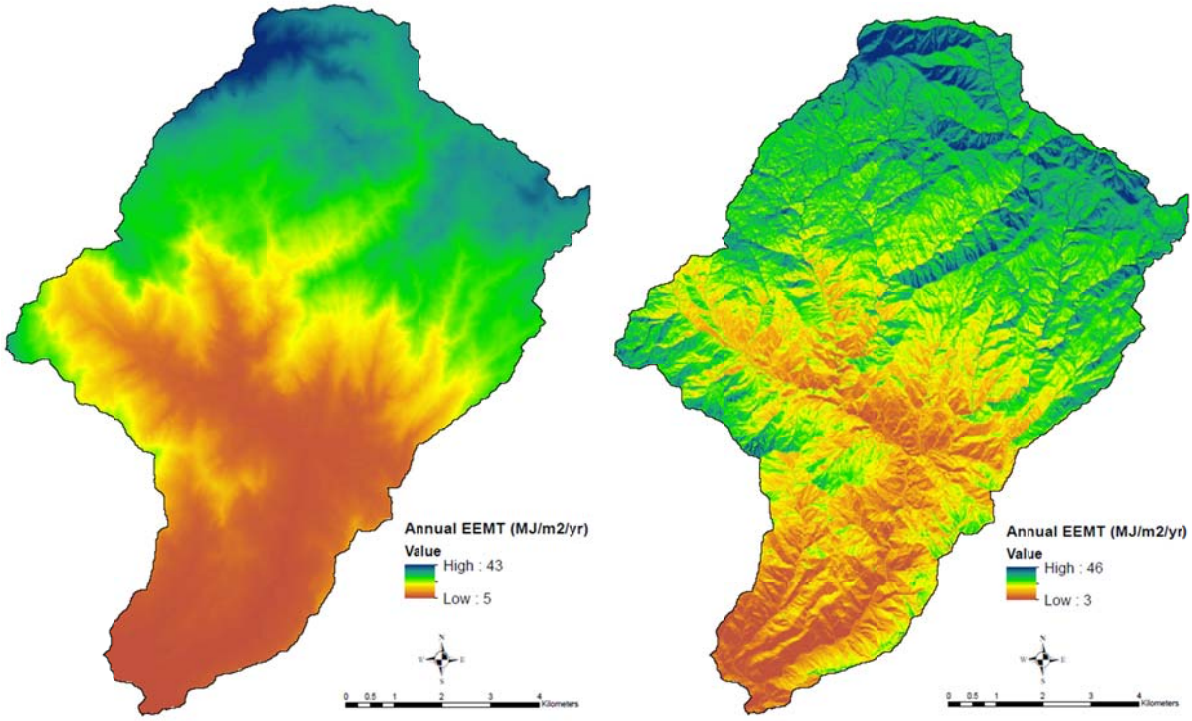


**Figure 53.** EEMT calculated for the Sabino Canyon watershed in the SCM using a) the traditional approach incorporating coarse resolution climate data and b) the modified approach that incorporated topographic and vegetation controls on evapotranspiration and water redistribution (Rasmussen et al.).

## 4. Data Management Activities

Our JRB-SCM CZO data management specialist, Dr. Matej Durcik, has been working closely with members of the cross-CZO data management team (PI Anthony Aufdenkampe, Stroud Water Research Center and associated scientists) to consolidate hydrologic, hydrochemical, meteoroligical and geochemical time series data in a CUAHSI and CZchem.db formats that can be posted on line at CZO home servers and then harvested by "CZO central", for uploading to the San Diego Super Computer. All data being generated by the CZO are being geared toward presentation in the requisite format. Geochemical data acquisition (spatial data on distribution of geochemical concentrations, mineralogical data, etc.) are being incorporated into the Penn State led geochemical data base program that will permit eventual inclusion of the data into EarthChem (PI Kirsten Lehnert).

## 5. Opportunities for Training, Development, and Mentoring Provided by the Project

The multiple graduate and undergraduate students involved in this project have gained invaluable field and laboratory skills, and research experience working as part of a large interdisciplinary team. In addition, funding of an REU site proposal at Biosphere 2 (B2) has provided excellent opportunities for collaboration with that program via undergraduate research experiences associated with the JRB-SCM CZO. Several B2 REU students were involved in CZO research during summers of 2010 and 2011, as described in "Personnel" section of this report. In addition to graduate and undergraduate training described in the activities and findings above, four postdoctoral scientists (Dr. Julia Perdrial, Dr. Adrian Harpold, Dr. Ciaran Harman, and Dr. Bhaskar Mitra) also received training and mentorship experience as part of this grant.

Caitlin Orem (LSE grad student) was trained in cosmogenic sample preparation for $^{10}$Be dating. Her PhD project integrates lab analysis of suspended sediment data, cosmogenic radionuclide dating, analysis of ground-based and airborne-lidar data, and numerical modeling.

PI Pelletier worked with UA's Flandrau Museum to construct a Sky Islands exhibit.

A summer intern and Northwestern University Undergraduate Earth Sciences major, Jessica Prescott-Smith, joined the CZO program for the summer 2012 (June 18th-August 24th) and focused on developing an independent research project in collaboration with Julia Perdrial, Michael Pohlmann and Jon Chorover entitled "Impact of storm events on stream water particulate and colloidal matter: resolving variation by colloid size fractionation." This summer project resulted in submission of an AGU fall 2012 meeting abstract.

The HWR 696G course entitled "Water-Rock-Microbial Interactions" taught by J. McIntosh utilized results from CZO research in integration of course topics.

Student research grants and awards that were leveraged by the JRB-SCM CZO include:
Xavier Zapata-Rios (PhD, Hydrology and Water Resources, major advisor)
- Geological Society of America Student Research Grant (2011)

Courtney Porter (MS, Hydrology and Water Resources, major advisor)
- SAHRA travel grant to Cornell University for instrumentation training (2011)
- Geological Society of America Student Research Grant (2012)

## 6. Outreach Activities Undertaken by the Project

The CZO project is developing a collaboration with the Biosphere 2 (B2), where CZO science and related findings will be displayed in conjunction with the B2-led "Landscape Evolution Observatory" (LEO) that involves conjunctive study of hydrologic, biogeochemical, and geomorphic process couplings in three replicated zero order basin hillslope models subjected to controlled environment inputs. The public display pertaining to LEO is going to focus on both LEO related activities and also complementary research occurring in CZO field sites,. A large display at B2 currently presents a description of the National CZO program. Public displays at Biosphere 2 provide unique opportunites to reach a very large number of public visitors each year.

A wide array of information, including data, personnel and interpretive media are being uploaded regularly at the Jemez-Santa Catalina CZO website (www.czo.arizona.edu). For example, a video originally generated before and during the CZO All Hands Meeting at Biosphere 2, and that has included new information, is now posted at that location.

## 7. Publications Resulting From Research

***Published, Submitted and In Prep. Papers (since last report):***

Adams, H. D., C. H. Luce, D. D. Breshears, C. D. Allen, M. Weiler, V. C. Hale, A. M. S. Smith, and T. E. Huxman. 2012. Ecohydrological consequences of drought- and infestation-triggered tree die-off: insights and hypotheses. Special feature: Ecohydrologic Connections and Complexities in Drylands – New Perspectives for Understanding Transformative Landscape Change. *Ecohydrology* 5: 145-159. DOI: 10.1002/eco.233.

Barron-Gafford G.A., R.L. Minor, C.L. Wright, and S.A. Papuga. Quantifying environmental and topographic controls on soil respiration in a montane drainage system. In final preparation for *Journal of Geophysical Research-Biogeosciences*.

Breshears, D. D., T. B. Kirchner, J. J. Whicker, J. P. Field, and C. D. Allen. 2012. Modeling aeolian transport in response to succession, disturbance and future climate: Dynamic long-term risk assessment for contaminant redistribution. Special Issue: International Aeolian research Conference VI. *Aeolian Research* 3: 445-457. DOI:10.1016/j.aeolia.2011.03.012.

Harman, C. J., K. A. Lohse, P. A. Troch, M. Sivapalan, Structure and processes controlling resource islands and microtopography on semi-arid hillslopes, submitted to *Journal of Geophysical Research – Biogeosciences*

Harpold, A.A., C. Stielstra, S. Rajogopalan, I. Heidebuchel, A. Jardine, and P.D. Brooks. Changes in snowpack volume and snowmelt timing in the Intermountain West. <in review at *Water Resources Research*>

Harpold, A.A., J. Biederman, K. Condon, M. Merino, and P.D. Brooks. Changes in winter season snowpack accumulation and ablation following the Las Conchas Forest Fire. <submitted to *Ecohydrology*>

Harpold, A.A., P.D. Brooks, J. Perdrial, J. McIntosh, T. Meixner, X. Zapata-Rios, A. Rios- Vasquez, and J. Chorover. Quantifying the variation in solute sources in montane headwater catchments <planned submission to *JGR-Biogeosciences*>

Krystine Nelson "*The Influence of Snow Cover Duration on Evaporation and Soil Respiration in Mixed-Conifer Ecosystems*", MS Thesis, SNRE, University of Arizona.

Law, D. J., D. D. Breshears, M. H. Ebinger, C. W. Myer, and C. D. Allen. 2012. Soil C and N patterns in a semiarid piñon-juniper woodland: Topography of slope and ephemeral channels add to canopy-intercanopy heterogeneity. *Journal of Arid Environments* 79:20-24. DOI:10.1016/j.jaridenv.2011.11.029.

Mahmood, T.H. 2012. "*Hillslope Scale Hydrologic Spatial Patterns in a Patchy Ponderosa Pine Landscape: Insights from Distributed Hydrologic Modeling*." PhD thesis in Geological Sciences, Arizona State University, 179 pp.

Mahmood, T.H. and Vivoni, E.R. 2011. A Climate-Induced Threshold in Hydrologic Response in a Semiarid Ponderosa Pine Hillslope. *Water Resources Research*. 47: W09529, doi: 10.1029/2011WR010384.

Mahmood, T.H. and Vivoni, E.R. 2011. Breakdown of Hydrologic Patterns upon Model Coarsening at Hillslope Scales and Implications for Experimental Design. *Journal of Hydrology*. 411(3-4): 309-321.

Mahmood, T.H. and Vivoni, E.R. 2012. Forest Ecohydrological Response to Bimodal Precipitation during Contrasting Winter to Summer Transitions. *Ecohydrology*. (In second review).

McDowell, N. G., D. J. Beerling, D. D. Breshears, R. A. Fisher, K. F. Raffa, and M. Stitt. 2012. The interdependence of mechanisms underlying climate-driven vegetation mortality. *Trends in Ecology and Evolution* 26: 523-532. doi:10.1016/j.tree.2011.06.003.

Neal, A.L., S. A. Kurc, P.D. Brooks, and R.L. Scott (In Revision) Environmental Controls on Ecosystem Respiration in Drylands: The Role of the Vertical Distribution of Soil Moisture. *Journal of Geophysical Research-Biogeosciences*

Nelson, K., Kurc, S.A., John, G.P., Minor, R., and G.A. Barron-Gafford. Influence of snow cover duration on soil evaporation and respiration efflux in mixed-conifer ecosystems, in review at *Ecohydrology*.

Orem, C.A., and J.D. Pelletier, Constraining frequency-magnitude-area relationships for precipitation and flood discharges using Next-Generation Radar (NEXRAD) and flow-routing models: Example applications in the Upper and Lower Colorado River Basins, *Journal of Hydrology*, in review.

Pelletier, J.D., A robust, two-parameter method for drainage network extraction from high-resolution DEMs, *Water Resources Research*, in review.

Pelletier, J.D., and J.T. Perron, Analytic solution for the morphology of a soil-mantled valley undergoing steady headward growth: Validation using case studies in southeastern Arizona, *Journal of Geophysical Research – Earth Surface*, 117, F02018, doi:10.1029/2011JF002281, 2012.

Pelletier, J.D., G.A. Barron-Gafford, D.D. Breshears, P.D. Brooks, J. Chorover, M. Durcik, C.J. Harman, T.E. Huxman, K.A. Lohse, R. Lybrand, T. Meixner, J.C. McIntosh, S.A. Kurc, C. Rasmussen, M. Schaap, T.L. Swetnam, and P.A. Troch, Coevolution of nonlinear trends in vegetation, soils, and topography with elevation and slope aspect: A case study in the sky islands of southern Arizona, *Journal of Geophysical Research - Earth Surface*, in review.

Pelletier, J.D., T.L. Swetnam, and T.W. Swetnam, Scaling and breaks in scaling in forest fires: The role of topographic slope and aspect, *Journal of Geophysical Research - Biogeosciences*, in review.

Perdrial, J. N., N. Perdrial, A. Harpold, X. Gao, R. Gabor, K. LaSharr, and J. Chorover. 2012. Impacts of sampling dissolved organic matter with passive capillary wicks versus aqueous soil extraction. Soil Sci. Soc. Am. J. https://www.soils.org/publications/sssaj/view/first-look/s12-0061.pdf

Perdrial, J., McIntosh, J., Harpold, A., Brooks, P., Zapata-Rios, X., Ray, J., Troch, P., Chorover, J. (in review) Impact of winter climate change and catchment aspect on carbon dynamics in snow-dominated headwater streams. Submitted to *Global Change Biology*.

Porter, C.M., McIntosh, J., Derry, L., Meixner, T., Chorover, J., Brooks, P., Rasmussen, C., Perdrial, J. (*in prep*) Determining solute inputs to soil and stream waters in a seasonally snow-covered mountain catchment in northern New Mexico, using Ge/Si, 87Sr/86Sr, and ion chemistry.

Rasmussen, C. 2011. Thermodynamic constraints on effective energy and mass transfer and catchment function. Hydrol. Earth Syst. Sci., 16, 725-739, 2012. doi:10.5194/hess-16-725-2012

Stielstra, C. M. Quantifying the role of hydrologic variability in controlling soil carbon flux, MS thesis, Hydrology and Water Resources, University of Arizona

Vazquez-Ortega, A., J. Perdrial, A. Harpold, X. Zapata, C. Rasmussen, J. McIntosh, M. Schaap, J. D. Pelletier, M. K. Amistadi, J. Chorover. 2012. Rare earth elements as reactive tracers of biogeochemical weathering in the Jemez River Basin Critical Zone Observatory. For submission to Chem. Geol.

Wilcox, B. P., M. S. Seyfried, D. D. Breshears and J. J. McDonnell. 2012. Preface: Ecohydrological connections and complexities in drylands: new perspectives for understanding transformative landscape change. Ecohydrology 5: 143-144. DOI: 10.1002/eco.1251.

Zapata-Rios, X., Troch, P., McIntosh, J., Broxton, P., Harpold, A., Brooks, P. (in prep) The effect of terrain aspect on interannual variability of hydrologic response in mountainous catchments in New Mexico.

**Published Abstracts & Presentations of Results (only those presented since last annual NSF report):**

Braun, Z., Rebecca L. Minor, Daniel L. Potts, and Greg A. Barron-Gafford. Quantifying thermal constraints on carbon and water fluxes in a mixed-conifer sky island ecosystem. Fall Meeting of the American Geophysical Union, December 2012.

Braun, Z., Rebecca L. Minor, Daniel L. Potts, Maggie Heard, and Greg A. Barron-Gafford. Quantifying temperature constraints on leaf-level carbon and water fluxes in a mixed-conifer sky island ecosystem. Undergraduate Research Opportunities Consortium (UROC) Summer Research Institute, August 2012.

Brooks, P. D., et al., Multi-scale Observations of Hydrologic Partitioning and Solution Chemistry Following Tree Mortality: Implications for Ecosystem Water and Biogeochemical Cycles, Ecological Society of America Annual Meeting, August 2012

Brooks, P., Litvak, M., Harpold, A., Molotch, N., McIntosh, J., Troch, P., Zapata, X. (2011) Non-linear feedbacks between climate change, hydrologic partitioning, plant available water, and carbon cycling in montane forests. AGU Fall Meeting.

Charaska, E., K.A. Lohse, C. Weber, P. Brooks, and J. Chorover. 2012. Nitrogen Cycling in Post-Fire Soils Across a Burn Intensity Gradient. Rocky Mountain Geological Society of America, Alburqueque, NM, May 7-10.

Chorover, J., Troch, P., Pelletier, J., Rasmussen, C., Brooks, P., McIntosh, J., Breshears, D., Huxman, T., Papuga, S., Lohse, K., Meixner, T., Schaap, M., Litvak, M., Harpold, A., Perdrial, J., Durcik, M. (2011) Carbon, water and weathering limitations in the semi-arid critical zone. AGU Fall Meeting.

Dannemann, F., Zapata, X., McIntosh, J., Perdrial, J., Books, P., Chorover, J., Lohse, K., Fricke, H. (2011) Temporal and spatial dynamics of carbon and nitrogen in headwater snow-dominated ctachments. AGU Fall Meeting.

Driscoll, J., Meixner, T., Molotch, N., Sickman, J., Williams, M., McIntosh, J., Brooks, P. (2011) Inverse geochemical reaction path modeling and the impact of climate change on hydrologic structure in snowmelt-dominated catchments in the southwestern USA. AGU Fall Meeting.

Harman, C. J., Can co-evolved spatial patterns of soils and topography improve upscaled representations of hydrologic processes? 2nd International Conference on Hydropedology, Leipzig, Germany, Jul. 2012

Harman, C. J., K. A. Lohse, P. A. Troch, M. Sivapalan, Do vegetated patches on hillslopes act like immobile zones with heavy-tailed residence times?, 3rd Workshop on Stochastic Transport and Emergent Scaling in Earth-surface Processes, Lake Tahoe, Oct.-Nov. 2011

Harman, C. J., P.A. Troch; K.A. Lohse; M. Sivapalan, Co-evolution of Vegetation, Sediment Transport and Infiltration on semi-arid hillslopes (Poster), American Geosciences Union Fall meeting, San Francisco, Dec. 2011, Abstract B33G-0555.

Harman, C. J., Troch, P. A., Pelletier, J., Rasmussen, C., Chorover, J., Critical zone evolution and the origins of organised complexity in watersheds, EGU General Assembly, Vienna, Austria, Apr. 2012

Harpold, A.A., J.A. Biederman, and P.D. Brooks. Changes in snow accumulation and ablation following the Las Conchas Forest Fire, NM, USA. CUASHI Biannual Conference 2012. Boulder, CO.

Harpold, A.A., P.D. Brooks, J.A. Biederman, and T. Swetnam. Estimating catchment-scale snowpack variability in complex forested terrain. Valles Caldera National Preserve, NM. AGU Fall Conference 2011. San Francisco, CA.

Lohse, K., Gallo, E., Carlson, M., Riha, K., Brooks, P., McIntosh, J., Sorooshian, A., Michalski, G., Meixner, T. (2011) Impacts of urbanization on nitrogen cycling and aerosol, surface and groundwater transport in semi-arid regions. AGU Fall Meeting.

Lohse, K.A., *E. Charaska, P. Brooks, C. Rassmussen, and J. Chorover. 2012. Soil carbon and nitrogen cycling in the Valles Caldera, NM: Initial responses to the Las Conchas fire. Tri-State EPSCoR Annual Meeting. Sun Valley, ID, April 2-6.

Lowry, F.; Papuga, S. A., Vegetation-infiltration relationships along an elevational gradient in the semiarid southwestern United States, American Geophysical Union, Fall Meeting 2011

Lybrand R. and C. Rasmussen. 2011. Chemical Weathering of Granitic Soils in the Santa Catalina Mountains, Arizona: Effects of Climate and Landscape Position. In Abstracts, International Annual Meeting, ASA-CSSA-SSSA, San Antonio, TX. 16 Oct-19 Oct. 2011. (Talk)

Lybrand R. and C. Rasmussen. 2011. Quantifying elemental compositions of primary minerals from granitic rocks and saprolite within the Santa Catalina Mountain Critical Zone Observatory. In Abstracts, American Geophysical Union Fall Meeting, San Francisco, CA. 5-9 Dec. 2011.

Lybrand R. and C. Rasmussen. March 29th, 2012. Quantifying microscale mineral transformations in granitic soils across the Santa Catalina Mountains of southern Arizona. In Abstracts, University of Arizona's EarthWeek Conference.

Mahmood, T.H. and Vivoni, E.R. 2012. Hydrologic Spatial Patterns in a Semiarid Ponderosa Pine Hillslope. National Hydrologic Research Centre, Saskatoon, SK, Canada.

McIntosh, J. (2012) How water, carbon and energy drive Critical Zone evolution: Jemez River Basin-Santa Catalina Critical Zone Observatory. University of Texas-El Paso, Geology Department Seminar.

Nelson, K.; Papuga, S. A.; John, G. P.; Minor, R.; Barron-Gafford, G. A., Influence of snow cover duration on soil evaporation and respiration efflux in mixed-conifer ecosystems. American Geophysical Union, Fall Meeting 2011

Pelletier, J.D., Scaling and breaks in scaling in forest fires: The role of topographic slope and aspect, STRESS III Workshop, Lake Tahoe, NV, November, 2011.

Pelletier, J.D., T. Swetnam, S.A. Papuga, K. Nelson, P.D. Brooks, A.A. Harpold, J. Chorover (2011) Distinguishing grass from ground using LiDAR: Techniques and applications. Abstract EP51E-05.

Perdrial, J. N., A. Vasquez-Ortega, J. McIntosh, A. Harpold, C. Porter, X. Zapata-Rios, L. Guthridge, P. Brooks, J. Chorover. Stream water organic matter characteristics after the Las Conchas wildfire : perspective from the critical zone. GSA meeting Rocky Mountain section, ABQ. May 9-11th.

Perdrial, J. N., N. Perdrial, A. Harpold, A. Peterson, A. Vasquez, J. Chorover. Probing dissolved organic matter in the critical zone: a comparison between in situ sampling and aqueous soil extracts. AGU 2011 Fall meeting, San Francinso, Dec.5-9. . B51A-0385.

Perdrial, J. N., P. Brooks, J. Chorover, K. Condon, A. Harpold, M. Holleran, D. Huckle, R. Lybrand, P. Troch, J. McIntosh, T. Meixner, R. Minor, B. Mitra, M. Pohlmann, C. Rasmussen, T. Swetnam, A. Vazquez-Ortega, X. Zapata-Rios. Do water and carbon fluxes control chemical denudation? Goldschmidt 2012, June 24-29, Montreal.

Porter, C., McIntosh, J., Derry, L., Meixner, T., Chorover, J., Rasmussen, C., Brooks, P., Perdrial, J. (2011) Determining solut inputs to soil and stream waters in a seasonally snow-covered mountain catchment in northern New Mexico using Ge/Si and 87Sr/86Sr ratios. AGU Fall Meeting.

Potts, D. L., Rebecca L. Minor, Zev Braun, and Greg A. Barron-Gafford. Species-specific and seasonal differences in chlorophyll fluorescence and photosynthetic light response among three evergreen species in a Madrean sky island mixed conifer forest. Fall Meeting of the American Geophysical Union, December 2012.

Swetish, J., S. A. Papuga, M. Litvak, G. Barron-Gafford, B. Mitra. 2011. Influence of understory greenness on trace gas and energy exchange in forested ecosystems, American Geophysical Union, Fall Meeting 2011

Zapata, X., McIntosh, J., Sorooshian, A., Lohse, K., Brooks, P., Troch, P., Chorover, J., Heidbuechel, I. (2011) Sources and amounts of nitrogen deposited in sky-island ecosystems. AGU Fall Meeting.

## 8. Contributions to within Discipline

As described in detail above, ongoing research in multiple coordinated projects is resulting in substantive, peer-reviewed contributions within the fields of ecology, geochemistry, hydrology, and geomorphology. These disciplinary contributions are strengthened by the inter-disciplinary linkages that are being made to allied disciplines via cross-cutting CZO science themes. Within field contributions include:

- Quantifying vegetation-topography interactions at hillslope scales
- Understanding winter-to-summer transitional periods in forested regions
- Quantifying the role of forest disturbance on snow water balance
- Understanding vegetation demography across complex terrain in the critical

## 9. Contributions to Resources for Research and Education

In so far as the principal intent of the CZOs is to establish natural laboratories for use by the broader earth sciences community, we have made significant progress in this respect through installations of sampling

equipment and sensors in the SCM at low, intermediate and high elevation sites, and intensive instrumentation array in the JRB at high elevation (mixed conifer) burned and unburned sites.

The JRB-SCM CZO is coordinating with the new Biosphere 2 REU/RET site to provide an exciting venue for their earth system sciences summer research program. Several of the CZO investigators hosted REU/RET students in their lab groups during summers of 2011 and 2012 focusing on CZO research.